AIR – WATER PARTITIONING OF VOLATILE ORGANIC COMPOUNDS AND GREENHOUSE GASES IN THE PRESENCE OF SALTS

A Thesis
Presented to
The Academic Faculty

by

James Benjamin Falabella

In Partial Fulfillment
of the Requirements for the Degree
Doctor of Philosophy in the
School of Chemical and Biomolecular Engineering

Georgia Institute of Technology
August 2007

AIR – WATER PARTITIONING OF VOLATILE ORGANIC COMPOUNDS AND GREENHOUSE GASES IN THE PRESENCE OF SALTS

Approved by:

Dr. Amyn S. Teja, Chair
School of Chemical and Biomolecular Engineering
Georgia Institute of Technology

Dr. Charles A. Eckert
School of Chemical and Biomolecular Engineering
Georgia Institute of Technology

Dr. James Frederick
School of Chemical and Biomolecular Engineering
Georgia Institute of Technology

Dr. Athanasios Nenes
School of Chemical and Biomolecular Engineering and School of Earth and Atmospheric Sciences
Georgia Institute of Technology

Dr. Paul H. Wine
School of Chemistry and Biochemistry and School of Earth and Atmospheric Sciences
Georgia Institute of Technology

Date Approved: April 30, 2007

To my Family

ACKNOWLEDGEMENTS

I would like to thank my PhD thesis advisor Professor Amyn S. Teja for the guidance and experience that he has shared with me during my time in his research group. I would also like to thank Professors Eckert, Frederick, Nenes, and Wine of my reading committee for their critical reviews of my research. Dr. Tongfan Sun's advice on thermodynamic modeling helped me to efficiently sort through the literature. I truly appreciate Dr. Xin-Sheng Chai's headspace gas chromatography advice, which helped me have a quick start in measuring the necessary Henry's constants.

All of my family members, particularly my parents and sister, have been a key source of moral support during my journey through graduate school.

My MS thesis advisor at Northeastern University, Professor Nurcan Baç, has helped me build a strong foundation for graduate work in the two years that I spent in his research group.

Imogene Baker, Gayle Burt, and Rochelle Moses in the School of Chemical and Biomolecular Engineering helped me procure the chemicals and equipment for my research and their very prompt ordering kept my project on schedule.

Advice and writing exercises from Jacqueline Mohalley-Snedeker of the ChBE writing program and Karen Head of the Center for the Enhancement of Teaching and Learning (CETL) have helped me further refined my technical writing skills.

Teja group members Michael Beck, Anupama Kasturirangan, Pei Yoong Koh, Angel Olivera Toro, and Chunbao Xu have been great friends and coworkers.

I truly appreciate the financial support provided by the Institute of Paper Science and Technology over the entire course of my project.

TABLE OF CONTENTS

LIST OF TABLES

Page

LIST OF FIGURES

Page

LIST OF SYMBOLS

A	Debye-Hückel constant
a^r	residual Helmholtz energy
A_{ij}, B_{ij}, C_{ij}	binary parameters
C_i^l	concentration of *i* in the liquid phase
C_i^v	concentration of *i* in the vapor phase
D	ternary salt effect parameter
f_i^v	fugacity of solute *i* in the vapor phase
G	NRTL interaction parameter
$g(\sigma)$	hard sphere correlation function
H_c	dimensionless Henry's constant
H_{ij}	thermodynamic Henry's constant
I_x	ionic strength on a mole fraction basis
k_s	Setchenov constant
K_{OW}	octanol-water partition coefficient
M_s	molar mass of the solvent
n_{ion}	# of moles of an ion
n_i^v	moles of *i* in the vapor phase
n_i^l	moles of *i* in the liquid phase
n^v	total vapor phase mole fraction
n^l	total liquid phase mole fraction
n_w	mass of water
P	total pressure

P_i^{sat}	saturated solvent vapor pressure
P_j^{sat}	saturated vapor pressure of solvent *j*
P_m^{sat}	saturated vapor pressure of a solvent mixture
x_i	mole fraction of solute *i* in the liquid phase
x_s	salt mole fraction
y_i	mole fraction of *i* in the vapor phase
R	gas constant
T	absolute system temperature
T_c	critical temperature
T_r	system temperature reduced relative to the solvent's critical point
$\bar{v}_i^{\infty}$	partial molar volume of solute *i* at infinite dilution
V_{crit}	critical volume of the volatile solute
V^v	volume of vapor
V^l	volume of liquid
z_{ion}	ion charge

Greek Symbols

α	NRTL nonrandomness factor
γ_i	activity coefficient of component *i*
γ_i^{∞}	limiting activity coefficient of component *i*
$\gamma_{\pm}^{(m)}$	mean ionic activity coefficient
ε_o	permittivity of a vacuum
Λ_{ijk}	third osmotic virial coefficient
λ_{ij}	second osmotic coefficient
τ	NRTL binary interaction parameter

ρ	closest approach parameter
σ_{ion}	ion diameter

SUMMARY

A new relative headspace gas chromatography method was developed to obtain Henry's constants of moderately volatile VOCs such as 1-alkanols, 2-ketones, and aromatics in aqueous salt solutions. In addition, a model based on dilute solution theory was developed to correlate and extrapolate data sets collected in this work and those from the literature.

The new Henry's constant measurement method compares the headspaces above two vials containing dilute VOC solutions in water with and without salt. Minimal headspaces are maintained above both liquid phases to ensure that the liquid-phase VOC concentration remains essentially unchanged when equilibrium is reached. Henry's constants obtained using the relative method agreed with those obtained using the differential method [1] within experimental error. In addition, partial molar excess enthalpies at infinite dilution of methanol, ethanol, 1-propanol, and 2-butanone obtained from the Henry's constant data agreed reasonably well with calorimetrically determined values.

A total of 39 systems containing a VOC + one or more salts + water were studied in this work. The VOCs studied included homologous series of 2-ketones and 1-alkanols, some of the components of gasoline (toluene, ethylbenzene, o-xylene, methyl *tert*butyl ether, and ethyl *tert*butyl ether), and organic sulfides, which are a nuisance around paper mills. The salts in these systems included NaCl, $CaCl_2$, Na_2CO_3 Na_2SO_4, $(CH_3)_4NBr$, and $(C_2H_5)_4NBr$. Several mixtures of NaCl and Na_2SO_4 were also used with a homologous

series of 2-ketones (2-propanone – 2-heptanone) to examine trends in salting out behavior.

The model based on dilute solution theory was modified to correlate air-water partitioning data for Henry's constants of VOCs and GHGs for temperatures up to 525 K, salt concentrations up to 4 molal, and pressures up to 1000 atm. The model is also capable of correlating Henry's constants in solutions containing mixtures of two salts. Within a homologous series of compounds, a linear relationship was found between the critical volume of the VOC and its salt effect parameter. This suggests that the salt effect parameter for a given VOC could be predicted given the salt effect parameters for previously measured homologues. Extrapolations of up to 50 K, and 1 molal salt and 100 bar pressure can also be performed to eliminate the need for additional experiments. When this model was used to calculate emissions of methane from produced water storage tanks, it was found that such emissions were 50 % below predictions from ASPEN Plus using default salt-GHG interactions.

1. INTRODUCTION

Knowledge of the air-water partitioning behavior of volatile organic compounds (VOCs) and greenhouse gases (GHGs) is important in a number of environmental applications. For example, VOCs emitted from open process streams in a paper mill can promote ground level ozone and lead to respiratory problems in humans. Therefore, it is important to have reliable estimates of the amount of VOCs in the atmosphere in contact with open process streams. In global climate models, the partitioning of carbon dioxide and methane between the atmosphere and ocean water is of current interest since oceans represent a substantial storage reservoir for these gases.

In the area of occupational safety, many of the same VOCs that industries are monitoring to maintain a healthy environment are also a concern for the safety of workers. The National Institute for Occupational Safety and Health (NIOSH) has determined that acetone and methyl ethyl ketone (MEK) may not exceed maximum threshold limit values (TLVs) of 200 parts per million volume (ppmv) [2] in the work environment.

Finally, VOC partitioning is also of interest to the biochemical industry in the manufacture of pharmaceuticals and some specialty chemicals where a gas must be dissolved in a liquid. The solubility of different growth hormones and some gases cannot easily be measured in growth media containing salts and must be determined from its concentration in the vapor space of the bioreactor [3].

In all of these instances, salts are commonly present in water at concentrations that are high enough to significantly alter the air-water partitioning behavior of the VOC or GHG. Accurate vapor-liquid partition coefficients and robust models are therefore necessary to yield reliable estimates of VOCs and GHGs in airborne environments to satisfy regulatory requirements.

It is common for aqueous electrolyte solutions such as spent pulping liquor to contain several electrolytes and many non-volatile organic compounds in addition to VOCs. Teja et al. [4] have demonstrated that the electrolyte concentration has the strongest influence on VOC Henry's constants in such solutions. The agreement between the Henry's constants of methanol in spent liquor samples and of methanol in simulated spent liquor consisting of water + salt + VOC can be seen in Figure 1. This allowed them to simulate spent liquors using model ternary systems consisting of water, a VOC and one salt thereby limiting the number of combinations necessary to develop a model.

Despite the great need for air-water partitioning data for many VOCs and GHGs, few data are available when salts are present. Furthermore, even when data exist, there are large disagreements between reported values from different research groups. It is therefore desirable to have sets of partition coefficients that are measured on one apparatus to observe trends as salt concentration and temperature are varied.

Dissolved electrolytes have a profound affect on the partitioning behavior of a VOC and can result in an increase in solubility ("salting-in") or a decrease in solubility ("salting-out") of the VOC. The salt effect must be taken into account in calculations

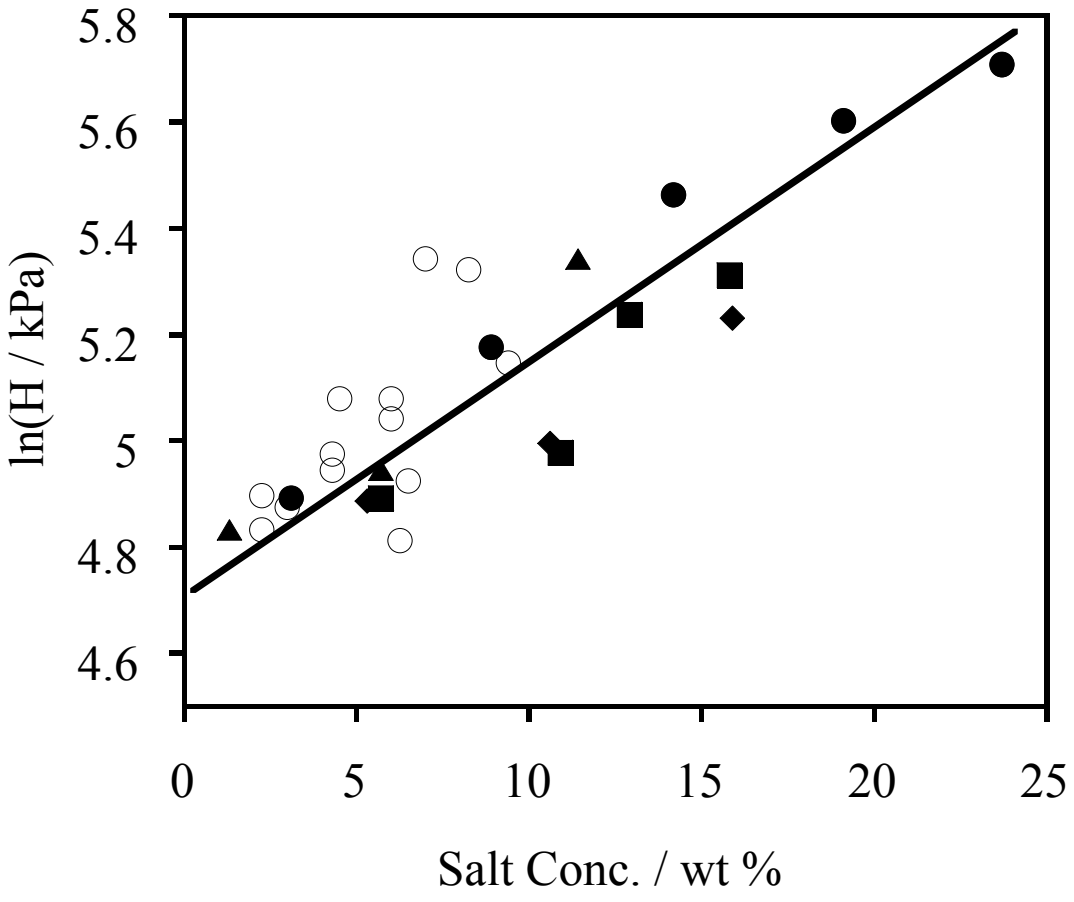

Figure 1. Henry's constants of methanol in (○) spent pulping liquor and simulated pulping liquor containing (●) sodium thiosulfate, (■) sodium chloride, and (▲) sodium sulfate, (◆) sodium carbonate [4].

since it can easily change the solubility of a VOC by up to 300 %. A reduction in VOC solubility is caused when salt ions bind more tightly to water than to the VOC. With fewer water molecules free to interact with the VOC, it will leave the water more freely resulting in an increased vapor space concentration. Solubility enhancements are the result of the salt ions breaking up the tight water structure and interacting with the VOC through dispersion forces both making the needed room for the VOC and pulling it into solution [5].

A common way to quantify the partitioning of VOCs between a liquid or vapor phase is by the use of Henry's constants. Henry's constant is defined as

$$H_{ij} = \lim_{x_i \to 0} \left(\frac{f_i^V}{x_i} \right) \qquad (1)$$

where H_{ij} is the Henry's constant, f_i^V is the fugacity of the VOC in the vapor phase and x_i is the mole fraction of the VOC in the liquid phase. At low pressures, the fugacity may be replaced by the partial pressure, so that

$$H_{ij} = \lim_{x_i \to 0} \left(\frac{y_i P}{x_i} \right) \qquad (2)$$

If y_i and x_i are expressed in terms of mole ratios,

$$H_{ij} = \left(\frac{n_i^v / n^v}{n_i^l / n^l} P \right). \qquad (3)$$

where n_i^v and n_i^l are the number of moles of i in the vapor and liquid phases and n^v and n^l are the total number of moles in the vapor and liquid phases respectively. In terms of concentration we obtain,

$$H_{ij} = \left(\frac{C_i^v V^v / n^v}{C_i^l V^l / n^l} P \right) \qquad (4)$$

where V^v and V^l are the total volume of the vapor and liquid phases. Simplifying further by substituting the molar volume, v, for V / n and substituting the ideal gas law we have,

$$H_{ij} = \left(\frac{C_i^v}{C_i^l} \frac{RT}{v^l} \right) = \left(H_c \frac{RT}{v^l} \right) \qquad (5)$$

where R is the gas constant, T is the system temperature, and v^l can be approximated as the molar volume of the solvent since the solution is dilute. The ratio of concentrations is called the dimensionless Henry's constant and is widely used in environmental applications.

The software package (WATER 9©) developed by the USEPA to estimate VOC emissions from aqueous streams employs dimensionless Henry's constants that have been averaged from various literature sources. In addition to being appropriate only for systems that contain no salt, the WATER9 Henry's constants used to estimate methanol emissions are approximately 30 % larger than recently published values [6]. The internal default values of WATER9 can therefore exert a large influence over emission estimates. Methanol emissions calculated from a cooling tower processing a typical wash water stream of 17,802,900 gal/day and containing 200 parts per million (ppm) of dissolved salts and 147 ppm methanol are 24 % lower if the data of Gupta et al. [6] are used in the calculations in place of the Henry's constants of Yaws used in WATER9. Such discrepancies between published Henry's constants are not rare.

Most published Henry's constants are for systems of VOCs in pure water. For example, Staudinger and Roberts [7, 8] have compiled Henry's constant vs. temperature correlations, based on van't Hoff's equation, for over 200 organic compounds. The DIPPR 911 [9] database also contains Henry's constants at 298 K for over 200 nonelectrolytes in water. Unfortunately, inconsistencies between the values reported by

DIPPR and results published by other investigators are quite common. Several examples have been compiled in Table 1. Infinite dilution activity coefficients, which are directly related to Henry's constants, have been reported for chlorinated and non-chlorinated aromatics in pure water and with electrolytes as a function of temperature [10]. However, many of the values at the same temperature differ by over 100 % when measured by different investigators [9, 11-16]. Clearly, it is necessary to resolve the discrepancy between published values and add partition coefficients for VOCs in the presence of dissolved salts since large industries rely on Henry's constants to prove their compliance with US environmental regulations.

In this work, Henry's constants for environmentally relevant VOCs will be measured with a single method to generate a data set with internal consistency and combined with literature data where available. The salts and VOCs were selected to provide a range of salt effects on homologous series of compounds. Consistency tests of the new data will be performed with independent measurements to cross check the measured Henry's constants. In addition, a model will be developed to calculate Henry's constants of VOCs and GHGs from ambient to geothermal conditions so that the entire range of applications can be addressed by one model. The ultimate goal of this work is to make *a priori* prediction of Henry's constants from independent measurements and/or molecular properties.

Table 1. Comparison of DIPPR 911 database values with literature values of Henry's constants.

Compound	CAS #	EPA Value (25 °C)*	DIPPR 911 (25 °C)*	Difference, %	Reference
2-butanone	78-93-3	1.30×10^{-4}	4.64×10^{-5}	64	[15]
trichloroethylene	79-01-6	8.33×10^{-3}	1.01×10^{-2}	21	[16]
benzal chloride	98-87-3	7.41×10^{-3}	1.48×10^{-3}	80	[17]
benzotrichloride	98-07-7	9.81×10^{-4}	3.09×10^{-4}	68	[17]
trichlorophenol 2,4,5	95-95-4	8.71×10^{-6}	1.97×10^{-5}	126	[17]
chlorophenol-2	95-57-8	8.28×10^{-6}	5.70×10^{-7}	93	[17]
o-xylene	95-47-6	4.00×10^{-3}	4.85×10^{-3}	21	[16]
benzo(b)pyridine	91-22-5	2.70×10^{-7}	1.65×10^{-6}	511	[17]
dibutylpthalate	84-74-2	2.81×10^{-7}	1.93×10^{-6}	586	[17]
acenapthene	83-32-9	7.71×10^{-3}	1.46×10^{-4}	98	[17]
ethanoic peroxyacid	79-21-0	1.19×10^{-6}	2.07×10^{-6}	74	[11]
chloroacetic acid	79-11-8	9.09×10^{-9}	7.34×10^{-8}	708	[12]
propanoic acid	79-09-4	1.75×10^{-7}	9.87×10^{-7}	462	[13]
methylbutadiene	78-79-5	3.57×10^{-2}	7.64×10^{-2}	114	[16]
ammonia	7664-41-7	1.64×10^{-5}	6.09×10^{-5}	272	[18]
chloroethane	75-00-3	1.12×10^{-2}	4.76×10^{-4}	96	[19]
methyl mercaptan	74-93-1	5.00×10^{-3}	3.17×10^{-3}	37	[20]
methyl amine	74-89-5	1.11×10^{-5}	4.14×10^{-5}	273	[21]
ethane	74-84-0	4.93×10^{-2}	4.80×10^{-1}	874	[17]
hexachloroethane	67-72-1	4.00×10^{-3}	8.32×10^{-3}	108	[7]
1-butene	106-98-9	4.09×10^{-8}	1.84×10^{-8}	122	[14]

*(atm m^3 mol^{-1})

2. LITERATURE REVIEW

The body of published Henry's constants spanning a range of temperatures and salt concentrations is a subset of the literature since the majority of the published Henry's constants in electrolyte systems are reported at either a single temperature and several salt concentrations [22, 23] or at just a single salt concentration over several temperatures [24, 25]. Other published data span narrow temperature ranges or explore only a range of electrolyte concentrations that is far less than 1 molal [16, 26].

2.1 Literature sources of Henry's constants in ternary systems.

Presently, there are just a few sources of Henry's constants where temperatures higher than 25 ^{o}C and salt concentrations in the molal-range are explored. Table 2 lists the available tabulations of Henry's constants. It should be noted that only 27 of the systems in Table 2 have been studied over a range of both temperature and salt concentration.

Table 2. Literature sources of Henry's constants.

Solute	Salt	T/ K	C_{salt} / mol/kg solvent	Source
benzene	NaCl	298	0.5	[23]
toluene	NaCl	298	0.5	[23]
ethylbenzene	NaCl	298	0.5	[23]
1,2-dimethylbenzene	NaCl	298	0.5	[23]
1,4-dimethylbenzene	NaCl	298	0.5	[23]
n-propylbenzene	NaCl	298	0.5	[23]
isopropylbenzene	NaCl	298	0.5	[23]
1,3,5-trimethylbenzene	NaCl	298	0.5	[23]
2-ethyl-1-methylbenzene	NaCl	298	0.5	[23]
3-ethyl-1-methylbenzene	NaCl	298	0.5	[23]
n-butylbenzene	NaCl	298	0.5	[23]
isobutylbenzene	NaCl	298	0.5	[23]
sec-butylbenzene	NaCl	298	0.5	[23]
t-butylbenzene	NaCl	298	0.5	[23]
1,2-diethylbenzene	NaCl	298	0.5	[23]
1,3-diethylbenzene	NaCl	298	0.5	[23]
1,4-diethlybenzene	NaCl	298	0.5	[23]
hexachlorocyclohexane	seawater	273-318	0.5	[27]
methyl chloride	seawater	273-293	0.5-0.6	[28]
methyl iodide	seawater	273-293	0.5-0.6	[28]
methyl dibromide	seawater	273-293	0.5-0.6	[28]
bromomethyl dichloride	seawater	273-293	0.5-0.6	[28]
methyl tribromide	seawater	273-293	0.5-0.6	[28]
methyl diiodide	seawater	273-293	0.5-0.6	[28]
methyl chloroiodide	seawater	273-293	0.5-0.6	[28]
trichloromethane	briny water	293	0.006-0.01	[24]
methyl dichlorobromide	briny water	293	0.006-0.01	[24]
methyl chlorodibromide	briny water	293	0.006-0.01	[24]
methyl tribromide	briny water	293	0.006-0.01	[24]
benzene	NaCl	298	0-5.0	[29]
toluene	NaCl	298	0-5.0	[29]
ethylbenzene	NaCl	298	0-5.0	[29]
1,2-dimethylbenzene	NaCl	298	0-5.0	[29]
1,3-dimethlybenzene	NaCl	298	0-5.0	[29]
1,4-dimethylbenzene	NaCl	298	0-5.0	[29]
chloroform	seawater	275-298	0-0.6	[16]
tetrachloromethane	seawater	275-298	0-0.6	[16]
1,1-dichloroethane	seawater	275-298	0-0.6	[16]
1,2-dichloroethane	seawater	275-298	0-0.6	[16]
1,1,1-trichloroethane	seawater	275-298	0-0.6	[16]

Table 2. Continued

trichloroethylene	seawater	275-298	0-0.6	[16]
tetrachloroethylene	seawater	275-298	0-0.6	[16]
benzene	seawater	275-298	0-0.6	[16]
toluene	seawater	275-298	0-0.6	[16]
ethylbenzene	seawater	275-298	0-0.6	[16]
o-xylene	seawater	275-298	0-0.6	[16]
m-xylene	seawater	275-298	0-0.6	[16]
p-xylene	seawater	275-298	0-0.6	[16]
Dimethyl sulfide	Na_2SO_4	313-343	0-3.6	[30]
Dimethyl disulfide	Na_2SO_4	313-343	0-3.6	[30]
methanol	Na_2CO_3	313-338	0-1.5	[4]
methanol	Na_2SO_4	313-338	0-0.8	[4]
methanol	NaCl	313-338	0.97-2.71	[4]
methanol	$Na_2S_2O_3$	313-338	0.20-1.50	[4]
methanol	KCl	313-338	0.34-2.72	[4]

2.2 Limiting activity coefficients for water + salt + VOC systems in the literature

The activity coefficient at infinite dilution, $\gamma_i^\infty = \lim_{x_i \to 0} \gamma_i$, is a source for dimensionless Henry's constants since,

$$\gamma_i^\infty = \frac{H_c RT}{v_j^L P_i^{sat}}, \quad (6)$$

where H_c is the dimensionless Henry's constant, v_j^L is the molar volume of the solvent, and P_i^{sat} is the saturated vapor pressure of the solute. If thermodynamic Henry's constants are desired, substitution of Eq. 5 will yield the relationship for conversion,

$$H_{ij} = P_i^{sat} \gamma_i^\infty . \quad (7)$$

The temperature of the system must be below the critical temperature of the VOC for Eq. 7 to be valid since it requires the vapor pressure of the VOC.

A compilation of γ_i^∞ for aqueous electrolyte systems in the literature is given in Table 3. The available data have several limitations including a relatively small database of γ_i^∞ for aqueous systems, a dearth of measurements on aqueous electrolyte solutions, data measured at 298 K and a single salt concentration [31-33], or salt concentration ranges well under 1 molal. Just 5 systems in Table 3 were studied over both a range of temperature and pressure.

Table 3. Literature sources of infinite dilution activity coefficients of aqueous volatile organic and salt solutions.

Solute	Salt	T / K	C_{salt} / mol/kg solvent	Source
chlorobenzene	NaCl	298	0.09-0.8	[34]
1,3-dichlorobenzene	NaCl	298	0.09-0.8	[34]
1,4-dichlorobenzene	NaCl	298	0.09-0.8	[34]
1,2,4-trichlorobenzene	NaCl	298	0.09-0.8	[34]
2,4-dichlorophenol	NaCl	298	0.09-0.8	[34]
2,4,6-trichlorophenol	NaCl	298	0.09-0.8	[34]
chlorobenzene	KCl	298	0.15-0.8	[34]
1,3-dichlorobenzene	KCl	298	0.15-0.8	[34]
1,4-dichlorobenzene	KCl	298	0.15-0.8	[34]
1,2,4-trichlorobenzene	KCl	298	0.15-0.8	[34]
chlorobenzene	Na_2CO_3	298	0.08-0.8	[34]
1,3-dichlorobenzene	Na_2CO_3	298	0.08-0.8	[34]
1,4-dichlorobenzene	Na_2CO_3	298	0.08-0.8	[34]
1,2,4-trichlorobenzene	Na_2CO_3	298	0.08-0.8	[34]
chlorobenzene	K_2SO_4	298	0.09-0.6	[34]
1,3-dichlorobenzene	K_2SO_4	298	0.09-0.6	[34]
1,4-dichlorobenzene	K_2SO_4	298	0.09-0.6	[34]
1,2,4-trichlorobenzene	K_2SO_4	298	0.09-0.6	[34]
chlorobenzene	$CaCl_2$	298	0.14-0.7	[34]
1,3-dichlorobenzene	$CaCl_2$	298	0.14-0.7	[34]
1,4-dichlorobenzene	$CaCl_2$	298	0.14-0.7	[34]
1,2,4-trichlorobenzene	$CaCl_2$	298	0.14-0.7	[34]
chlorobenzene	$(C_2H_5)_4NBr$	298	0.2-1.0	[34]
1,3-dichlorobenzene	$(C_2H_5)_4NBr$	298	0.2-1.0	[34]
1,4-dichlorobenzene	$(C_2H_5)_4NBr$	298	0.2-1.0	[34]
1,2,4-trichlorobenzene	$(C_2H_5)_4NBr$	298	0.2-1.0	[34]
dichloromethane	NaCl	283-313	0-2.5	[35]
chloroform	NaCl	283-313	0-2.5	[35]
1,2-dichloroethane	NaCl	283-313	0-2.5	[35]
trichloroethylene	NaCl	283-313	0-2.5	[35]
benzene	NaCl	283-313	0-2.5	[35]

2.3 Vapor liquid equilibrium data.

Henry's constants may also be obtained from vapor-liquid equilibrium (VLE) data and several data sources of VLE data are available for 1-alkanols including methanol, ethanol, 1-propanol, 2-propanol, allyl alcohol, and benzene with inorganic salts. A summary of temperature and salt concentration ranges for several salts is provided in Table 4. Just 2 of these systems were determined over a range of temperatures and salt concentrations. Larger compilations have been published by Furter [36, 37] and for some 100 aqueous systems by Ohe [38]. However, the majority of the data was collected at a single temperature and ambient pressure.

Infinite dilution activity coefficient can be determined by the extrapolation of VLE data to zero concentration [39]. The extrapolation of VLE data with the Wilson equation [40] is generally satisfactory for binary systems where γ_i^∞ is under 10. With water as the solvent, however, γ_i^∞ is on the order of 100 to several thousand for toluene, ethylbenzene, xylene or trichloroethylene that pollute many underground aquifers. Thus the extrapolation method cannot be used on most systems of environmental relevance.

The model of Sun et al. [41] may also be used for extrapolation, but is still very susceptible to error in the VLE data. It yields an average error of 20 % for Henry's constants obtained from extrapolated VLE data.

Table 4. Literature sources of VLE data of VOCs in aqueous salt solutions.

Solute	Salt	T / K	P / atm	Salt Conc. / molal	Source
methanol	NaCl	298	1	0-4	[42]
methanol	KCl	298	1	0-1.5	[42]
methanol	NaBr	298	1	0-4	[42]
methanol	$CaCl_2$	298	1	0-1.4	[43]
ethanol	NaCl	343	1	0-2.3	[44]
ethanol	$CaCl_2$	343	1	0-2.3	[44]
ethanol	NH_4Cl	343	1	0-2.3	[44]
ethanol	SrCl	343	1	0-1.3	[45]
ethanol	$CaCl_2$	298	1	0-1.4	[43]
1-propanol	NaCl	333	1	0.2-6	[46]
1-propanol	$CaCl_2$	333	1	0.5	[46]
1-propanol	NH_4Cl	333	1	0.5	[46]
1-propanol	$CaCl_2$	298	1	0-1.4	[43]
2-propanol	LiCl	348	1	0-6	[47]
2-propanol	LiBr	348	1	0-6	[47]
2-propanol	$CaCl_2$	348	1	0-4	[47]
2-propanol	NaCl	348	1	0-5	[48]
2-propanol	$CaCl_2$	348	1	0-3	[48]
2-propanol	$(C_3H_7)_4NBr$	369-356	1	1-3	[49]
2-propanol	$MgBr_2$	358-353	1	3-18	[50]
allyl alcohol	$CaCl_2$	298	1	0-1.4	[43]
benzene	ZnCl	363	1	0-3	[48]
benzene	$CaCl_2$	363	1	0-3	[48]
benzene	NaCl	363	1	0-5	[48]

2.4 Measurement Methods.

2.4.1 Determining infinite dilution activity coefficients in water + salt + VOC systems at ambient pressure.

Differential ebulliometry [51-54] can be used to determine γ_i^∞ by measuring the difference in the boiling temperature between several solutions containing a single solute at different concentrations and a set pressure. This method works well with systems having a relative volatility of between 0.3 and 20 according to Sherman et al. [55]. However, most organic solutes of interest for environmental impact and remediation have relative volatilities in water far exceeding the optimal range for this method.

A dew point sensor was employed by Trampe and Eckert [56] to obtain γ_i^∞ for binary mixtures of volatile organic solutes in water. This technique is limited to even lower limiting relative volatilities between 0.01 and 0.40 [55], preventing its use on most VOC-water systems of environmental interest.

In gas liquid or dynamic chromatography [57, 58] γ_i^∞ is calculated by measuring the retention time of a volatile solute in a capillary column that is coated with a given solvent. An inert carrier gas such as helium is used to flush the solute as a vapor through the column. This method is ideal for highly volatile substances that dissolve in the stationary phase. However, this method will not be at all practical for solvents containing dissolved salts since the salt may crystallize in portions of the capillary. Also, changing the salt concentration would require fabrication of separate capillary tubes.

Inert gas stripping [59-62] has proven to be a useful technique for dilute solutions of water and a highly volatile solute. This technique employs a stream of inert gas at constant temperature bubbling through a dilute solution that contains the VOC. A gas

chromatograph monitors the offgas from the liquid and γ_i^∞ is determined from the decay curve that results as the VOC is stripped from the solvent. Measurement of γ_i^∞ on the order 1000 has been reported [55]. This technique is suitable for salt solutions since the analysis is primarily on the vapor phase. However, inert gas stripping would not be suitable for several important VOCs such as methanol, 2-propanone, and 2-butanone since their γ_i^∞ values are well below 1000.

A differential static cell has been employed to create another simple technique appropriate for high relative volatility systems. Wright et al. [63] determined γ_i^∞ by the pressure difference between the pure solvent and the volatile solute at the same temperature. As with gas stripping, solutes such as methanol, 2-propanone, and 2-butanone in water are well below the sensitivity threshold for this method.

Inverse solubility [64, 65] is one of the oldest techniques for measuring γ_i^∞ in a particular solute. If the solute is sparingly soluble so that it forms a saturated solution in the dilute regime, γ_i^∞ is equal to the inverse mole fraction of the solute. In a saturated solution, the partial pressure of the VOC is equal to its vapor pressure in the saturated solution. Thus at moderate pressure we obtain,

$$\gamma_i^\infty = \frac{y_i P}{x_i P_i^{sat}} = \frac{P_i^{sat}}{x_i P_i^{sat}} = \frac{1}{x_i}, \qquad (8)$$

where P_i^{sat} saturated vapor pressure of the solute, y_i is its vapor phase mole fraction, and x_i is its liquid phase mole fraction.

Headspace gas chromatography (HSGC) overcomes many of the limitations of the aforementioned methods including the need to know the concentration of solute in the

liquid phase, restriction to either low or high γ_i^∞, laborious sample preparation, and long wait time per data point. Since its introduction by Hussam and Carr [66], the method has been used for measuring Henry's constants of methanol in water by Chai and Zhu [1, 67]. The values of γ_i^∞ are well below 10 for methanol representing the low end of environmentally significant compounds. Shortly after the work of Chai and Zhu, Brendel and Sandler [68] reported γ_i^∞ of chlorinated organic compounds and benzene from 10 to 40 ^oC in pure water and with 0.2 to 2.5 molal NaCl. The highest γ_i^∞ measured with HSGC was nearly 10,000.

The HSGC method generally employs several vials filled with solutions of interest. Different HGSC methods differ in the number of vials used and in the range of γ_i^∞ values that they can measure with precision. The details of several methods will be discussed in later sections. In all methods, the vials are brought to equilibrium at the desired temperature, and the concentration of volatile solute in the vapor space is measured by gas chromatography. After the concentration of solute in the headspace of all vials has been determined, γ_i^∞ or the Henry's constant can be computed.

2.4.2 Determining Henry's constants at ambient pressure

Henry's constants of a VOC in a solution of interest below the boiling temperature of the solvent at ambient pressure can be determined by analyzing the concentration of the volatile solute in the liquid and vapor phases in an equilibrium cell. The presence of non-volatile electrolytes, however, reduces the number of experimental techniques available for direct liquid-phase composition measurement to ultraviolet spectroscopy. On the other hand, several headspace gas chromatography (HSGC) methods can be used to determine the vapor phase concentration. Some of these techniques are reviewed in the following section.

2.4.2.1 *Purge and trap*

Dacey et al. [26] measured Henry's constants for dimethyl sulfide (DMS) by bubbling a stream of helium containing DMS vapor through either pure water, or water containing salts. Both liquid and vapor phases were analyzed. A 6 ml sample of the exiting DMS-laden carrier gas was obtained from the top of the bubble column and subsequently analyzed by direct injection into a GC. A 1 ml liquid sample was withdrawn from the bottom of the bubble column and sparged with pure helium to strip out all DMS. The stripped DMS was captured in a cryogenic trap and subsequently flushed into a GC with helium to determine the liquid phase DMS concentration. Dacey et al. claimed that the standard error in their Henry's constants ranged from 1 to 4 %. However, to consistently attain this low experimental error, precise control is needed to strip and collect the DMS from each liquid sample. Also, their apparatus required great skill to operate. Finally, measurement of Henry's constants of more than one system is laborious

since a single bubble column is used in all experiments and therefore must be cleaned and refilled with salt solution for each run.

2.4.2.2 *Sealed vial methods*

Sealed vial methods are a class of methods using a closed system that is at thermodynamic equilibrium. Either the vapor phase or the liquid phase can be sampled. However, the presence of a non-volatile electrolyte prevents the analysis of the liquid phase with gas chromatography, which provides the highest sensitivity for the dilute concentrations of dissolved organics.

When a non-volatile electrolyte is present in the liquid phase, UV spectroscopy is the most straightforward technique to implement for sparingly soluble solutes such as aromatics. With the proper sealed vial, spectroscopy can be performed directly through the walls of the vial. In a recent study of Setchenov constants, Xie et al. [69] first calibrated their temperature-controlled UV spectrophotometer with solutions containing known VOC concentrations, and then allowed sealed vials with increasing amounts of salt to attain equilibrium in order to determine the liquid phase VOC concentration. In the concentration range of Beer's law, the UV absorbance of a liquid sample is given by:

$$\log(A_o/A) = \log(S_o/S) = k_S x_s \qquad (9)$$

where A_o is the absorbance of the sample without salt, A is the absorbance of the sample of interest with electrolyte, S_o is the solubility of the nonelectrolyte in pure water, and S is its solubility in the sample containing electrolyte. The electrolyte concentration in moles / kg solvent is represented by x_s.

UV spectroscopy allows the direct analysis of the liquid phase VOC concentration that is much higher than the vapor phase VOC concentration in pure water. However,

only one nonelectrolyte can be studied at a time. The method is several orders of magnitude less sensitive than gas chromatography and is therefore not capable of resolving small changes in the concentration. The lower sensitivity and small changes in liquid-phase nonelectrolyte concentration makes UV spectrophotometry a poor option for many low-volatility VOCs that are of interest to environmental modelers and process designers.

Headspace gas chromatography (HSGC) can rapidly determine Henry's constants of several VOCs simultaneously. Although the headspace VOC concentration is much lower than the liquid phase concentration, precision can be maintained since the GC detector is several orders of magnitude more sensitive than a UV spectrophotometer.

HSGC methods that require one or no calibrations have been proposed by Kolb et al. [70], as well as by McAullife [71] and others [67, 72, 73]. Analysis of the headspace vapor was accomplished with either a stepwise extraction [71] or a vapor-phase calibration [70]. Ettre et al. [74] proposed an indirect method [71] termed phase ratio variation (PRV) that requires no calibration and uses several samples with different liquid volumes. The PRV method requires the analysis of headspaces in two vials with different vapor-to-liquid volume ratios. Additional vials with different vapor-to-liquid volumes may also be used to improve precision, check detector linearity and gauge method performance. The method is not suitable, however, for systems in which dimensionless Henry's constants are smaller than 0.007 [75].

The lower limit of the PRV method prevents its use for determining Henry's constants of less volatile nonelectrolytes such as methanol. To remedy this shortcoming, Chai and Zhu [1, 67] developed an indirect headspace method called the differential

method that requires no calibration and uses two vials with different volumes of the same solution. The headspace in each vial is analyzed, and the Henry's constant is determined directly from these analyses via mass balances. The liquid volumes of the two vials must be chosen carefully to minimize experimental error. Chai and Zhu's differential method is a PRV method that is similar, in principle, to the Equilibrium Partitioning in Closed Systems (EPICS) method developed by Lincoff and Gossett [19, 76]. Chai and Zhu demonstrated the capability of their method by determining Henry's constants of methanol and other n-alkanols in water, salt solutions, and industrial process liquors [4, 6, 77].

Several setups are available for acquiring a sample of the vapor space in a closed vial at ambient pressure. The most direct of these withdraws a fraction of the headspace after the contents attain thermodynamic equilibrium. Commercial headspace samplers perform the equilibration, sampling and injection into a GC with precise timing to yield Henry's constants of high accuracy and ± 4 to 10 % relative error. This method is the easiest to implement due to complete automation.

The VOC can also be extracted from the headspace using a solid phase microextraction (SPME) technique. A polymer phase is coated onto a glass filament that is housed in a syringe, which allows the investigator to handle the extremely delicate fiber. Common solid-phase coatings consist of polydimethylsiloxane and polyacrylate [78]. The investigator can implement SPME manually to keep the equipment cost low. However, automation will greatly increase the experimental precision since it is governed by the fiber exposure time in the headspace [78, 79].

Nazarenko [80] proposed a liquid phase microextraction (LPME) method as a simple, lower-cost alternative to SPME. A drop of distilled water was used in place of a polymer-coated fiber to capture a VOC sample. In his LPME technique, a 10 μL syringe containing water was pierced through a polymer septum. A drop of water was produced at the tip of the syringe by depressing the plunger slightly. The drop was exposed to the headspace vapor for a given period of time to capture a sample of the VOC. When the adsorption stage was complete, the water drop was retracted and the needle was pulled away from the septum. The water in the syringe was immediately injected into a gas chromatograph.

2.4.3 Determining Henry's constants at high pressures.

Gas solubility at high pressure is often measured by sampling of the saturated liquid phase. O'Sullivan and Smith [81] performed solubility measurements on methane between 100 and 600 atmospheres and between 324.65 and 398.15 K by bringing water and methane to equilibrium in a 1-gallon stainless steel autoclave and rocking the autoclave for 2 – 48 hours. The liquid phase was sampled by slowly withdrawing a 10 cm^3 volume and allowing the methane to flash from the solution. Once at equilibrium, replicate samples could be taken 3 to 4 hours later.

Gas solubilities at pressures between 136 - 1500 atmospheres, temperatures from 373.15 – 513.15 K, and sodium chloride concentrations from 5 - 15 weight percent were measured by Price and coworkers [82] using a stainless steel pressure vessel containing a Teflon vessel that was pressure balanced by distilled water outside. A lengthy equilibration time of up to two days was required and replicate samples were taken 3 to 4 hours after equilibrium was attained.

2.5 Modeling the solubility of nonelectrolytes in aqueous systems

2.5.1 Correlating Henry's constants in water-VOC systems

Few models for the temperature behavior of Henry's constants of nonelectrolytes in electrolyte solutions are available. The familiar van't Hoff equation has been used in several studies [6-8, 30] to correlate Henry's constants in both pure solvent and with an electrolyte. However, the van't Hoff equation

$$\ln(H) = a - b/T \qquad (10)$$

is a poor choice for correlating data over wide temperature ranges because the natural log of the Henry's constants actually follows a nonlinear trend as temperature rises. The constant *a* in Eq. 10 is often called the van't Hoff entropy of solution and *b* the van't Hoff enthalpy of solution for the volatile solute.

The simplest correlation for Henry's constants over greater than a 50 K span is a polynomial expansion in inverse temperature:

$$ln(H) = A_0 + A_1/T + A_2/T^2 + A_3/T^3 \qquad (11)$$

This relationship contains enough parameters to correlate Henry's constants over a wide temperature range, although extrapolation is only successful over approximately 50 K as shown in Figure 2.

Clarke and Glew [83] replaced the last two terms of Eq. 11 with a logarithmic and linear term to better extrapolate to higher temperatures.

$$ln(H) = A_0 + A_1/T + A_2\, ln\, T + A_3 T \qquad (12)$$

While the extrapolations with this model were better than the simple polynomial expansion in Eq. 11 there is still room for improvement as shown in Figure 2.

Alvarez et al. [84] replaced the 4th term of Eq. 11 with a term that was designed to diverge as the critical point of the solvent is approached so as to more closely match the behavior of Henry's constants near the critical point of the solvent.

$$ln(H) = A_0 + A_1/T + A_2/T^2 + B_0\left[\left(T_{c,1} - T\right)/T\right] ln\left[\left(T_{c,1} - T\right)/T_{c,1}\right] \quad (13)$$

This model allows for better extrapolation of data to high temperatures because of its asymptotic behavior as $T_{c,1}$ is approached.

Fernandez-Prini and Crovetto [85] have set B_0 to –1 in the above expression in order to reduce the number of adjustable parameters

$$ln(H) = A_0 + A_1/T + A_2/T^2 + A_3/T^3 - \left[\left(T_{c,1} - T\right)/T\right] ln\left[\left(T_{c,1} - T\right)/T_{c,1}\right], \quad (14)$$

but extrapolations in temperature diverged quickly as shown in Figure 2.

Krause and Benson [86] developed a correlation that improved on the performance of Eqs. 11 through 14 with just three adjustable parameters.

$$T^{*2}\, ln\, H = T^{*2} A_0 + A_1\left(1 - T^*\right)^{1/3} + A_2\left(1 - T^*\right)^{2/3} \quad (15)$$

The exponent of the third term is extremely close to the exponent predicted by dilute solution theory, so that Eq. 15 displays the best extrapolation capabilities to this point. This is despite the fact that the relationship is empirical and the parameters are not related to any independently measurable thermodynamic quantities [86].

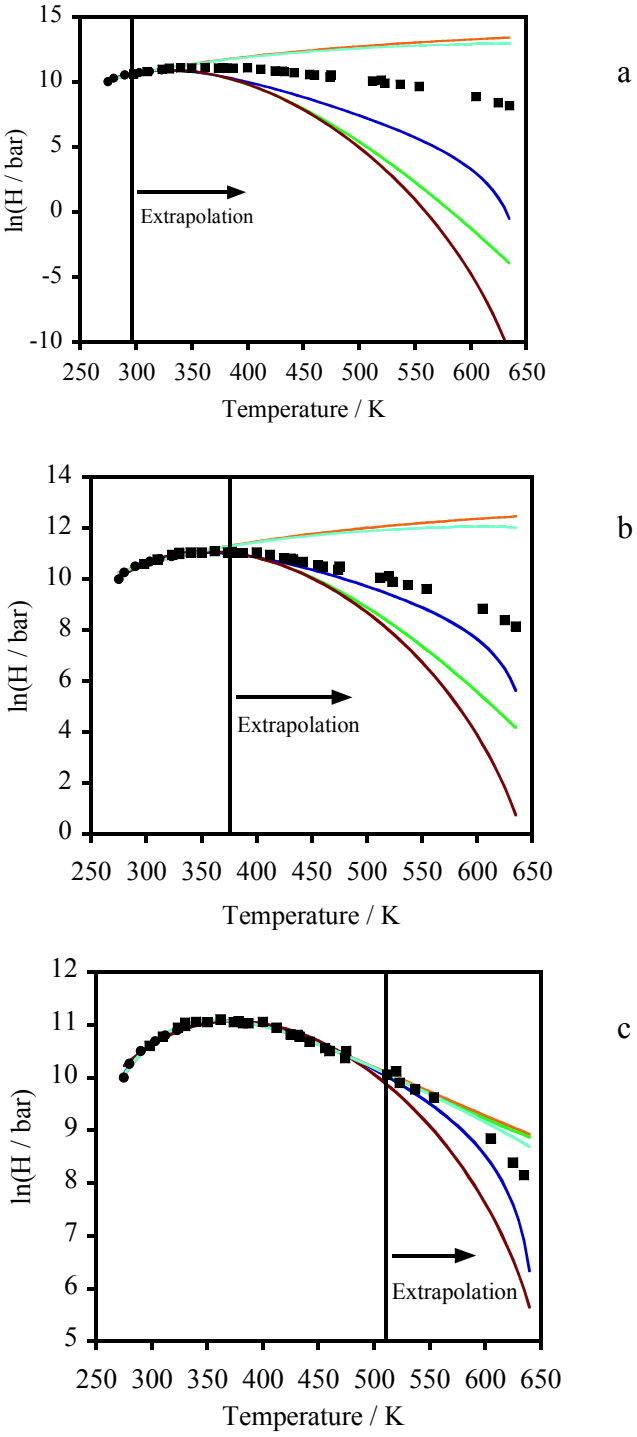

Figure 2. Henry's constants of methane gas in pure water (●) IUPAC [87] and (■) Fernandez-Prini et al. [85] extrapolated after (a) 298, (b) 373, and (c) 512 K with models: (—) polynomial expansion in temperature, (—) Fernandez-Prini et al. [85], (—) Krause and Benson [86], (—) Clarke and Glew [83], (—) Alvarez et al. [84].

2.5.2 Modeling Setchenov constants.

Setchenov studied the solubility of carbon dioxide in blood and other electrolyte solutions over one hundred years ago and proposed the equation that bears his name [88]:

$$ln\frac{x_i^0}{x_i} = k_s \cdot x_s, \qquad (16)$$

where x_i^0 is the mole fraction of the volatile solute in electrolyte-free water, x_i is its mole fraction in water containing electrolyte, x_s is the mole fraction of the electrolyte, and k_s is the Setchenov constant. This relationship can be derived by equating chemical potentials for a salt containing VOC solution and a salt free VOC solution with a common headspace as shown in Figure 3. Thus:

$$\mu_i^G = \mu_i^{0'} + RT\,ln\left(m_i^{'}\right) = \mu_i^{0''} + RT\,ln\left(m_i^{''}\right) \qquad (17)$$

where $\mu_i^{0'}$ and $\mu_i^{0''}$ are reference state chemical potentials with and without electrolyte respectively, μ_i^G is the VOC chemical potential in the gas phase, and m is the liquid phase VOC concentration. If Eq. 17 is rearranged so that the reference state fugacities are on one side of the expression, the difference in reference state chemical potentials can be expressed as a power series,

$$RT\,ln\left(\frac{x_i^{'}}{x_i^{''}}\right) = \mu_i^{0''} - \mu_i^{0'} = RT\,ln\left(k_s x_s\right) + \cdots, \qquad (18)$$

where k_s is Setchenov's constant and x_s is the salt concentration. Substituting the definition of the Henry's constant for moderate pressures ($p_i = H_{ij} \cdot x_i$) in Eq. 18 yields the following [89]:

$$ln\frac{H_i^{''}}{H_i^{'}} = k_s \cdot x_s \ , \qquad (19)$$

where $H_i^{''}$ and $H_i^{'}$ are Henry's constants for the nonelectrolyte in aqueous solution with and without an electrolyte.

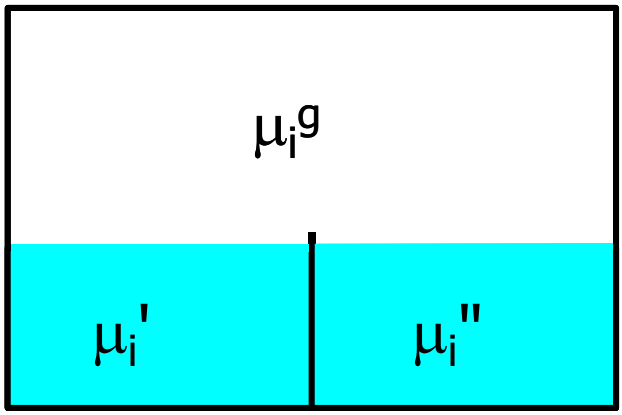

Figure 3. Common headspace method for Setchenov relationship at constant temperature and pressure.

2.5.2.1 *Electrostatic models for predicting the Setchenov constant*

Several theories have been developed to estimate the Setchenov constant for an electrolyte-nonelectrolyte pair by treating the solvent as a continuum with a uniform dielectric constant and using physical data for pure substances. Debye and McAulay [90] assumed that the salt effect on a nonelectrolyte arises from Columbic forces and proposed the following relationship:

$$k_s = \frac{\beta \cdot e^2 \cdot N_0}{4.606 \times 10^3 \cdot k \cdot T \cdot D_0} \cdot \sum_j \frac{v_j \cdot z_j^2}{r_j}, \qquad (20)$$

where e is the electronic charge, N_0 is Avogadro's number, D_0 is the dielectric constant of water, k is the Boltzmann constant, T is the absolute temperature, r_j is the radius of ion j, v_j is the number of ions of type j with a valence z_j. The factor β is defined according to Saylor's method [91] as:

$$\beta = \frac{(D_0 - D) \cdot V_n}{D_0}, \qquad (21)$$

where D is the dielectric constant of the nonelectrolyte and V_n is its molar volume. However, the model grossly over-predicts k_s for VOCs in the presence of anions that are larger than bromine [92].

McDevit and Long [22] proposed a model based on the assumption that compression of the solvent occurs due to the presence of ions. This results in a higher internal pressure and reduces the available space for the nonelectrolyte, pushing it out of the liquid phase. Kirkwood's method was employed to calculate the electrostatic energy between an ion and a neutral molecule so that the following expression results for the Setchenov constant:

$$k_s = \frac{V_n^0\left(V_s - V_s^0\right)}{2.303 \cdot R \cdot T \cdot \beta_0} \cdot \frac{a}{a+b} \quad , \qquad (22)$$

where V_n^0 and V_s^0 are the partial molar volumes of the nonelectrolyte and the salt at infinite dilution, V_s is the molar volume of the salt in the molten state, β_0 is the compressibility of pure water, the constant a is the average radius of the cation and anion, and b is the radius of the nonelectrolyte. Bockris et al. [93] modified McDevit and Long's model with a term whose sign depends on the relative polarizabilities of the organic solute and water [92]. Their model has proved useful for predicting trends in salt effects related to ions of different size. However, the parameters to calculate the Setchenov constant are not available for many systems [92]. Xie et al. [69] introduced an additional improvement using Latimer's radii (r_L) to replace the ionic radii from crystal structure. Latimer's radii are based on the Pauling radii (r_P) as follows $r_L^+ = r_P^+ + 0.85$ Å and $r_L^- = r_P^- + 0.10$ Å. Latimer's radii for the cation and anion are averaged for use in Eq. 22 so that $a = (r_L^+ + r_L^-) / 2$ and the radius of the nonelectrolyte molecule is:

$$b = \left(\frac{3 \cdot 0.7402 \cdot V_n}{4 \cdot \pi \cdot N_0} \right)^{1/3} \quad , \qquad (23)$$

where N_0 is Avogadro's number. This yields a marginal improvement in performance.

Scaled particle theory has been used to predict Setchenov constants in several studies [94, 95]. Pierotti [96, 97] adapted the Reiss [98, 99] scaled particle theory to nonelectrolytes in pure water, by expressing the solubility in terms of two free energy terms: the work required to create a cavity that is large enough to accommodate the nonelectrolyte molecule, and the energy of interaction between the nonelectrolyte and the surrounding solvent. Shoor and Gubbins [100] extended the model to the solubility of a nonelectrolyte in an aqueous salt solution; and Masterton and Lee [92] extended this

further to create a generalized expression for Setchenov constants for electrolyte-nonelectrolyte pairs. The expression for the solubility is

$$-\log S = \frac{g_1^h}{2.3 \cdot k \cdot T} + \frac{g_1^s}{2.3 \cdot k \cdot T} + \log(k \cdot T) \cdot \sum_{j=i}^{4} \rho_j \,, \qquad (24)$$

where g_1^h is the free energy change when a cavity large enough to hold the nonelectrolyte is formed, and g_1^s is the free energy change when the nonelectrolyte is introduced into the cavity. The third term is a standard state correction that is only used if the concentrations are not in terms of molarity. To arrive at the Setchenov constant, Eq. 24 is differentiated with respect to salt concentration c as follows:

$$k_s = \left[\frac{d\left(g_1^h / 2.3 \cdot k \cdot T\right)}{d(c)}\right]_{c \to 0} + \left[\frac{d\left(g_1^s / 2.3 \cdot k \cdot T\right)}{d(c)}\right]_{c \to 0} + \left[\frac{d\left(\log \sum \rho_j\right)}{d(c)}\right]_{c \to 0} \qquad (25)$$

Each term requires the diameters of the nonelectrolyte and the salt ions, the polarizability of the salt and its apparent molal volume at infinite dilution. The weakness of scaled particle theory is that it is sensitive to the ionic radii, which are seldom known to any significant accuracy [92]. Masterton and Lee [101] performed a sensitivity analysis to demonstrate the effect of variation in several key physical parameters in their scaled particle theory for several nonelectrolyte-electrolyte pairs. This variation is shown in Table 5 where it can be seen that sensitivity to small variations in the ionic radius clearly results in large variation in the Setchenov constant. The sensitivity in k_s is nearly as large as the Setchenov constant shown below in Table 6.

Agreement between experimental Setchenov constants and those predicted with scaled particle theory can be improved by modifying the interaction energy parameter for salt ions. Masterton and Lee showed that increasing the diameter of the iodide ion by 0.1 Å leads to predicted Setchenov constants that are within a few percent of experimental

values. However, Setchenov constants for benzene in aqueous solutions with small and large salt ions were in poor agreement with predictions for salts such as cesium chloride and rubidium chloride [92]. It should be mentioned that the model of Masterton and Lee [92] is only appropriate for non-polar nonelectrolytes and must be modified for polar nonelectrolytes as shown by Xie and Yang [102]. However, the complexity of the model increases considerably in that case.

Table 5. Sensitivity of k_s to 5 % variations in interaction energy (ε_1), nonelectrolyte diameter (σ_1), cation (σ_3) and anion (σ_4) diameters for scaled particle theory [92].

System	$\Delta\varepsilon_1 / \varepsilon_1$	$\Delta\sigma_1 / \sigma_1$	$\Delta\sigma_3 / \sigma_3$	$\Delta\sigma_4 / \sigma_4$
H_2 - NaCl	-0.001	0.008	0.005	0.022
H_2 - KI	-0.001	0.006	0.011	0.035
CH_4 - NaCl	-0.002	0.010	0.010	0.039
CH_4 - KI	-0.003	0.006	0.020	0.062
SF_6 - NaCl	-0.005	0.015	0.022	0.078
SF_6 - KI	-0.006	0.009	0.042	0.123

Table 6. Comparison of Setchenov constants calculated from scaled particle theory (a) [92] and McDevit-Long theory (b) [22] for nonelectrolytes with NaCl and KI.

nonelectrolyte	NaCl			KI		
	observed	a	b	observed	a	b
He	0.081[c]	0.102	0.151	0.083[c]	0.076	0.070
Ne	0.097[c]	0.100	0.080	0.080[c]	0.067	0.037
Ar	0.133[c]	0.117	0.132	0.108[c]	0.067	0.061
Kr	0.146[c]	0.114	0.160	0.120[c]	0.060	0.074
H_2	0.114[d]	0.111	0.123	0.081[e]	0.080	0.057
O_2	0.141[d]	0.129	0.146	…	0.082	0.068
N_2	0.121[e]	0.137	0.188	0.100[e]	0.085	0.087
CH_4	0.127[e]	0.131	0.184	0.097[e]	0.076	0.086
C_2H_4	0.127[e]	0.132	0.236	0.061[e]	0.065	0.109
C_2H_6	0.162[e]	0.134	0.260	0.101[e]	0.062	0.120
SF_6	0.195[e]	0.202	0.358	0.145[c]	0.113	0.166

[c]Morrison and Johnstone [103]; [d]Long and McDevit [104]; [e]Morrison and Billett [105]

Tiepel and Gubbins [106] employed perturbation theory to calculate Setchenov constants from equilibrium data on binary systems: gas in pure water and salt in pure water. Their model couples the more plentiful water-VOC data with more available electrolyte-water data to predict the Setchenov constant of a VOC in a ternary system. Their expression for k_s is:

$$k_s = a_s + b_s \times (\varepsilon/k)_{gas} \quad , \qquad (26)$$

where ε is the Lennard-Jones energy parameter for the gas and k is Boltzmann's constant. The parameters a_s and b_s are temperature dependant. They also extended Eq. 26 to correlate the temperature dependence of Setchenov constants as follows:

$$k_s = a_{is} + a_{2s}T + (b_{1s} + b_{2s}T) \times (\varepsilon/k)_{gas} \quad , \qquad (27)$$

In Eq. 27, the parameters a_{is}, a_{2s}, b_{1s}, and b_{2s} are specific to the salt and must be estimated from the Setchenov constants for individual ions.

Xie et al. [107] attempted to develop an empirical linear correlation between the Setchenov constants and the molar volume of the nonelectrolyte estimated at its normal boiling point using the group contribution method of Le Bas [108]. The correlation was of the type ($k_s = \phi \cdot V_{Le\ Bas}$) with $\phi = 0.0018 \pm 0.0005$. Where, $V_{Le\ Bas}$ is the molar volume of the solute at its normal boiling point that was estimated by the method of Le Bas [108]. However, the fit is poor for most compounds, as shown in Figure 4.

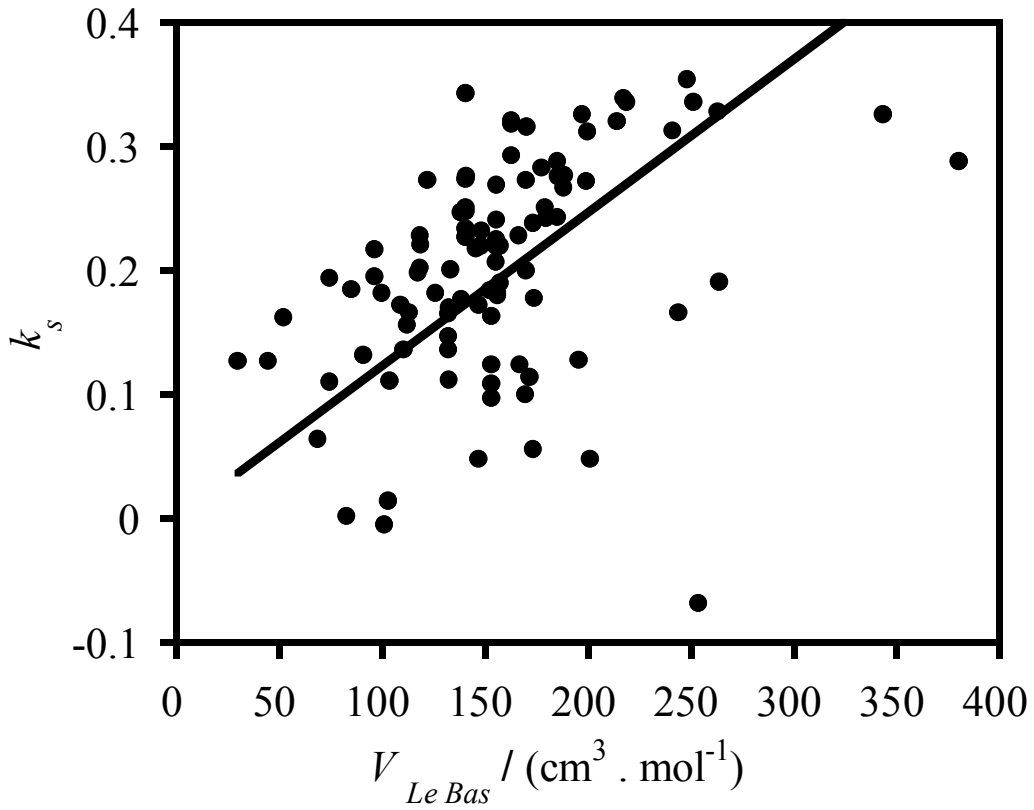

Figure 4. Setchenov constants 25 ^{o}C for organic solutes in aqueous sodium chloride as a function of the molar volume of the organic solute from Xie et al. [107] (R^2 = 0.0363).

An obvious problem with the method of Le Bas is that isomers are assigned identical molar volumes because they have the same number and type of residues. Thus, the Le Bas molar volume represents a low-resolution scale for correlating Setchenov constants. The clearest trends in k_s as a function of Le Bas molar volume can be seen within a homologous series of alkanes or organic acids in Figure 5.

Ni et al. [109, 110] developed another simple linear relationship between k_s and the logarithm of the octanol water partition coefficient (K_{ow}). Octanol water partition coefficients provide a direct measure of the polarity of a particular solute [111]. Since adding an electrolyte creates spheres of ordered water molecules around each ion, the organic nonelectrolyte has less available space to reside in the liquid phase and fewer water molecules to interact with, forcing the VOC to exit to the vapor phase. Eq. 28 was obtained by regressing 62 experimentally measured Setchenov constants and their corresponding log K_{ow} values from ClogP® software, which makes use of the Quantitative Structure Activity Relationships (QSAR) to determine the log K_{ow} [112]

$$k_s = 0.040\, log\, K_{ow} + 0.114\,. \qquad (28)$$

This correlation is somewhat better than the correlation of Xie et al. [107] and k_s for alkanes, organic acids and chlorinated benzenes exhibit regular behavior as shown by the closed points in Figure 6.

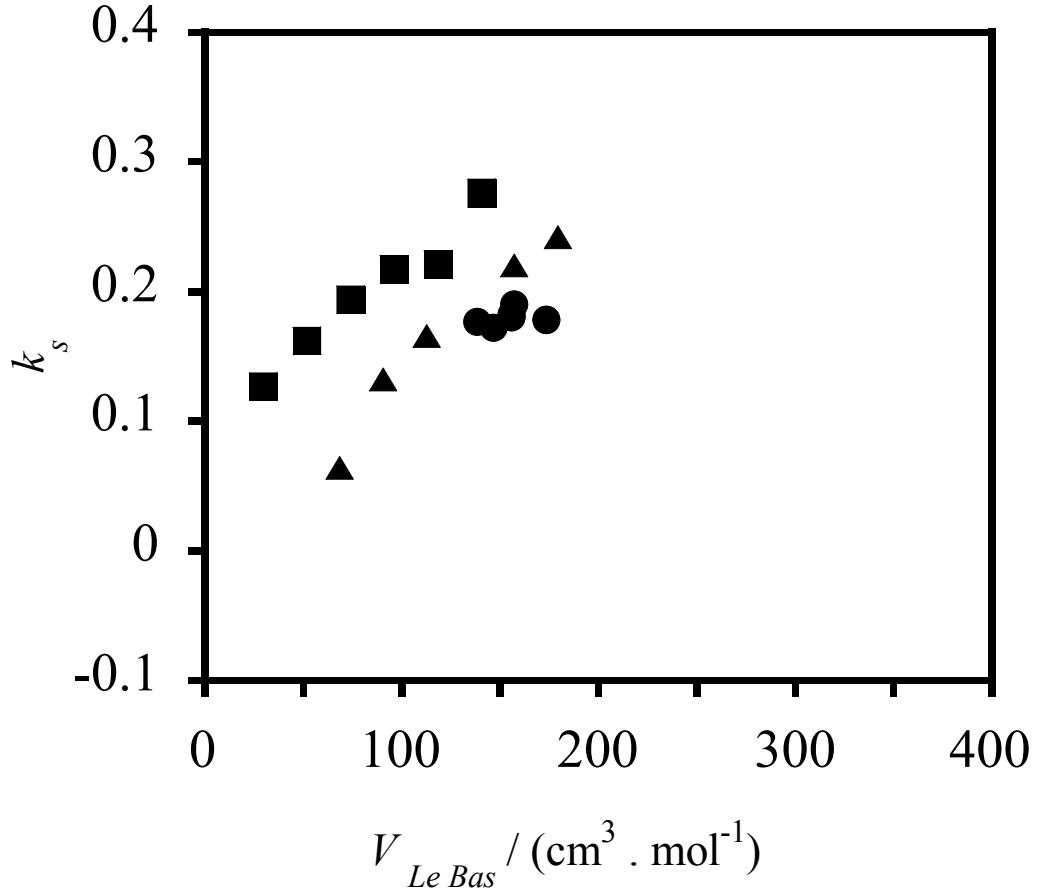

Figure 5. Setchenov constants for n-alkanes (■) [113], aliphatic organic acids (▲) [114], and aromatic organic acids (●) [113] in aqueous NaCl solution at 25 ^{o}C.

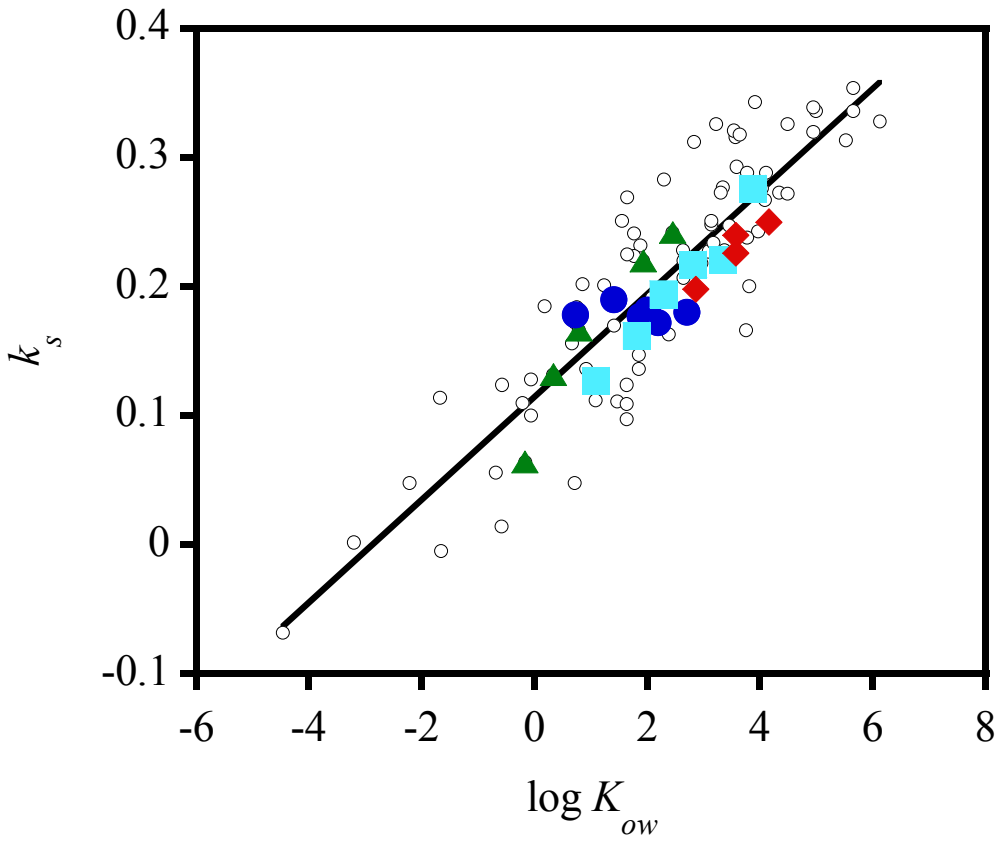

Figure 6. Setchenov constants for alkanes (■) [113], chlorinated aromatics (◆) [34, 113], aliphatic organic acids (▲) [114], aromatic organic acids (●) [113], and other organic solutes (○) [34, 101, 113, 115] in aqueous NaCl solution at 25 ^{o}C (R^2 = 0.7717).

2.5.2.2 *Group contribution model for predicting Setchenov constants.*

Schumpe [116] introduced model based on the work of van Krevlen and Hoftijzer [117] who first suggested that the Setchenov constant be described in terms of two ion specific parameters and a gas specific parameter. The Setchenov relationship was then written as:

$$log\left(c_{G,0}/c_G\right)=\left(h_+^{'}+h_-^{'}+h_G^{'}\right)I\,, \qquad (29)$$

where $h_+^{'}$ and $h_-^{'}$ are specific to the cation and anion respectively and were considered temperature independent. The gas specific constant h_G' was tabulated at discrete temperatures. To extend the model of van Krevlen and Hoftijzer to mixtures of salts, Danckwerts [118] and Onda et al. [119] were able to correlate experimental Setchenov constants at a single temperature by simply summing the salt effects of each salt

$$log\left(c_{G,0}/c_G\right)=\sum\left(h_+^{'}+h_-^{'}+h_G^{'}\right)_j I_j\,, \qquad (30)$$

In both Eqs. 29 and 30 the use of total ionic strength makes the equations skewed by the charge on the cation which has a lesser effect on the Setchenov constant than the anion. The effect of cations and anions on the salt effect was described in terms of individual salt effect parameters, J_i, for each salt ion and multiplied by its respective ionic strength I_i.

$$log\left(c_{G,0}/c_G\right)=\sum J_i I_i \qquad (31)$$

where I_i is the molal ionic strength contribution of ion I that is defined as

$$I_i=\frac{1}{2}\sum m_i z_i^2\,, \qquad (32)$$

and m_i is the concentration of ion i, and z is the valence of the ion.

Schumpe decomposed the salt effect into a salt specific coefficient and a gas specific coefficient to better match experimentally observed salt effects.

$$log\left(c_{G,0}/c_G\right)=\left(H_s+H_G\right)c_s \quad (33)$$

The salt parameter, H_s, consists of a sum of the salt effects for each ion

$$H_s=0.5\sum H_i n_i z_i^2\,, \quad (34)$$

where n_i is the index of the ion in the formula of the salt and can be defined as the concentration of the ion, c_i, over the concentration of the salt, c_s

$$n_i=c_i/c_s \quad (35)$$

Eq. 34 can be simplified by combining all constants including the ion valence, z_i, into a modified salt specific parameter, h_i,

$$H_s=\sum h_i n_i\,. \quad (36)$$

Likewise, the gas specific parameter, H_G, was comprised of a modified gas-specific parameter multiplied by the ion index, n_i

$$H_G=\sum h_G n_i \quad (37)$$

When Eqs. 36 and 37 are substituted into Eq. 33 the following relationship results

$$log\left(c_{G,0}/c_G\right)=\left(\sum h_i n_i+\sum h_G n_i\right)c_s\,, \quad (38)$$

Eq. 35 can be used to simplify Eq. 38 and yield the following expression

$$log\left(c_{G,0}/c_G\right)=\sum\left(h_i c_i+h_G c_i\right) \quad (39)$$

Extensive sets of parameters have been generated for many salts that reduce VOC solubility giving it relatively high accuracy. However, nearly all of the volatile solutes listed for this model are inorganic gases or straight-chain aliphatic hydrocarbons. In

addition, mostly small inorganic salts have been used to test this model. Thus, this model may not quantitatively predict the effects of larger salts.

2.6 Dilute solution theory for water + salt + VOC mixtures

The theory of dilute solutions has been well studied over the past two decades [120-129]. It is based on a Taylor expansion of the Helmholtz energy about the critical point of the solvent and yields simple expressions for Henry's constants among other thermodynamic properties for dilute binary mixtures. The ideal Helmholtz energy must be subtracted since it diverges at infinite dilution. The resulting expression for residual Helmholtz energy at infinite dilution, a^r, is as follows:

$$a^r(T,v,x) = a(T,v,x) - RT\left[x\,ln\,x + (1-x)ln(1-x)\right] \qquad (40)$$

The residual Helmholtz energy can be manipulated to yield an expression for Henry's constant. Harvey's expression [125, 129] for this property is given by

$$ln\left(H_{2,1}\right) = ln\,P_1^{sat} + \frac{A_{ij}}{T_r} + B_{ij}\,\frac{(1-T_r)^{0.355}}{T_r} + C_{ij}\,\frac{exp(1-T_r)}{T_r^{0.41}}, \qquad (41)$$

where A_{ij}, B_{ij}, are temperature-independent binary parameters, C_{ij} is a temperature-independent empirical parameter for correlations below the boiling point of the solvent, T_r is the reduced temperature, and P_1^{sat} is the saturated vapor pressure of the solvent. Harvey's model was extended to ternary mixtures of solids in supercritical CO_2 + an organic cosolvent by Mendez-Santiago and Teja [130]. Teja et al. [4] further extended this model for use with VOCs in a salt solution. The derivations for both models are reproduced here. The subscript *1* refers to the solvent, *2* to the solid solute, and *3* to the cosolvent. Henry's constant is given by:

$$H_{2,m} = \lim_{x_2 \to 0}\left(\frac{f_2}{x_2}\right) = \lim_{x_2 \to 0}\left(\frac{x_2 \phi_2 P}{x_2}\right) = \lim_{x_2 \to 0}\left(\phi_2 P\right) = \phi_2^{\infty} P \qquad (42)$$

With the fugacity coefficient given by [131]:

$$\ln \phi_2 = \int_0^P \left(\frac{\bar{v}_2}{RT} - \frac{1}{P}\right) dP \qquad (43)$$

and the molar volume of the mixture by:

$$v = x_1 \bar{v}_1 + x_2 \bar{v}_2 + x_3 \bar{v}_3 \qquad (44)$$

When Eq. 44 is differentiated with respect to x_2 at constant temperature and pressure it yields:

$$\left(\frac{\partial v}{\partial x_2}\right)_{T,P} = x_1\left(\frac{\partial \bar{v}_1}{\partial x_2}\right)_{T,P} + x_2\left(\frac{\partial \bar{v}_2}{\partial x_2}\right)_{T,P} + x_3\left(\frac{\partial \bar{v}_3}{\partial x_2}\right)_{T,P} + \bar{v}_1\left(\frac{\partial x_1}{\partial x_2}\right)_{T,P} + \bar{v}_2\left(\frac{\partial x_2}{\partial x_2}\right)_{T,P} + \bar{v}_3\left(\frac{\partial x_3}{\partial x_2}\right)_{T,P} \qquad (45)$$

By the Gibbs-Duhem equation,

$$x_1\left(\frac{\partial \bar{v}_1}{\partial x_2}\right)_{T,P} + x_2\left(\frac{\partial \bar{v}_2}{\partial x_2}\right)_{T,P} + x_3\left(\frac{\partial \bar{v}_3}{\partial x_2}\right)_{T,P} = 0 \qquad (46)$$

Thus,

$$\left(\frac{\partial v}{\partial x_2}\right)_{T,P} = \bar{v}_1\left(\frac{\partial x_1}{\partial x_2}\right)_{T,P} + \bar{v}_2\left(\frac{\partial x_2}{\partial x_2}\right)_{T,P} + \bar{v}_3\left(\frac{\partial x_3}{\partial x_2}\right)_{T,P} \qquad (47)$$

Solving for $\bar{v}_2$,

$$\bar{v}_2 = \left(\frac{\partial v}{\partial x_2}\right)_{T,P} - \bar{v}_1\left(\frac{\partial x_1}{\partial x_2}\right)_{T,P} - \bar{v}_3\left(\frac{\partial x_3}{\partial x_2}\right)_{T,P} \qquad (48)$$

Substituting into Eq. 43,

$$\ln \phi_2 = \int_0^P \left[\frac{1}{RT} \left(\frac{\partial v}{\partial x_2} \right)_{T,P} - \frac{\bar{v}_1}{RT} \left(\frac{\partial x_1}{\partial x_2} \right)_{T,P} - \frac{\bar{v}_3}{RT} \left(\frac{\partial x_3}{\partial x_2} \right)_{T,P} - \frac{1}{P} \right] dP \qquad (49)$$

for a ternary mixture,

$$x_1 + x_2 + x_3 = 1 \qquad (50)$$

differentiating with respect to x_2 yields:

$$\left(\frac{\partial x_1}{\partial x_2} \right)_{T,P} + 1 + \left(\frac{\partial x_3}{\partial x_2} \right)_{T,P} = 0 \qquad (51)$$

It is assumed that the ratio x_1/x_3 remains constant as x_2 approaches zero, then

$$\left[\frac{\partial (x_1 / x_3)}{\partial x_2} \right]_{T,P} = 0, \qquad (52)$$

using the Chain Rule, Eq. 52 becomes,

$$\frac{-x_1}{(x_3)^2} \left(\frac{\partial x_3}{\partial x_2} \right)_{T,P} + \frac{1}{x_3} \left(\frac{\partial x_1}{\partial x_2} \right)_{T,P} = 0 \qquad (53)$$

Combining Eqs. 53 and 51,

$$\left(\frac{\partial x_1}{\partial x_2} \right)_{T,P} = -\frac{x_1}{x_1 + x_3} \qquad (54)$$

and

$$\left(\frac{\partial x_3}{\partial x_2} \right)_{T,P} = -\frac{x_3}{x_1 + x_3} \qquad (55)$$

Also,

$$\left(\frac{\partial v}{\partial x_2} \right)_{T,P} = -\left(\frac{\partial P}{\partial x_2} \right)_{v,T} \left(\frac{\partial v}{\partial P} \right)_{T,x_2} \qquad (56)$$

Substituting Eqs. 53, 54 and 55 into Eq. 48 yields,

$$\ln \phi_2 = \int_{\infty}^{V} -\frac{1}{RT}\left(\frac{\partial P}{\partial x_2}\right)_{v,T} dV + \int_{0}^{P}\left[\left(\frac{x_1}{x_1 + x_3}\right)\frac{\bar{v}_1}{RT} + \left(\frac{x_3}{x_1 + x_3}\right)\frac{\bar{v}_3}{RT} - \frac{1}{P}\right]dP \qquad (57)$$

At infinite dilution for component *2*,

$$\lim_{x_2 \to 0}\left(\frac{x_1}{x_1 + x_3}\right) \to x_1 \qquad (58)$$

and

$$\lim_{x_2 \to 0}\left(\frac{x_3}{x_1 + x_3}\right) \to x_3 \qquad (59)$$

Therefore,

$$\lim_{x_2 \to 0}\left[\left(\frac{x_1}{x_1 + x_3}\right)\frac{\bar{v}_1}{RT} + \left(\frac{x_3}{x_1 + x_3}\right)\frac{\bar{v}_3}{RT}\right] = \frac{x_1\bar{v}_1 + x_3\bar{v}_3}{RT} = \frac{v}{RT} \qquad (60)$$

Then Eq. 57 becomes,

$$\ln \phi_2^{\infty} = \int_{\infty}^{V} -\frac{1}{RT}\left(\frac{\partial P}{\partial x_2}\right)_{v,T}^{\infty} dV + \int_{0}^{P}\left[\frac{v}{RT} - \frac{1}{P}\right]dP \qquad (61)$$

The second integral of Eq. 61 corresponds to the fugacity coefficient of the mixed solvent. The first integral of Eq. 61 is the derivative of the residual Helmholtz energy; therefore,

$$ln\,\phi_2^{\infty} = \frac{1}{RT}\left(\frac{\partial a^r}{\partial x_2}\right)_{v,T}^{\infty} + ln\,\phi_m, \qquad (62)$$

where ϕ_m is the fugacity coefficient of the mixed solvent.

Performing a Taylor expansion on the Helmholtz energy derivative,

$$\left(\frac{\partial a^r}{\partial x_2}\right)_{v,T}^{\infty}\Bigg|_{x_3=0} = \left(\frac{\partial a^r}{\partial x_2}\right)_{v,T}^{\infty}\Bigg|_{x_3=0} + (x_3 - 0)\left[\frac{\partial}{\partial x_3}\left(\frac{\partial a^r}{\partial x_2}\right)\right]_{v,T}^{\infty}\Bigg|_{x_3=0} \qquad (63)$$

The first term in Eq. 63 can also be expressed in terms of a Taylor expansion,

$$\left(\frac{\partial a^r}{\partial x_2}\right)_{v,T}^{\infty}\Bigg|_{x_3=0,v_1=v_{c,1}} = \left(\frac{\partial a^r}{\partial x_2}\right)_{v_1,T}^{\infty,c}\Bigg|_{x_3=0,v_1=v_{c,1}} + (v_1 - v_{c,1})\left[\frac{\partial}{\partial v}\left(\frac{\partial a^r}{\partial x_2}\right)_{V,T}^{\infty,c}\right]\Bigg|_{x_3=0,v_1=v_{c,1}} \quad (64)$$

We now substitute Eqs. 63 and 64 into Eq. 62, and since they are asymptotically equivalent, we substitute $(\rho_1 - \rho_{c1})$ for $(v_1 - v_{c1})$:

$$RT\,ln\,\phi_2^{\infty} = \left(\frac{\partial a^r}{\partial x_2}\right)_{v,T}^{\infty,c}\Bigg|_{x_3=0,v_1=v_{1c}} + (\rho_1 - \rho_{c1})\left[\frac{\partial}{\partial v}\left(\frac{\partial a^r}{\partial x_2}\right)_{v,T}^{\infty,c}\right]\Bigg|_{x_3=0,v_1=v_{c1}} + (x_3)\left[\frac{\partial}{\partial x_3}\left(\frac{\partial a^r}{\partial x_2}\right)_{v,T}^{\infty}\right]\Bigg|_{x_3=0} + RT\,ln\,\phi_m \quad (65)$$

The second term on the right hand side of Eq. 65 is a significant thermodynamic parameter called the Krichevsky parameter and is equal to the second derivative of the Helmholtz energy, *a*, with respect to molar volume, *v*, and mole fraction of the volatile solute, x_2. To simplify Eq. 65 we substitute coefficients for the derivatives of the Helmholtz energy:

$$RT\ln\phi_2^{\infty} = A' + B'(\rho_1 - \rho_{c,1}) + kx_3 + RT\ln\phi_m\,. \quad (66)$$

Then, substituting Eq. 66 into 42,

$$RT\,ln\left(\frac{H_{2,m}}{f_m}\right) = A' + B'(\rho_1 - \rho_{c,1}) + Dx_3 \quad (67)$$

At low temperature with a volatile solute, it is necessary to add the empirical term given by Harvey [129]. Eq. 67 then becomes:

$$RT\,ln\left(\frac{H_{2,m}}{f_m}\right) = A' + B'\left(\rho_1 - \rho_{c1}\right) + C'T\rho_1\,exp\left(\frac{273.15 - T}{\tau}\right) + Dx_3 \qquad (68)$$

where $\tau = 50\ K$. Since the density scales with temperature, i.e. $\left|\rho_1 - \rho_{c,1}\right| \propto \left|T_1 - T_{c,1}\right|$, Eq. 68 can be rewritten as,

$$ln\left(H_{2,m}\right) = ln\,P_m^{sat} + \frac{A'}{T_r} + B'\frac{\left(1 - T_r\right)^{0.355}}{T_r} + C'\frac{exp\left(1 - T_r\right)}{T_r^{0.41}} + Dx_3 \qquad (69)$$

where T_r is the reduced temperature of pure solvent *1* (water) and the fugacity of the mixed solvent, f_m, is approximated by the vapor pressure of solvent + salt, P_m^{sat}. Using this equation, the Henry's constants of a VOC in an aqueous salt solution can be correlated over a wide range of temperatures. Teja et al. [4, 132] showed that the saturated vapor pressure of the solvent alone can be used in place of P_m^{sat} to further simplify the use of Eq. 69. The excellent performance of Eq. 69 over a 300 K temperature range, relative to several other Henry's constant models in the literature can be seen in Figure 7.

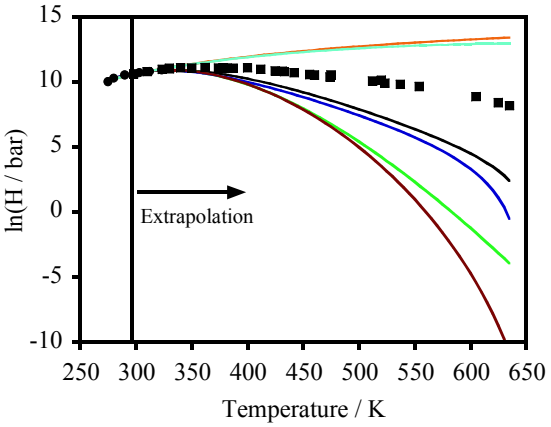

a

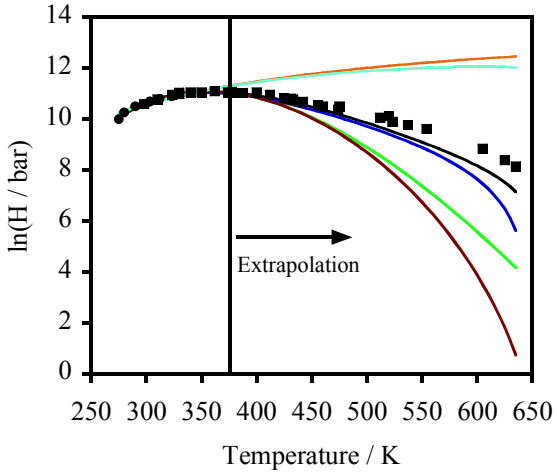

b

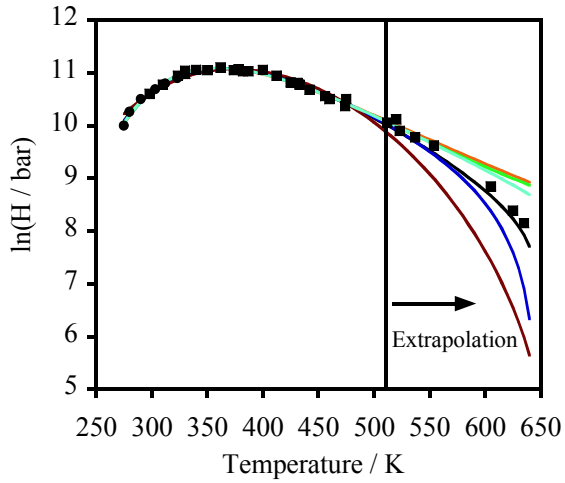

c

Figure 7. Henry's constants of methane gas in pure water (●) IUPAC [87] and (■) Fernandez-Prini et al. [85] extrapolated after (a) 298, (b) 373, and (c) 512 K with models: (—) Teja et al. [4], (—) polynomial expansion in temperature, (—) Fernandez-Prini et al. [85], (—) Krause and Benson [86], (—) Clarke and Glew [83], (—) Alvarez et al. [84].

2.6.1 Models for activity coefficients of water + salt + VOC systems.

There is a large body of literature on activity coefficient models for aqueous electrolyte systems. The Debye-Hückel limiting law [133] was developed for a single salt and solvent pair when the salt concentration is below an ionic strength of 0.01 mol/kg [131]. Its inability to treat higher electrolyte concentration originates from the fact that the limiting law is based purely on electrostatics, and addresses long-range forces but not the shorter-range dipole-dipole and dipole-ion interactions. The activity coefficient $\gamma_{\pm}^{(m)}$ for an ionic species with the Debye-Hückel limiting law is given by:

$$ln\,\gamma_{\pm}^{(m)} = -A_{\gamma}\left|z_{+}z_{-}\right|I^{1/2} \qquad (70)$$

where z is the charge on an ion, A_{γ} is the Debye constant, and I is the ionic strength of the salt defined as,

$$I_i = 0.5\sum_i m_i z_i^2 \qquad (71)$$

where m_i is the molal concentration of ion i, and z_i is the valence of ion i. The mean ionic activity coefficient, $\gamma_{\pm}^{(m)}$, is defined as follows:

$$\gamma_{\pm}^{(m)} = \left(\gamma_{+}^{\nu_{+}}\,\gamma_{-}^{\nu_{-}}\right)^{1/(\nu_{+}\ +\ \nu_{-})} \qquad (72)$$

where ν_{+} is the number of positive charges per cation, and ν_{-} is the number of negative charges per anion. The Debye constant A_{γ} is given by:

$$A_{\gamma} = \left(\frac{e^2}{\varepsilon_o \varepsilon_r RT}\right)^{3/2} \frac{N_A^2}{8\pi}\left(2d_s\right)^{1/2} \qquad (73)$$

where e is the charge of an electron (1.60218 x 10^{-19} coulombs), ε_o is the permittivity of a vacuum, ε_r is the dielectric constant, N_A is Avogadro's number, and d_s is the solvent density.

Guggenheim [134, 135] extended the Debye-Hückel limiting law to 0.1 molal in salt concentration as follows

$$\gamma_{R,X}^{(m)} = -A_\gamma Z_R |Z_X| \frac{I^{1/2}}{1+I^{1/2}} + \frac{2\nu_+}{\nu_- + \nu_+} \sum_{X'} \beta_{R,X'} m_{X'} + \frac{2\nu_-}{\nu_+ + \nu_-} \sum_{R'} \beta_{R',X} m_X \,, \qquad (74)$$

where $\gamma_{R,X}^{(m)}$ is equivalent to $\gamma_{\pm}^{(m)}$ in Eq. 70, Z_R is the number of positive charges per cation, Z_x is the number of positive charges per anion, $\beta_{R,X}$ is the interaction parameter between cation R and anion X, m_X is the (molal) concentration of anions, and m_R is the (molal) concentration of cations.

Pitzer [136-138] modified the Debye-Hückel law to account for short-range forces and was able to correlate data up to 6 molal of dissolved electrolytes. The enhancements that allow it to operate with significantly higher electrolyte concentrations originate from terms employed to account for the hard-core and Columbic interactions between ions in a concentrated solution. The hard-core and Columbic forces are represented as follows,

$$\Phi_{ij}^{HC} = \infty \quad r < r_o \qquad (75)$$

$$\Phi_{ij}^{C} = \frac{z_i z_j e^2}{4\pi\varepsilon_o D_s r} \quad r > r_o \qquad (76)$$

The radial charge distribution function for the system is then

$$g_{ij}(r) = exp\left[\left(\frac{z_i z_j e^2}{4\pi\varepsilon_o \varepsilon_r}\right)\left(\frac{exp(\kappa r_o)}{1+\kappa r_o}\right)\left(\frac{exp(-\kappa r)}{r}\right)\right] \qquad (77)$$

where z is the charge number of the ion, D_s is the dielectric constant of the solvent, ε_o is the permittivity of a vacuum, r is the distance from an ion to its neighbors, e is the charge of an electron, and κ is the total concentration of ions (molal). Pitzer's excess Gibbs energy expression can be written as follows:

$$\frac{G^E}{RT} = n_w A(I) + \frac{1}{n_w}\sum_i\sum_j \lambda_{ij}(I) n_i n_j + \frac{1}{n_w^2}\sum_i\sum_j\sum_k \Lambda_{ijk} n_i n_j n_k \,, \qquad (78)$$

where $A(I)$ is a Debye-Hückel term for long-range electrostatic ion-ion effects, n_i is the number of moles of species i, n_w is the mass of water, $\lambda_{ij}(I)$ is the second osmotic virial coefficient, and Λ_{ijk} is the third osmotic virial coefficient. The $A(I)$ term depends on temperature, solvent density, and dielectric constant, whereas $\lambda_{ij}(I)$ depends on ionic strength. The term Λ_{ijk} accounts for triple ion interactions and is assumed constant with ionic strength. The difficulty in obtaining the third osmotic virial coefficient for aqueous salt solutions through independent experiments or through models makes this equation particularly difficult to apply without extensive data.

The expression for the activity coefficient of species i is,

$$\ln \gamma_i = \frac{z_i^2}{2}\frac{\partial A}{\partial I} + 2\sum_j \lambda_{ij} m_j + \frac{z_i^2}{2}\sum_j\sum_k \frac{d\lambda_{ik}}{dI} m_j m_k + 3\sum_j\sum_k \Lambda_{ijk} m_j m_k \qquad (79)$$

where $m_i = n_i / n_w$. With the derivative of A abbreviated as A' and that for λ abbreviated as λ', the mean activity coefficient for an electrolyte is as follows,

$$\ln \gamma_{\pm}^{(m)} = \frac{|z_+ z_-|}{2} A' + \frac{2\nu_+}{\nu_+ + \nu_-}\sum_j \lambda_{(+)j} m_j + \frac{2\nu_-}{\nu_+ + \nu_-}\sum_j \lambda_{(-)j} m_j + \frac{|z_+ z_-|}{2}\sum_j\sum_k \lambda'_{jk} m_j m_k + \frac{3\nu_+}{\nu_+ - \nu_-}\sum_j\sum_k \Lambda_{(+)jk} m_j m_k + \frac{3\nu_-}{\nu_+ + \nu_-}\sum_j\sum_k \Lambda_{(-)jk} m_j m_k \qquad (80)$$

where subscripts (+) and (-) denote the positive or negative species. It is clear that the number of parameters increases dramatically with the number of ionic species. The large number of temperature - dependent binary and ternary parameters required in the Pitzer model make it unwieldy for use for systems containing more than two electrolytes.

Chen et al. [139, 140] developed a modified form of the non-random two liquid model (NRTL) of Renon and Prausnitz [141] to address systems of multiple electrolytes and mixed solvents. Their model accounts for ions and neutral molecules by assuming a neutral local composition balanced by equal numbers of cations and anions. They also added interaction parameters for the repulsion of like ions. The excess Gibbs energy for their electrolyte NRTL (eNRTL) model is given by:

$$\frac{G^E}{RT} = \frac{G^E_{PDH}}{RT} + \frac{G^E_{LC}}{RT} \qquad (81)$$

where G^E_{PDH} is the contribution of the long-range electrostatic interactions and G^E_{LC} is the contribution of the short-range interactions represented by the modified NRTL model. The long-range interaction term G^E_{PDH} is represented by the Pitzer-Debye-Hückel equation [142],

$$\frac{G^E_{PDH}}{RT} = -\left(\sum n_k\right)\left(1000/M_s\right)^{\frac{1}{2}}\left(4AI_x/\rho\right)ln\left(1+\rho I_x^{1/2}\right) \qquad (82)$$

where M_s is the molar mass of the solvent in moles/kg, I_x is the ionic strength on a mole fraction basis, and ρ is the closest approach parameter. The summation is over all n_k ionic and neutral species. The activity coefficient resulting from the derivative of Eq. 82 is as follows,

$$ln\,\gamma_i^{PDH} = -\left(1000/M_s\right)^{1/2} A\left[\left(2z_i^2/\rho\right)ln\left(1+\rho I_x^{1/2}\right)+\left(z_i^2 I_x^{1/2} - 2I_x^{3/2}\right)/\left(1+\rho I_x^{1/2}\right)\right] \qquad (83)$$

The NRTL local composition term for the molecular species activity constants is as follows,

$$ln\gamma_m^{LC} = \frac{\sum_j X_j G_{jm}\tau_{jm}}{\sum_k X_k G_{km}} + \sum_{m'} \frac{X_{m'} G_{mm'}}{\sum_k X_k G_{km'}} \left(\tau_{mm'} - \frac{\sum_k X_k G_{km'} \tau_{km'}}{\sum_k X_k G_{km'}} \right) +$$
$$\sum_c \sum_{a'} \frac{X_{a'}}{\sum_{a''} X_{a''}} \frac{X_c G_{mc,a'c}}{\sum_k X_k G_{kc,a'c}} \left(\tau_{mc,a'c} - \frac{\sum_k X_k G_{kc,a'c} \tau_{kc,a'c}}{\sum_k X_k G_{kc,a'c}} \right) + , \quad (84)$$
$$\sum_a \sum_{c'} \frac{X_{c'} X_a G_{ma,c'a}}{\sum_{c''} X_{c''} \sum_k X_k G_{ka,c'a}} \left(\tau_{ma,c'a} - \frac{\sum_k X_k G_{kc,c'a} \tau_{ka,c'a}}{\sum_k K_k G_{ka,c'a}} \right)$$

where X is the effective liquid phase mole fraction of a species, τ is the NRTL binary interaction parameter, the subscripts *a*, *a'*, and *a''* denote the anion, subscripts *c*, *c'*, and *c''* denote the cation, *ca* represents the un-dissociated salt, *m* denotes a molecular species, and *i*, *j*, *k* represent any species. G is a combination of τ and a nonrandomness factor α,

$$G_{ji,ki} = exp\left(-\alpha_{ji,ki}\tau_{ji,ki}\right) \quad (85)$$

The local composition term for the cation is as follows,

$$\frac{1}{Z_c} ln\gamma_c^{LC} = \sum_{a'} \frac{X_{a'}}{\sum_{a''} X_{a''}} \frac{\sum_k X_k G_{kc,a'c} \tau_{kc,a'c}}{\sum_k X_k G_{kc,a'c}} + \sum_m \frac{X_m G_{cm}}{\sum_k X_k G_{km}} \left(\tau_{cm} - \frac{\sum_k X_k G_{km} \tau_{km}}{\sum_k X_k G_{km}} \right) +$$
$$\sum_a \sum_{c'} \frac{X_{c'}}{\sum_{c''} X_{c''}} \frac{X_a G_{ca,c'a}}{\sum_k X_k G_{ka,c'a}} \left(\tau_{ca,c'a} - \frac{\sum_k X_k G_{ka,c'a} \tau_{ka,c'a}}{\sum_k X_k G_{ka,c'a}} \right) \quad (86)$$

where Z_c is the absolute value of the cation charge. The activity coefficient for the anion is as follows,

$$\frac{1}{Z_a} ln\gamma_a^{LC} = \sum_{c'} \frac{X_{c'}}{\sum_{c''} X_{c''}} \frac{\sum_k X_k G_{ka,c'a} \tau_{kc,a'c}}{\sum_k X_k G_{ka,c'a}} + \sum_m \frac{X_m G_{am}}{\sum_k X_k G_{km}} \left(\tau_{am} - \frac{\sum_k X_k G_{km} \tau_{km}}{\sum_k X_k G_{km}} \right) + \sum_c \sum_{a'} \frac{X_{a'}}{\sum_{a''} X_{a''}} \frac{X_c G_{ac,a'c}}{\sum_k X_k G_{kc,a'c}} \left(\tau_{ac,a'c} - \frac{\sum_k X_k G_{kc,a'c} \tau_{kc,a'c}}{\sum_k X_k G_{kc,a'c}} \right) \quad (87)$$

The final expression for the activity coefficient of species *i* is the linear combination of Eqs. 83, 84, 86, and 87 for the anion, cation, or solvent denoted as *i*,

$$ln\gamma_i = ln\gamma_i^{PDH} + ln\gamma_i^{LC} . \quad (88)$$

The eNRTL model of Chen et al. eliminates the need for ternary interaction parameters. However, the binary parameters remain a function of temperature making it necessary to regress the T-xy data for water + salt + VOC systems. As has been shown in Chapter 2 [38], only limited VLE data are available for ternary systems.

In order to treat VLE of solutions where site-specific associations play a role, Chapman et al. [143, 144] developed the statistical associating fluid theory (SAFT) to model the phase behavior of pure fluids and mixtures. The equation of state of Chapman et al. is based on an expansion of the residual Helmholtz energy, a^r, of Wertheim [145]. This expansion is composed of three separate terms,

$$a^r = a^{seg} + a^{chain} + a^{assoc} \quad (89)$$

where a^{seg} accounts for segment-segment interactions and is defined as,

$$a^{seg} = a_o^{seg} \sum_i X_i m_i \quad (90)$$

where a_o^{seg} is the Helmholtz energy of non-associating spherical segments and the summation yields the ratio of segments to the number of molecules in the fluid, m_i is the number of spherical segments in molecules of component *i*, and X_i is the mole fraction of

component *i*. The term a^{chain} is derived from associating fluid theory [145] and accounts for covalent bonds that result in chain formation,

$$a^{chain} = RT\sum_i X_i(1-m_i)ln\left(g_{ii}(d_{ii})^{hs}\right) \qquad (91)$$

where g_{ii} is the hard sphere correlation function for the interaction of two spheres, *i*, in a mixture of spheres evaluated at the hard sphere contact distance d_{ii}. The term a^{assoc} accounts for specific interactions among segments such as hydrogen bonding and is defined as,

$$a^{assoc} = RT\sum_i X_i\left[\sum_{A_i}\left[ln\,X^{A_i} - \frac{X^{A_i}}{2}\right] + \frac{1}{2}M_i\right], \qquad (92)$$

where M_i is the number of association sites on molecule *i*, X^{A_i} is the mole fraction of component *i* not bonded at site *A*.

Wu and Prausnitz [146] expressed the Helmholtz energy of mixtures of water + salt + hydrocarbon in terms of four parts,

$$a = a^{ref} + a^{assoc} + a^{Born} + a^{Coloumb} \qquad (93)$$

where a^{ref} is the Helmholtz energy of a mixture of normal (not ionized or hydrogen bonded) fluids that takes into account short-range repulsive interactions and van der Waal attractive forces of molecules or ions, a^{assoc} adds hydrogen bonding and electrostatic interactions between water and ions, a^{Born} takes into account the Helmholtz energy of ion formation in a continuous medium, and $a^{Coulomb}$ is the Helmholtz energy from ion-ion interactions. The PR EOS was used to calculate a^{ref},

$$\frac{a^{ref}}{nRT} = \frac{a^{IG}}{nRT} + ln\left(\frac{v}{v-b}\right) + \frac{q}{2\sqrt{2}bRT}ln\left(\frac{v+\left(1-\sqrt{2}\right)b}{v+\left(1+\sqrt{2}\right)b}\right) \qquad (94)$$

where *v* is the molar volume and other terms are defined below for hydrocarbons only,

$$q_i = q_i^o\left[1+\left(0.37464+1.54226\omega_i-0.26992\omega_i^2\right)\left(1-\sqrt{T/T_c}\right)\right]^2 \quad (95)$$

$$q_i^o = 0.45724\frac{R^2T_{ci}^2}{P_{ci}} \quad (96)$$

$$b_i = 0.07780\frac{RT_{ci}}{P_{ci}} \quad (97)$$

where ω_i is the Pitzer acentric factor for component i, T is the temperature in Kelvin, T_c is the critical temperature of the mixture, T_{ci} is the critical temperature of component i, P_{ci} is the critical pressure of component i, R is the gas constant. The mixing rules for q_i and b_i are as follows

$$\begin{aligned} q &= \sum_i\sum_j x_i x_j\left(q_i q_j\right)^{1/2}\left(1-k_{ij}\right) \\ b &= \sum_i x_i b_i \end{aligned} \quad (98)$$

In order to treat water q^o and b are calculated with Eqs. 96 and 97 and q for water is calculated as follows,

$$q_w = q_w^o\left(1+k_a\left(1-\sqrt{T/T_{cw}}\right)\right)^2 \quad (99)$$

where k_a is an adjustable parameter. Association due to hydrogen bonding is accounted for as follows,

$$\frac{a^{Assoc}}{nRT} = x_w\sum_S\left(ln\,X^S+\frac{1-X^S}{2}\right) \quad (100)$$

where x_w is the mole fraction of water and X^S is the mole fraction of water molecules not bonded to site S.

The Helmholtz energy of forming ions in the a medium with a dielectric constant D is calculated from an equation proposed by Born,

$$a^{Born} = \sum_{ions} \frac{(z_{ion} e)^2 N_A}{4\pi\varepsilon_o D \sigma_{ion}} n_{ion}\,, \qquad (101)$$

where the summation is over all ionized species, n_{ion} is the moles of ions, D is the dielectric constant, σ_{ion} is the ion diameter.

Columbic forces between ions are accounted for by a term based on the mean spherical approximation (MSA) [147],

$$a^{Coulomb} = -\frac{Ve^2}{4\pi\varepsilon_o D}\left[\Gamma\sum_{ions}\rho_{ion} z_{ion}^2 \Big/ \left(1+\Gamma\sigma_{ion}\right) + \frac{\pi}{2\Theta}\Omega P_n^2\right] + \frac{V\Gamma^3}{3\pi} kT \qquad (102)$$

where ρ_{ion} is the molecular number density of ions, V is the total volume and the parameters P_n, Θ, Ω, and Γ are defined in the following relationships that must be solved iteratively,

$$\Theta = 1 - \frac{\pi}{6}\sum_{ions}\rho_{ion}\sigma_{ion}^3 \qquad (103)$$

$$\Omega = 1 + \frac{\pi}{2\Theta}\sum_{ions}\frac{\rho_{ion}\sigma_{ion}^3}{1+\Gamma\sigma_{ion}} \qquad (104)$$

$$P_n = \frac{1}{\Omega}\sum_{ions}\frac{\rho_{ion}\sigma_{ion} z_{ion}}{1+\Gamma\sigma_{ion}} \qquad (105)$$

$$\Gamma = \frac{1}{2}\frac{e}{\sqrt{\varepsilon_o kTD}}\left\{\sum_{ions}\rho_{ion}\left[\left(z_{ion} - \frac{\pi}{2\Theta}\sigma_{ion}^2 P_n\right)\Big/\left(1+\Gamma\sigma_{ion}\right)\right]^2\right\}^{1/2} \qquad (106)$$

Wu and Prausnitz were successful in using this equation to correlate P-x-y data for water + salt + hydrocarbon above 473 K where hydrophobic effects are not pronounced. Another model must be employed at lower temperatures.

To develop a model that is not based on temperature-dependent interaction parameters, Li et al. [148] combined the theory of Guggenheim [134, 149] and the universal quasi-chemical (UNIQUAC) theory [150] to model the interactions in systems

of mixed solvents and electrolytes. Results from the model are not reliable outside of the data that was regressed to obtain the model parameters. This restricts predictions to below the normal boiling temperature of the systems since the systems are at ambient pressure. Their new model is called LIQUAC. The excess Gibbs energy for their LIQUAC model is composed of three terms,

$$G^E = G^E_{LR} + G^E_{MR} + G^E_{SR} \quad (107)$$

where the subscript *LR* stands for long-range or electrostatic forces, *MR* stands for medium-range forces that consist of ion-dipole and ion-induced dipole interactions (proportional to inter-molecular distances (*r*) as high as r^{-2} to as low as r^{-4}), *SR* stands for short-range interactions.

Long-range electrostatic forces were defined as follows,

$$G^E_{LR} = -(3D)^{-1} \sum_{i=1}^{ion} s_i z_i^2 e^2 \tau(\kappa a) \quad (108)$$

$$\tau(\kappa a) = 3(\kappa a)^{-3}\left[ln(1+\kappa a) - \kappa a + (\kappa a)^2/2\right] \quad (109)$$

where *D* is the dielectric constant of the mixed solvent, s_i is the number of ions *i* in the system, z_i is the charge number of an ion, κ is the inverse Debye length, and *a* is the distance of closest approach. Activity coefficients for the ions, *i*, and solvents, *s*, are calculated with their appropriate partial derivatives with respect to the moles of ions and solvent molecules,

$$ln\,\gamma_j^{LR} = -\left[z_j^2 e^2/(2DkT)\right]\left[\kappa/(1+x)\right] + \left[\bar{v}_j/(24\pi N_A a^3)\right]x^3\sigma(x), \quad (110)$$

$$ln\,\gamma_s^{LR} = \left[\bar{v}_s/(24\pi N_A a^3)\right]x^3\sigma(x), \quad (111)$$

where *k* is the Boltzmann constant, $\bar{v}_s$ is the partial molar volume of the solvent, $\bar{v}_j$ is the partial molar volume of the ion, and $\sigma(x)$ is defined as follows,

$$\sigma(x) = 3x^{-3}\left[1 + x - (1+x)^{-1} - 2ln(1+x)\right], \quad (112)$$

where x is a liquid phase mole fraction.

The middle-range interactions between ions and molecules was formulated for moderately concentrated electrolyte solutions where forces between similarly charged ions are neglected,

$$\frac{G^E_{MR}}{RT} = (n_{kg})^{-1}\left[\sum_{sol}\sum_{ion} B_{sol,ion}(I) n_{sol} n_{ion} + \sum_{c}\sum_{a} B_{ca}(I) n_c n_a\right], \quad (113)$$

where n_{kg} is the mass of solvent in kg, $B_{sol,ion}$ is a binary interaction parameter for solvent and ions, n_{sol} is the quantity of solvent molecules in moles, n_{ion} is the moles of ions, n_c is the number of moles of cations, and n_a is the number of moles of anions. Activity coefficients for the solvent molecules γ_s^{MR} and the ions γ_j^{MR} are as follows,

$$\begin{aligned} ln\,\gamma_s^{MR} = {} & \sum_{ion} B_{s,ion}(I) m_{ion} - (M_s/M_m)\sum_{sol}\sum_{ion}\left[B_{sol,ion}(I) + IB'_{sol,ion}(I)\right] x'_{sol} m_{ion} - \\ & M_s \sum_{c}\sum_{a}\left[B_{ca}(I) + IB'_{ca}(I)\right] m_c m_a \end{aligned} \quad (114)$$

$$\begin{aligned} ln\,\gamma_j^{MR} = {} & (M_m)^{-1}\sum_{sol} B_{j,sol}(I) X'_{sol} + \left[z_j^2/(2M_m)\right]\sum_{sol}\sum_{ion} B'_{sol,ion}(I) X'_{sol} m_{ion} + \\ & \sum_{a} B_{j,a}(I) m_a + (z_j^2/2)\sum_{c}\sum_{a} B'_{ca}(I) m_c m_a - B_{j,s}(I)/M_s \end{aligned} \quad (115)$$

where $B'(I) = dB(I)/dI$, X'_{sol} is the salt free mole fraction of solvent, *sol*, and M_m is the mean molecular weight of the mixed solvent.

Short-range interactions were modeled by the UNIQUAC expression [150]. The activity coefficient for the solvent molecules can be modeled with an unmodified version of UNIQUAC,

$$ln\,\gamma_s^{SR} = ln\,\gamma_s^C + ln\,\gamma_s^R \quad (116)$$

where the superscripts *C* and *R* stand for combinatorial and residual contributions respectively. The combinatorial and residual portions of the activity coefficient for solvent molecules are calculated as follows,

$$ln\gamma_s^C = 1 - V_s + lnV_s - 5q_s\left[1 - V_s/F_s + ln\left(V_s/F_s\right)\right] \quad (117)$$

$$ln\gamma_s^R = q_s\left\{1 - ln\left(\sum_l q_l x_l \Psi_{ls} \Big/ \sum_l q_l x_l\right) - \sum_l \left[q_i x_l \Psi_{kl} \Big/ \left(\sum_k q_k x_k \Psi_{kl}\right)\right]\right\} \quad (118)$$

$$V_s = r_s \Big/ \sum_l r_l x_l \quad (119)$$

$$F_s = q_s \Big/ \sum_l q_i x_l \quad (120)$$

$$\Psi_{ls} = exp\left(-a_{ls}/T\right) \quad (121)$$

where q is a surface interaction parameter, a is a UNIQUAC binary interaction parameter. The ions are treated with Eqs. 117 and 118 and the following equations,

$$ln\gamma_{j(B)}^c = 1 - r_j/r_s + ln\left(r_j/r_s\right) - 5q_j\left[1 - r_j q_s/\left(r_s q_j\right) + ln\left(r_j q_s/r_s q_j\right)\right] \quad (122)$$

$$ln\gamma_{j(B)}^R = q_j\left(1 - ln\,\Psi_{sj} - \Psi_{js}\right) \quad (123)$$

The equations for the activity coefficient are added together to yield the short-range contribution from the ions.

$$ln\gamma_j^{SR} = ln\gamma_j^c - ln\gamma_{j(B)}^c + ln\gamma_j^R - ln\gamma_{j(B)}^R \quad (124)$$

The LIQUAC model of Li et al. successfully correlated T-x-y data for 1-alkanols and water as well as non-aqueous methanol-acetone mixtures with inorganic salts such as NaCl, $CaCl_2$, and KCl to within a few percent deviation. All calculations were performed near atmospheric pressure.

The literature is lacking a model for water + salt + VOC systems that not only correlates data as a function of temperature but also as a function of pressure. The starting

point for such a model must be based on thermodynamic arguments to allow it to extrapolate properly if no data are available. The selection of a model with temperature-independent parameters will also make extrapolations in temperature possible. For these reasons, the model of Mendez-Santiago and Teja was selected as the basis for correlating and extrapolating data with temperature and salt concentration.

Headspace gas chromatography with the differential method of Chai and Zhu [1, 67] was selected to collect new Henry's constants for its excellent performance with low volatility as well as high volatility VOCs. The fact that this method is indirect allows the use of a highly sensitive flame ionization detector and removes the added complication of sampling a liquid phase with dissolved salts.

3. HEADSPACE GAS CHROMATOGRAPHY METHODS

3.1 Indirect differential headspace gas chromatography.

The differential method of Chai and Zhu [1, 67] is an efficient and accurate method to use for a wide range of VOC volatilities. A detailed derivation of the working equation is contained in this section. A material balance for the VOC is applied to the mixture in two vials. For each vial, the initial mass of solute (equal to the concentration multiplied by the volume) is equal to the sum of the mass in the liquid phase and the mass in the vapor phase after equilibrium is reached. For vessel 1:

$$C_{L1}^{0} V_{L1}^{0} = C_{L1} V_{L1} + C_{G1} V_{G1} \quad (125)$$

where C^{0}_{L1} is the initial solute concentration in the vial, V^{0}_{L1} is the initial volume of the solution in the vial, C_{L1} is the solute concentration in the liquid phase after equilibrium is attained, C_{G1} is the solute concentration in the gas phase (headspace) at equilibrium, and V_{G1} is the headspace volume. Similarly, for vial 2:

$$C_{L2}^{0} V_{L2}^{0} = C_{L2} V_{L2}^{0} + C_{G2} V_{G2} \quad (126)$$

It is assumed that the changes of liquid phase volumes in both vials during equilibration are negligible (so that $V^{0}_{L1} = V_{L1}$ and $V^{0}_{L2} = V_{L2}$). Also, $C^{0}_{L1} = C^{0}_{L2}$. The dimensionless Henry's constant is then given by:

$$H_c = C_{G1} / C_{L1} = C_{G2} / C_{L2} \quad (127)$$

After rearranging Eqs. 125 and 126 and eliminating liquid phase concentrations, the following expression for the dimensionless Henry's constant is obtained:

$$H_c = \frac{V_{L1}(1 - C_{G1}/C_{G2})}{(C_{G1}/C_{G2})(V_t - V_{L1}) - (V_{L1}/V_{L2})(V_t - V_{L2})} \quad (128)$$

The solute concentration in the vapor phase C_G is proportional to the peak area from the gas chromatogram:

$$C_{G1} / C_{G2} = A_1 / A_2 \qquad (129)$$

where $V_t = V_{L1} + V_{G1} = V_{L2} + V_{G2}$ represents the total volume of each vial and each vial is of the same size. Hence Eq. 128 becomes:

$$H_c = \frac{V_{L1}(1 - A_1/A_2)}{(A_1/A_2)(V_t - V_{L1}) - (V_{L1}/V_{L2})(V_t - V_{L2})} \qquad (130)$$

Thus the Henry's constant can be obtained from the ratio of the peak areas if the initial liquid volumes and the total volume of the vessels are known.

3.2 Validation of Henry's constants from the differential method.

Henry's constants obtained using the differential method can be validated by deriving the partial molar excess enthalpy of the volatile solute at infinite dilution, $\bar{h}_i^{ex,\infty}$, and comparing with literature values obtained from calorimetry. The partial molar excess enthalpy is defined by,

$$\bar{h}_i^{ex,\infty} \equiv \left(\frac{\partial H^E}{\partial n_i} \right)_{T,P,n_j} . \qquad (131)$$

where H^E is the excess enthalpy, and n_i is the number of moles of component *i*.

The Henry's constants from this work were converted into $\bar{h}_i^{ex,\infty}$, by way of the activity coefficients at infinite dilution, γ_i^{∞}. The temperature derivative of the resulting γ_i^{∞} was calculated with Eq. 6 to yield $\bar{h}_i^{ex,\infty}$,

$$\left| \frac{\partial\left(ln\,\gamma_i^{\infty}\right)}{\partial\left(1/T\right)} \right|_{P,x} = \frac{\bar{h}_i^{ex,\infty}}{R} . \qquad (132)$$

A comparison of the partial molar excess enthalpy of solution at infinite dilution from calorimetry and from experimentally determined Henry's constants is shown in Table 7. Only 1-alkanols and one 2-ketone with water as the solvent have been tabulated in the literature only allowing a comparison between these compounds in this work. The difference between excess partial molar enthalpies of solution from this work and the literature are far larger than the experimental error for individual Henry's constants, however, the difference is not unusual considering the severity of the test.

Table 7. Comparison of data from headspace gas chromatography and data from calorimetry.

	$\bar{h}^{ex,\infty}$ from H_c / (J/mol)	$\bar{h}^{ex,\infty}$ from Calorimetry / (J/mol)	
methanol	-7,916[a]	-7,000[c]	-7,050[e]
ethanol	-9,069[a]	-10,020[c]	-9,750[e]
1-propanol	-3,419[a]	-9,900[c]	-9,810[e]
2-butanone	-6,433[b]	-10,500[d]	

a: From data of Gupta et al. [6]
b: From data of Falabella et al. [151]
c: Trampe and Eckert [152]
d: Hovorka et al. [153]
e: Korolev et al. [154]

3.3 Modified relative method of headspace gas chromatography of salt containing solutions.

A modified relative method was developed in this work and published [155]. The new method maintains the precision of the differential method and reduces the number of samples necessary to obtain a data point over previous methods [1, 67, 71-74]. A larger amount of liquid is necessary to implement the relative method compared to the differential method.

For equilibrium between the vapor and liquid phases of a binary solution (VOC + water) in a closed vial, we may write:

$$m_l = C_l V_l \qquad (133)$$

and

$$m_g = C_g V_g \qquad (134)$$

where m, C, and V are the mass of the VOC, concentration of the VOC, and total volume of the phase respectively; and subscripts g and l refer to the vapor and liquid phases. The total mass m_0 of VOC in the vial is then given by:

$$m_0 = m_g + m_l = C_{l,0} V_l \qquad (135)$$

where $C_{l,0}$ is the concentration of the VOC in the initial liquid sample. The dimensionless Henry's constant H_c can now be expressed as follows:

$$H_c = \frac{C_g}{C_l} = \frac{(m_0 - m_l)}{m_l \beta} \qquad (136)$$

where the phase ratio $\beta = V_g/V_l$. Eq. 136 can be rearranged to give the ratio α of the mass of VOC in the equilibrated liquid phase to the mass of VOC in the initial liquid sample:

$$\alpha = \frac{m_l}{m_0} = \frac{1}{(H_c \cdot \beta + 1)} \qquad (137)$$

Note that in Eq. 137, $\alpha \rightarrow 1$ as the product $(H_c \cdot \beta) \rightarrow 0$; that is, the mass of VOC in the liquid phase at equilibrium is equal to the mass of the VOC in the initial liquid sample when β is small (and H_c is not very large). The concentration of the VOC in the liquid phase at equilibrium may then be obtained from the mass of VOC in the initial liquid sample, eliminating the need for analysis of the liquid phase at equilibrium.

The VOC concentration in the vapor phase can be obtained by GC analysis of the headspace and is proportional to the peak area A on the corresponding chromatogram. Thus, $C_g = kA$, where k is the response factor for the GC detector. The dimensionless Henry's constant of the VOC can now be expressed as:

$$H_c = \frac{C_g}{C_l} = \frac{kA}{C_l} \qquad (138)$$

Eq. 138 also applies to VOC + water + salt systems, if the salt is non-volatile and does not partition between the vapor and liquid phases. We may therefore eliminate the response factor k by analyzing the headspaces over two aqueous solutions, one containing the salt and one without the salt. Eq. 138 can then be written for the VOC + water solution (VOC concentration = $C_{l,s}$), and for a VOC + water + salt solution (VOC concentration = $C_{l,x}$). Dividing the resulting expressions leads to:

$$H_{c,x} = H_{c,s} \frac{A_x C_{l,s}}{A_s C_{l,x}} \qquad (139)$$

where $H_{c,s}$ and $H_{c,x}$ are dimensionless Henry's constants of the VOC in pure water and in the salt solution, respectively. When the VOC concentration in pure water is essentially the same as that in the salt solution, then $C_{l,s} = C_{l,x}$, and Eq. 139 further simplifies to:

$$H_{c,x} = H_{c,s} \frac{A_x}{A_s} \qquad (140)$$

Thus, the desired Henry's constant, $H_{c,x}$, can be obtained from two peak areas that correspond to two headspace analyses, and the reference value, $H_{c,s}$, from the literature or from a separate experiment.

3.4 Time for equilibration

Lincoff and Gossett [76] noted that the time for a liquid sample to attain equilibrium in a vial in HSGC experiments is related to the volume of the liquid in that vial. The times required to equilibrate 15 ml and 5 ml samples, used in data collection procedures in the following Chapter, were therefore obtained by analyzing the headspaces over test samples as a function of time until steady state conditions were attained. The 15 ml sample was analyzed at 5 min intervals for 60 min at 50 ^{o}C. Figure 8a is a plot of the GC peak area count vs. time and clearly shows that the area count approaches a constant value after about 45 min. All 15 ml samples were therefore equilibrated for 45 min in this work. Figure 8b shows similar data for the 5 ml sample at 40 ^{o}C. In this case, the area count approached a constant value after about 25 minutes, so that a 25 min equilibration time was used in all experiments carried out with 5 ml or smaller samples.

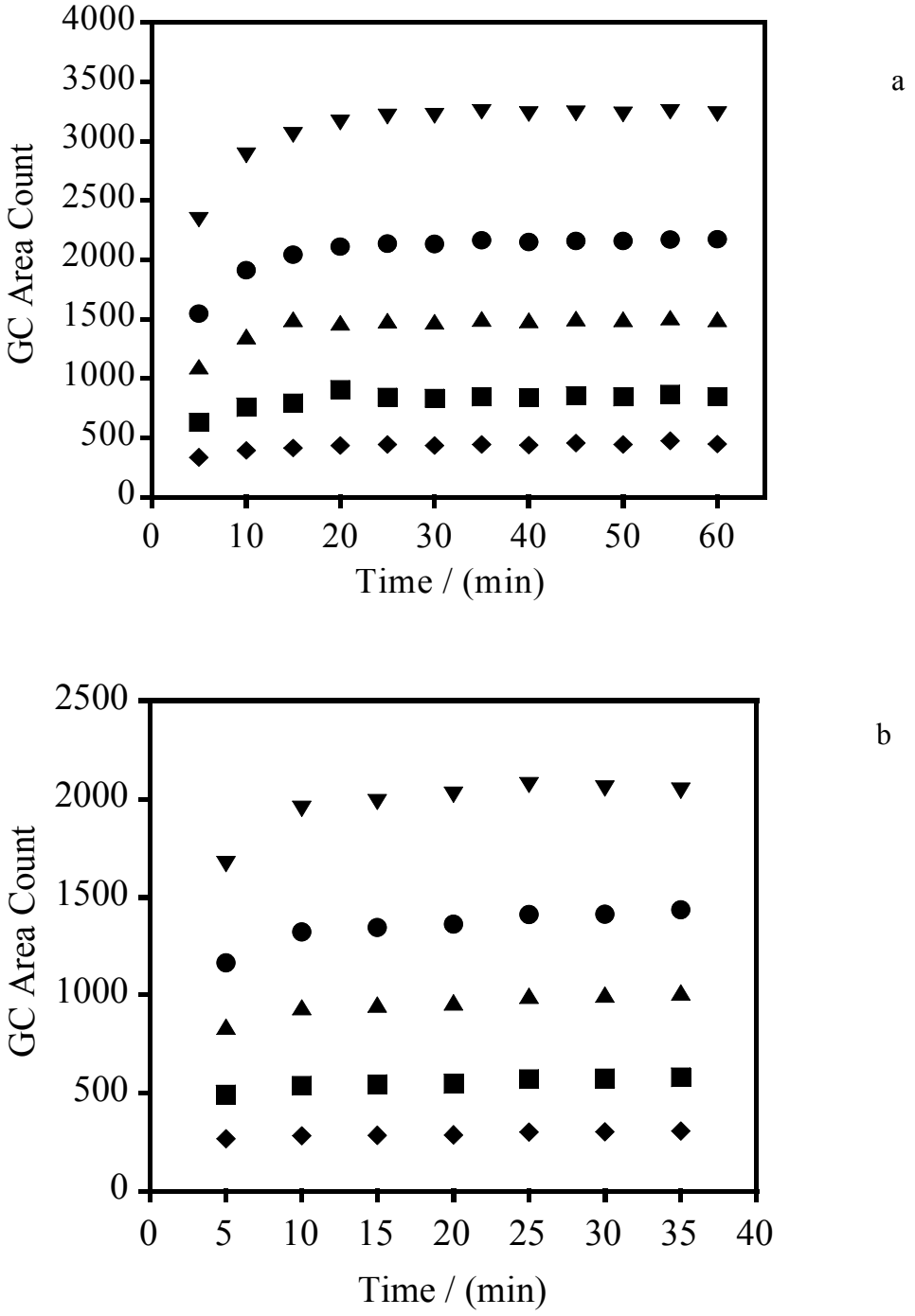

Figure 8. GC signal count vs. time for equilibrating different volumes of salt-free ketone solutions a) 15 ml at 50 ^{o}C; b) 5 ml at 40 ^{o}C. Data for: (◆) 2-propanone, (■) 2-butanone, (▲) 2-pentanone, (●) 2-hexanone, (▼) 2-heptanone [155].

3.5 Phase ratio selection for the relative method

A proper choice of phase ratio (β) is essential to ensure negligible concentration differences in the liquid phases at equilibrium (so that $m_{l,s} \approx m_{l,x}$). Figure 9a and 9b show the relationship between VOC mass ratio (α) and the phase ratio (β), or the liquid volume (V_l), for several values of Henry's constants. Figure 9b shows that a liquid volume of 15 ml (the maximum allowable volume for headspace sampling equipment) in a 21.6 ml sample vial corresponds to (α) values between 0.99 and 0.96 for dimensionless Henry's constants between 0.01 and 0.10. However, (α) values decrease to 0.88 for Henry's constants of ~ 0.3. This obviously invalidates the assumption (that $\alpha \rightarrow 1$) made in the derivation of Eq. 140 and therefore represents the upper limit of Henry's constants that can be measured in the vials. The upper limit of 0.10 for dimensionless Henry's constants allows one to measure 2-ketones (2-propanone to 2-heptanone) with up to 1.0 molal sodium sulfate and 353 K. 2-ketones with up to 1.2 molal sodium chloride can be determined up to 363 K and not exceed dimensionless Henry's constants of 0.10. 1-alkanols (methanol to 1-hexanol) also have Henry's constants below this threshold up to 363 K in the presence of up to 1.2 molal sodium sulfate and could also be used in the relative method. Note that the largest liquid volume employed in these experiments was 15 ml so that the liquid level would always be below the tip of the sampling needle.

To measure larger Henry's constants, it is necessary to decrease the vapor volume (or β) in each vial in order to minimize depletion of VOC in the liquid phase. The limitation imposed by the depth of penetration of the needle can be addressed by using a vapor-well [155].

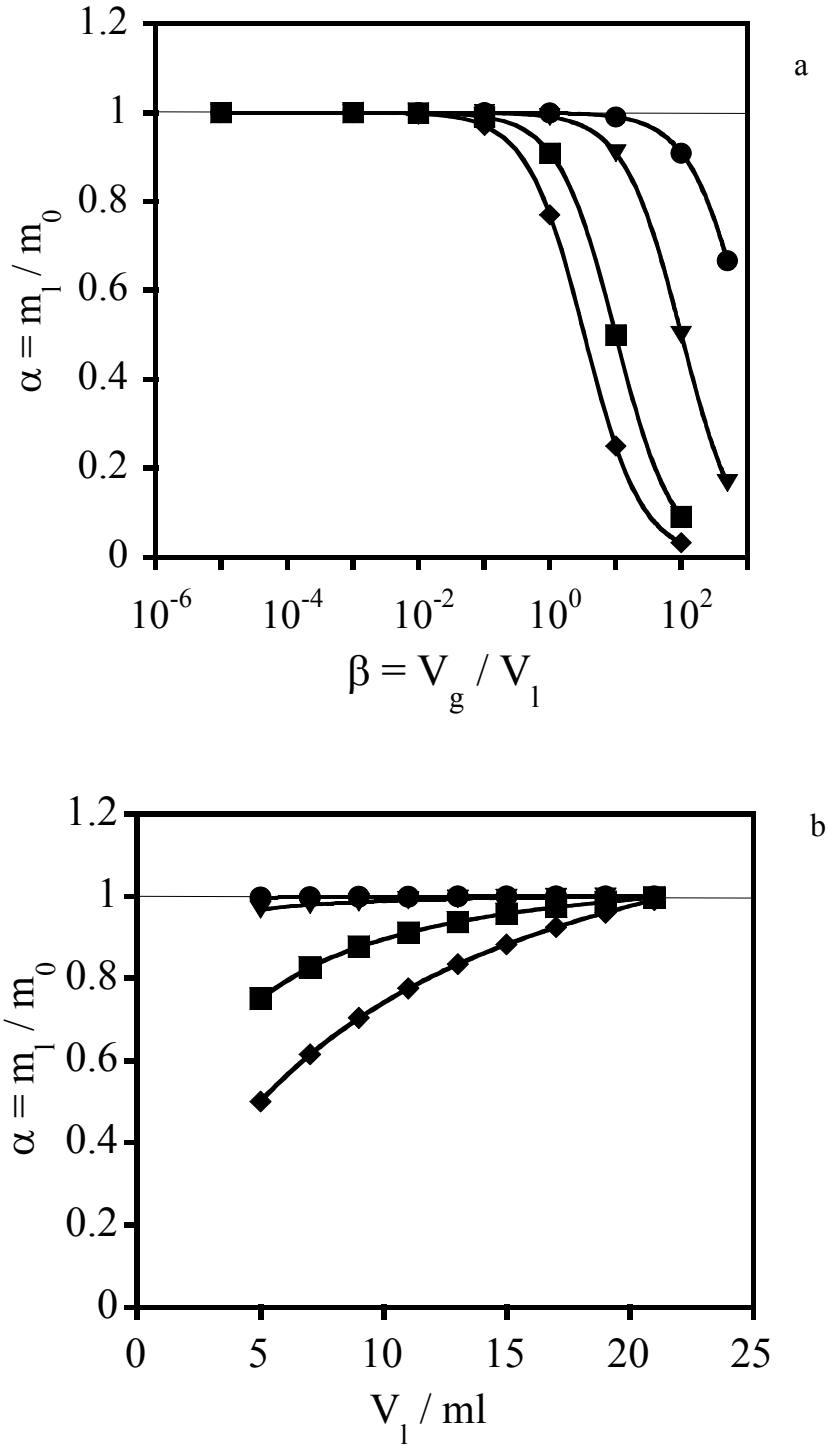

Figure 9. Partitioning of a VOC when Henry's constant = (◆) 0.3; (■) 0.1; (▼) 0.01 and (●) 0.001 as a function of phase ratio variation if (a) vial volume is arbitrary (b) vial volume = 21.6 ml.

3.6 Validation of relative headspace method against the differential method

Dimensionless Henry's constants of the five 2-ketones in 1.0 M solutions of sodium sulfate at 80 ^{o}C were measured using both the relative technique of this work and the differential technique of Chai and Zhu. The data are shown in Table 8 and agree within the reported experimental errors of both techniques. Note that Henry's constants for all five ketones at a given temperature and salt concentration were obtained in a single experiment because the solutions were dilute, and five separate peaks could be obtained in a single headspace analysis, as shown in Table 12.

Table 8. Henry's constants of 2-ketones in 1.0 molal Na_2SO_4 solutions at 353 K [155].

	H_c x 100		
	Relative HSGC	Differential HSGC*	% Difference
2-propanone	2.6	2.7	-6
2-butanone	5.5	5.7	-3
2-pentanone	11.0	10.8	2
2-hexanone	18.4	17.3	6
2-heptanone	31.3	28.1	10

* method of Chai and Zhu [67]

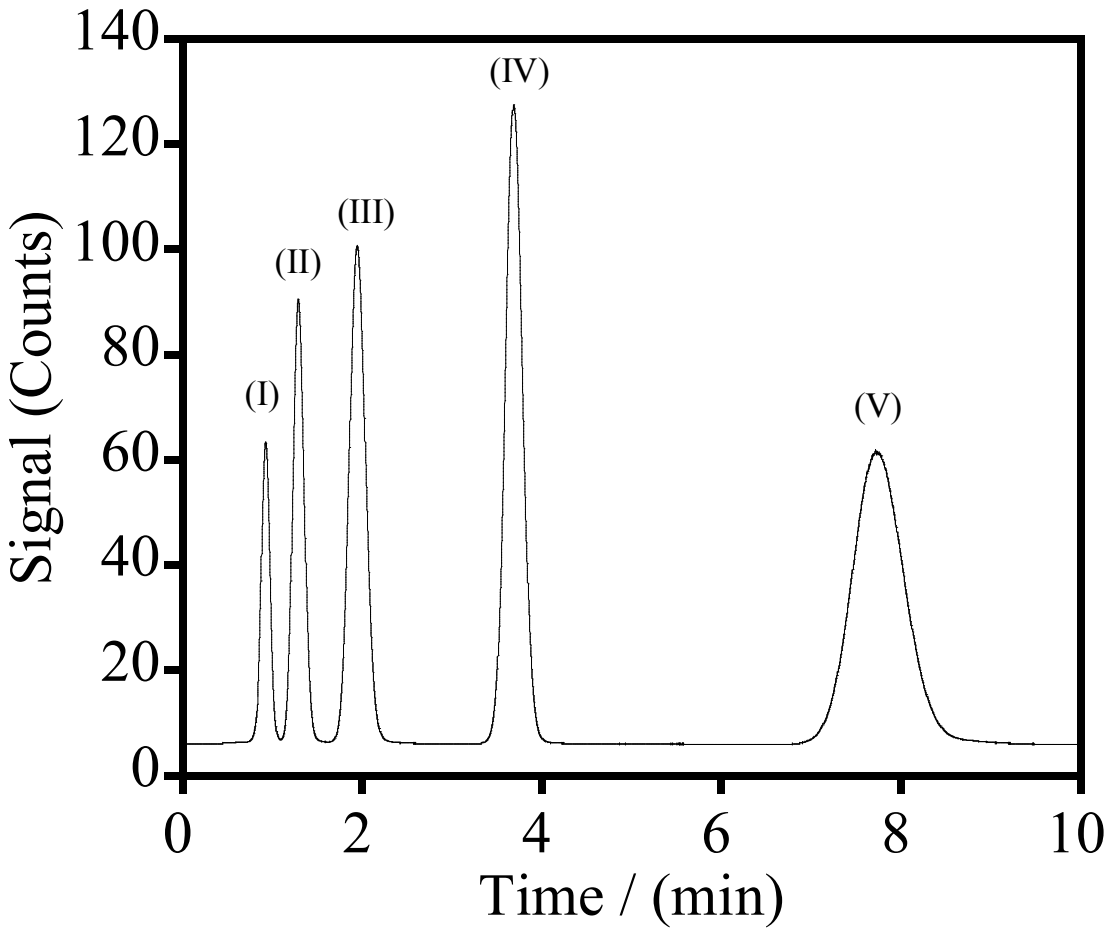

Figure 10. Representative chromatogram for multiplexed ketones (I) 2-propanone, (II) 2-butanone, (III) 2-pentanone, (IV) 2-hexanone, (V) 2-heptanone [155].

4. MEASUREMENT OF HENRY'S CONSTANTS WITH HEADSPACE GAS CHROMATOGRAPHY

4.1 Apparatus

A Hewlett-Packard (HP7694 Palo Alto, CA) automatic headspace sampler and a Hewlett-Packard (HP 6890) gas chromatograph (GC), shown in Figure 11, were used in this work. At the beginning of each experiment, a volume of solution (with or without electrolyte) was dispensed with a pipette into a glass vial (volume = 21.6 ± 0.1 ml) (Supelco, Bellefonte, PA) and the vial was immediately capped with a 20 mm diameter Teflon-faced butyl rubber septum (Supelco) and aluminum crimp ring to prevent loss of the VOC during equilibration and sampling. Each sealed vial was then placed in the 44-vial rack of the automatic sampler for equilibration in the headspace oven.

The GC was equipped with an HP INNOWax capillary column (length 15 m x inside diameter 0.53 mm with a 1 μm-thick cross linked poly(ethylene glycol) stationary phase), splitless injector port configuration and a flame ionization detector (FID), which is ideal for detecting hydrocarbons. Other typical GC conditions were: column temperature of 38 - 60 °C, injector port temperature of 250 ^{o}C, helium carrier gas flow of 10.6 ml min^{-1}, hydrogen flow rate of 40 ml min^{-1}, air flow rate of 400 ml min^{-1}, FID temperature of 250 ^{o}C, 15 - 45 min of gentle shaking for equilibration, vial pressurization time of 0.70 min, sample loop fill time of 0.02 - 0.10 min, loop equilibration time of 0.05 min and an injection time of 1.00 min. Ultra high purity helium (Air Products, 99.9995 % purity) was injected into each vial to create a pressure head and hence transfer 1 ml of the vapor phase into a heated sample loop. The vapor in the sample loop was then transferred to the GC by flow of helium carrier gas.

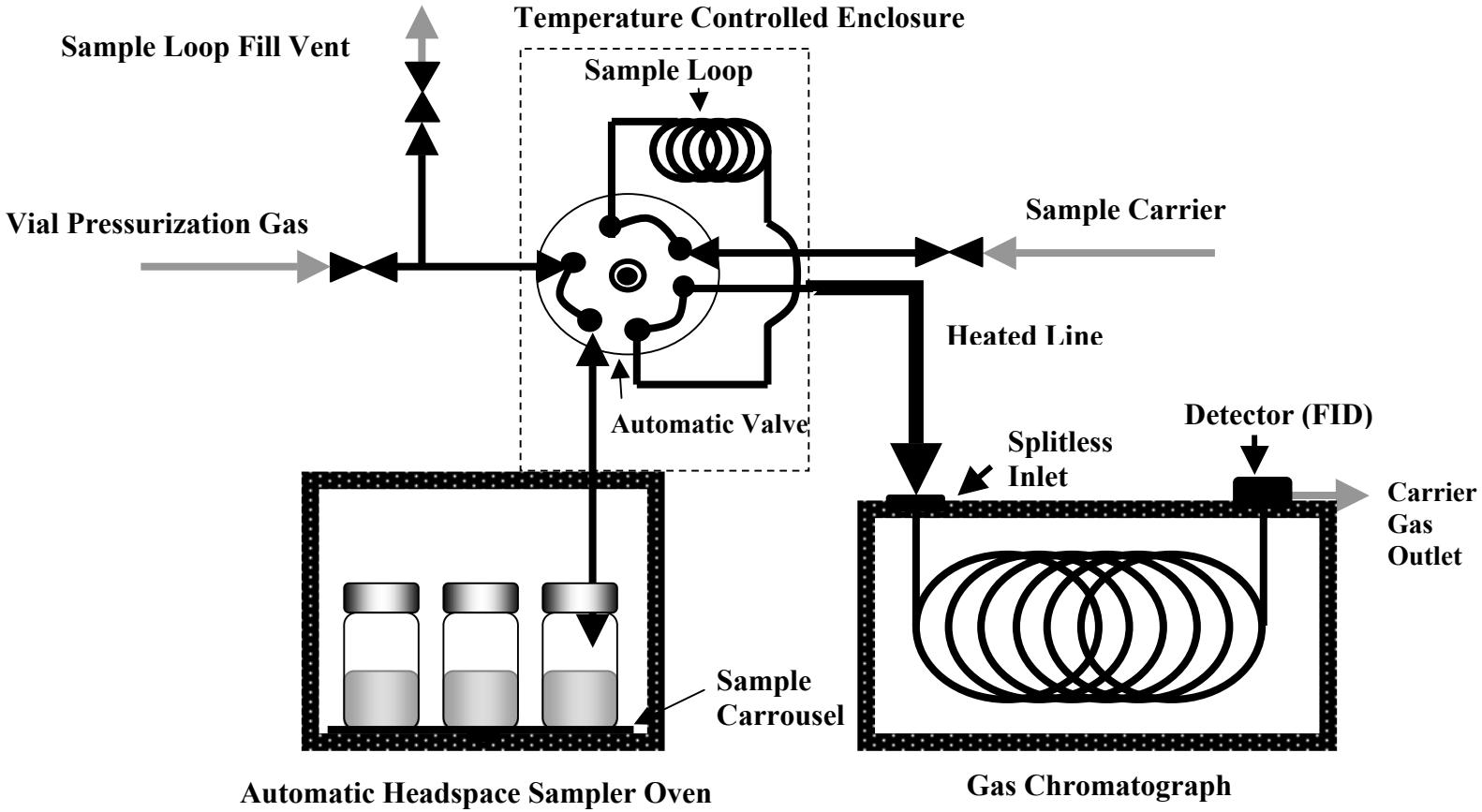

Figure 11. Schematic of the apparatus used in this work.

4.2 Materials.

1-alkanols and 2-ketones in Table 9 were selected to investigate the effects of an increasingly longer hydrophobic chain with a polar end group. Transportation fuel components in Table 9 were chosen to investigate the behavior of aromatics and *tert*butyl ethers with of alkyl substituents. Two organic sulfides in Table 9 with one and two sulfurs were chosen to investigate the effect of the disulfide bond in aqueous salt solution. The salts used in this work consisted of totally inorganic structures and structures with an organic cation. The inorganic salts in Table 10 were chosen because they reduce the solubility of organic VOCs and GHGs while the two salts with organic cations generally enhance the solubility of VOCs. The homologous 2-ketones were measured with both inorganic and organic salts to demonstrate trends that can be used to make *a priori* predictions of the salt effect.

Table 9. VOCs selected for measurements in this work.

1-alkanols	2-ketones	Transportation fuel components	sulfides
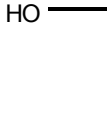	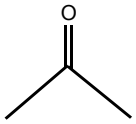	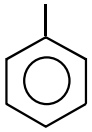	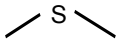
methanol	2-propanone	toluene	dimethyl sulfide
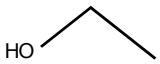	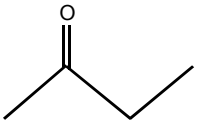	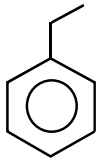	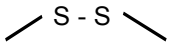
ethanol	2-butanone	ethylbenzene	dimethyl disulfide
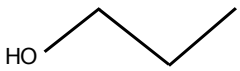	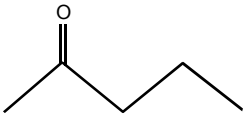	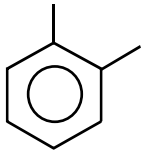	
1-propanol	2-pentanone	o-xylene	
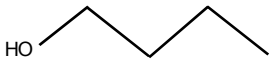	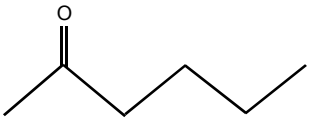	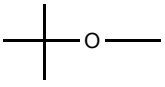	
1-butanol	2-hexanone	MTBE	
	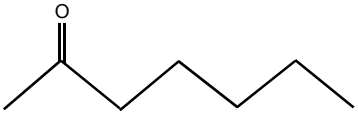	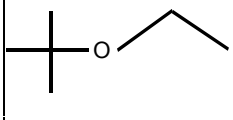	
1-pentanol	2-heptanone	ETBE	
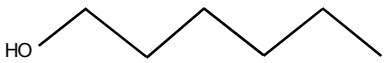			
1-hexanol			

Table 10. Salts used for experiments in this work.

Inorganic Salts	Organic Salts
Na^{+} Cl^{-} sodium chloride	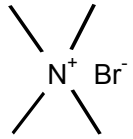 tetramethylammonium bromide
Ca^{+2} Cl_2^{-} calcium chloride	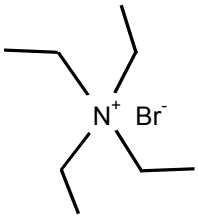 tetraethylammonium bromide
Na_2^{+} SO_4^{-2} sodium sulfate	
K_2^{+} SO_4^{-2} potassium sulfate	
Na_2^{+} CO_3^{-2} sodium carbonate	

The VOCs in Table 9 were purchased from Aldrich (Milwaukee, WI) including 1-alkanols, 2 ketones, sulfides, aromatics, and used as received. Their structures are summarized in Table 9. Purities of the VOCs are as follow: 2-propanone (> 99.5 %), 2-butanone (> 99 %), 2-pentanone (> 99.5 %), 2-hexanone (> 98 %), 2-heptanone (> 99 %), ethanol (absolute), 1-propanol (> 99 %), 1-butanol (> 99.5 %), 1-pentanol (> 98 %), 1-hexanol (> 99 %), methyl *tert*butyl ether (99.8 %), ethyl *tert*butyl ether (99 %), ethylbenzene (99.8 %), o-xylene (98 %), p-xylene (> 99 %), dimethyl sulfide (purity > 99.8 %), dimethyl disulfide (purity > 98 %).

The salts in Table 10 were purchased from Aldrich and their purities were as follows: sodium chloride (> 99.5 %), calcium chloride (> 99.5 %), sodium sulfate (> 99.9 %), potassium sulfate (> 99.9 %), sodium carbonate (> 99.9 %), tetraethylammonium bromide (> 99 %), and tetramethylammonium bromide (> 98 %). Their structures are summarized in Table 10.

Gases used for headspace analysis were purchased from Air Products (Allentown, PA) and had the following purities: ultra high purity helium (99.9995 %), ultra high purity hydrogen (99.9995 %), and ultra zero air.

4.3 Procedures

4.3.1 Systems explored with the relative method

4.3.1.1 *2-Ketones with sodium sulfate*

Several test solutions were prepared by adding 100 g of stock solution (containing 50 ppmv of each ketone) and different amounts of sodium sulfate crystals to a tared flask and weighing to ± 0.02 g on a Sartorius electronic balance (model 1404). Note that although each test solution contained different amounts of salt, the ketone concentration

in the solution was identical to that in the stock solution on a salt-free basis. The stock solution was also employed to obtain reference values of Henry's constants in the present study.

At the beginning of each experiment, 15 ± 0.06 ml of solution (with or without salt) were dispensed with a pipette into a glass vial (volume = 21.6 ± 0.1 ml) (Supelco, Bellefonte, PA) and the vial was immediately capped with a 20 mm diam. Teflon-faced butyl rubber septum (Supelco) to prevent loss of the volatile ketones. Each vial was then placed into the headspace sampler of Figure 11 for analysis. GC conditions were: column temperature of 38 °C, injector port temperature of 250 ^{o}C, helium carrier gas flow of 10.6 ml min^{-1}, hydrogen flow rate of 40 ml min^{-1}, air flow rate of 400 ml min^{-1}, FID temperature of 250 ^{o}C, 45 min of gentle shaking for equilibration, vial pressurization time of 0.70 min, sample loop fill time of 0.10 min, loop equilibration time of 0.05 min and an injection time of 1.00 min.

Reference values of Henry's constants of the VOC in pure water were obtained using the differential headspace technique of Chai and Zhu [67]. 5.00 ± 0.01 ml, 1.00 ± 0.01 ml or 0.050 ± 0.001 ml of the salt-free solution (VOC + water) were dispensed into glass vials with a glass pipette (Fisher) or a 50 μL micro-syringe (Supelco). A liquid ratio (ratio of initial liquid volumes in two vials) of 5 ml : 0.050 ml was employed for measurements at 50 ^{o}C and 60 ^{o}C, and a ratio of 1 ml : 0.050 ml was employed for measurements at 70 ^{o}C and 80 ^{o}C.

4.3.2 Henry's constants from the differential method

It is necessary to employ the differential method when the VOC is very sparingly soluble or if the salt is available in very limited quantities.

4.3.2.1 *Aromatics, ethers, and sulfides*

A water and VOC stock solution was prepared by adding several microliters of each VOC to two liters of water and stirring to obtain a homogeneous solution (Table 11). The dimethyl sulfide and dimethyl disulfide stock solution was prepared separately from the stock solution containing transportation fuel components. Since the INNOWAX GC column could not resolve signals for MTBE and ETBE mixed together, it was necessary to prepare two stock solutions: one containing MTBE and aromatics and another containing ETBE and aromatics. The aromatics had sufficiently high retention times to not interfere with MTBE and ETBE and were included in both stock solutions to verify consistency of the measurements. To formulate each of the stock solutions at different salt concentrations, different amounts of salt were added to tared flasks each containing 100 g of the stock solution. Stock solution was weighed on an electronic balance (Sartorius model 1404, Edgewood, NY) and salt was weighed on an analytical balance (Mettler model AE 163, Hightstown, NJ).

Test samples containing MTBE, ETBE, and aromatics were prepared by dispensing a 5.00 ± 0.06 ml major volume with a glass volumetric pipette (VWR, West Chester, PA) of a test solution into a 21.6 ± 0.1 ml glass vial (Agilent, Palo Alto, CA). A 1.00 ± 0.01 ml minor volume was pipetted into an identical glass vial using a Fisher (Fair Lawn, NJ) Finnpipette®. Test samples containing disulfides and sodium sulfate were prepared by dispensing a 5.00 ± 0.06 ml major volume of the test solution into a 21.6 ± 0.1 ml glass vial with a volumetric glass pipette and a 0.25 ± 0.01 ml minor volume was

Table 11. Component concentrations for aromatics, ethers, and sulfides.

VOC	VOC Concentration in Stock Soln. (ppmv**)	Salt	Salt Concentration Range (m*)
MTBE	24	NaCl	0.5, 1.0
ETBE	24	NaCl	0.5, 1.0
toluene	20	NaCl	0.5, 1.0
o-xylene	20	NaCl	0.5, 1.0
ethylbenzene	20	NaCl	0.5, 1.0
dimethyl sulfide	12	Na_2SO_4	0.6
dimethyl disulfide	6	Na_2SO_4	0.6

**parts per million on a volumetric basis.
*molality

pipetted into an identical glass vial using a Fisher Finnpipette®. After each vial was filled with VOC-containing solution, the vials were immediately capped with 20 mm diameter Teflon-faced butyl rubber septa (Agilent) to prevent loss of the VOC. The headspace sampler carrousel was loaded with the vials and the set for each temperature included 4 vials (two identical major and minor liquid volumes to gauge reproducibility within a run) for the Henry's constant in pure water and with two salt concentrations listed in Table 11 for a total of 16 vials analyzed at each temperature listed in Tables 18 and 19. Three runs were performed (one per day) with new samples at each of the four temperatures to obtain the standard deviation for each reported Henry's constant in Tables 18 and 19.

The GC peak area count vs. equilibration time was plotted as described previously [155] for the largest sample size of 5.0 ml and showed that the area count approached a constant value after 15 min for gasoline components (aromatics and ethers) at 313 K. This equilibration time was therefore used for both 1 ml and 5 ml samples. The 5.00 ml samples of sulfides and water were found to equilibrate in 25 minutes at 313 K. Therefore an equilibration time of 25 minutes was assumed for both 0.25 ml and 5.00 ml samples containing the sulfides.

4.3.2.2 *2-Ketones with tetraalkylammonium bromide salts.*

A fresh water and VOC stock solution was prepared for use with tetraethylammonium bromide and tetraethylammonium bromide by adding 50 microliters of each 2-ketone (2-propanone to 2-heptanone to one liter of water and stirring to obtain a homogeneous solution. To formulate each of the stock solutions at the three concentrations, different amounts of salt were added to tared flasks each containing 60 g

of the stock solution to minimize salt usage for each day's run. Stock solution was weighed on an electronic balance (Sartorius model 1404, Edgewood, NY) and salt was weighed on an analytical balance (Mettler model AE 163, Hightstown, NJ).

Test samples containing 2-ketones with and without tetraalkylammonium salts were prepared by dispensing a 5.00 ± 0.06 ml major volume with a glass volumetric pipette (VWR, West Chester, PA) of a test solution into a 21.6 ± 0.1 ml glass vial (Agilent, Palo Alto, CA). A 100 ± 0.1 μl minor volume was pipetted into an identical glass vial using a Fisher (Fair Lawn, NJ) Finnpipette®. After each vial was filled with VOC-containing solution, the vials were immediately capped with 20 mm diameter Teflon-faced butyl rubber septa (Agilent) to prevent loss of the VOC. The headspace sampler carrousel was loaded with the vials and the set for each temperature included 4 vials (two identical major and minor liquid volumes to gauge reproducibility within a run) for the Henry's constant in pure water and with three salt concentrations ranging from 0.5 to 3.0 molal for a total of 12 vials analyzed at each temperature listed in Tables 16 and 17. Three runs were performed (one per day) with new samples at each of the four temperatures to obtain the standard deviation for each reported Henry's constant in Tables 16 and 17.

4.3.2.3 *2-Ketones with mixtures of sodium sulfate and sodium chloride.*

A water and VOC stock solution for use with the salt mixture in this study was prepared by adding 50 microliters of each 2-ketone (2-propanone to 2-heptanone) to one liter of water and stirring to obtain a homogeneous solution. To formulate each of the stock solutions at different salt concentrations, different amounts of salt were added to tared flasks each containing 100 g of the stock solution. The total salt concentration was held constant at two molal for all solutions created from salt mixtures, while the composition was adjusted to vary the molar ratio of NaCl to Na_2SO_4 from 0.25 : 0.75 to

0.75 : 0.25. Stock solution was weighed on an electronic balance (Sartorius model 1404, Edgewood, NY) and salt was weighed on an analytical balance (Mettler model AE 163, Hightstown, NJ).

Test samples containing 2-ketones were prepared by dispensing a 5.00 ± 0.06 ml major volume with a glass volumetric pipette (VWR, West Chester, PA) of a test solution into a 21.6 ± 0.1 ml glass vial (Agilent, Palo Alto, CA). A 100 ± 0.1 μl minor volume was pipetted into an identical glass vial using a Fisher (Fair Lawn, NJ) Finnpipette®. After each vial was filled with VOC-containing solution, the vials were immediately capped with 20 mm diameter Teflon-faced butyl rubber septa (Agilent) to prevent loss of the VOC. The headspace sampler carrousel was loaded with the vials and the set for each temperature included 4 vials (two identical major and minor liquid volumes to gauge reproducibility within a run) for the Henry's constant in pure water and with three salt compositions for a total of 12 vials analyzed at each temperature listed in Table 15. Three runs were performed (one per day) with new samples at each of the four temperatures to obtain a standard deviation for each reported Henry's constant in Table 15.

4.4 Results: Measured Henry's constants.

4.4.1 2-Ketones + water + Na_2SO_4.

Reference values of dimensionless Henry's constants of the five 2-ketones in pure water were measured at 50 ^{o}C to 80 ^{o}C using the differential method of Chai and Zhu [1, 67]. The Henry's constants with 0.2 to 1.0 molal sodium sulfate were measured with the relative method of Chai et al. [155]. The Henry's constants of all 2-ketones increase as temperature increases, indicating a decrease in VOC solubility due to enthalpic effects [131]. Increasing the sodium sulfate concentration also increases the Henry's constants

for 2-ketones and decreases the VOC solubility. The salt effect observed for inorganic salts is caused by the salt fixing water molecules, which reduces the number of water molecules available to solvate the VOC. The salt has a more pronounced salting out effect on the 2-ketones of higher molecular weight since their longer hydrophobic tail makes them less likely to dissolve in water [156]. The results are presented in Table 12 together with their experimental errors (< 14 %).

Measured Henry's constants of 2-ketones and sodium chloride, as well as sodium chloride and 1-alkanols are listed in Table 13. Experimental uncertainties were less than 13 %. As can be deduced from data in Table 13, the 2-ketones and the alkanols were "salted out" by sodium chloride. The salt effect was noticeably less with sodium chloride on the molal basis. This can be attributed to the chloride ion's inability to fix as many water molecules around itself as the sulfate ion [156]. Solubility of 2-ketones also decreases as the molecular weight increases showing that it is increasingly a challenge to keep the more hydrophobic molecule in solution with the addition of more sodium chloride.

Measured Henry's constants of 2-ketones are listed in Table 15. Experimental uncertainties were less than 12 % for all 2-ketones with the exception of one data point for 2-hexanone at 353 K and one for 2-heptanone at 353 K with a 0.25 : 0.75 molal ratio. As can be deduced from Table 15, the 2-ketones were also "salted out" by mixtures of sodium chloride and sodium sulfate. Henry's constants for 2-hexanone with pure NaCl at 1.0 molal and pure Na_2SO_4 were plotted in Figure 13 along with the systems with NaCl / Na_2SO_4 mixtures to examine the consistency of the mixture Henry's constants. The additive effects of the salts in the mixture were scaled appropriately with molal ionic

strength causing the Henry's constants of 2-hexanone in the presence of the $NaCl/Na_2SO_4$ salt mixture with an ionic strength of 3 to equal the 2-hexanone Henry's constants with a pure sodium sulfate solution having an ionic strength of 3.

To examine the effect of salts with organic cations on the solubility of the homologous 2-ketones series, tetraethylammonium bromide (TEA-Br) and tetramethylammonium bromide were selected since they are soluble in water to over 3 molal and have a simple inorganic anion. It was found that TEA-Br enhanced the solubility of 2-propanone to 2-heptanone and reduced the solubility of 2-propanone as the salt concentration was increased from 0.5 to 3.0 molal. The salting in effect with 2-heptanone is shown in Figure 14 and the salting out effect with 2-butanone is shown in Figure 15. The Henry's constants for 2-propanone, 2-pentanone, 2-hexanone and 2-heptanone with TEA-Br were determined with an experimental error not exceeding 13 %. The 2-butanone Henry's constants could not be resolved as a unique signal since an impurity peak had the same retention time.

The influence of tetramethylammonium bromide (TMA-Br) on the homologous 2-ketone series was also investigated to examine the effect of lower dispersion forces from the cation. The Henry's constants of 2-heptanone with TMA-Br were plotted from 313 to 343 K in Figure 16 and show that the solubility enhancement remains constant with temperature just as with TEA-Br and the salt effect of TMA-Br is significantly lower than TEA-Br from 0.5 to 3.0 molal showing the difference that one carbon unit makes. The experimental error for most Henry's constants was below 15 %. Two volatile impurities were eluted from the column at the same retention times as 2-propanone and 2-butanone thereby obscuring their signals.

Measured Henry's constants of 1-alkanols are listed in Table 14. Experimental uncertainties were less than 15 %. As can be deduced from these tables, the 1-alkanols were also salted out by sodium sulfate. A representative plot of the Henry's constants of 1-butanol with sodium sulfate is shown by Figure 12. The degree of the salt effect was noticeably lower per molal of salt for 1-alkanols in the presence of sodium sulfate. The lower salt effect can be attributed to the fact that 1-alkanols can hydrogen bond to water keeping them in the liquid phase more so than the carbonyl dipole of the 2-ketones.

Table 12. Henry's constants for 2-ketones in aqueous Na_2SO_4 solutions.

	T / K	pure water		0.2 molal		0.4		0.6		0.8		1.0	
		H/kPa	err*/kPa	H	err	H	err	H	err	H	SD	H	err
	323	690	16	780	97	900	38	1060	36	1220	46	1430	33
	333	1020	22	1160	130	1340	86	1520	24	1800	40	2060	31
2-propanone	343	1490	40	1690	120	1910	130	2170	130	2400	120	2870	130
	353	2090	23	2360	54	2640	71	2980	120	3500	96	4120	130
	323	1170	26	1370	52	1650	46	1990	44	2390	61	2900	41
	333	1780	30	2110	34	2530	36	3010	49	3700	48	4420	44
2-butanone	343	2670	100	3140	230	3680	240	4380	250	5030	240	6250	260
	353	3730	73	4400	145	5110	200	5990	290	7250	240	8840	260
	323	1820	32	2230	37	2760	65	3420	98	4280	75	5310	86
	333	2830	42	3500	67	4280	71	5260	108	6670	58	8230	98
2-pentanone	343	4300	130	5230	180	6280	180	7720	194	9120	196	11720	198
	353	6290	180	7770	320	9300	440	11240	571	13850	500	17410	380
	323	2430	90	3190	108	4100	120	5180	160	6740	140	8520	150
	333	3820	117	5070	220	6440	180	8100	210	10610	153	13370	220
2-hexanone	343	5730	570	7400	630	9300	680	11670	720	14180	780	17930	870
	353	9370	860	11890	1070	14760	1250	18020	1440	22530	1450	29190	1150
	323	3630	45	4890	130	6360	96	8280	81	11180	111	14550	150
	333	5680	510	7720	590	9930	570	12900	585	17370	650	22520	780
2-heptanone	343	9510	1040	12560	1200	15910	1380	20570	1416	25810	1490	33070	1750
	353	15830	1530	20550	2120	25850	2310	31970	2481	40350	2670	49550	3010

*err = experimental error determined with Eq. 157

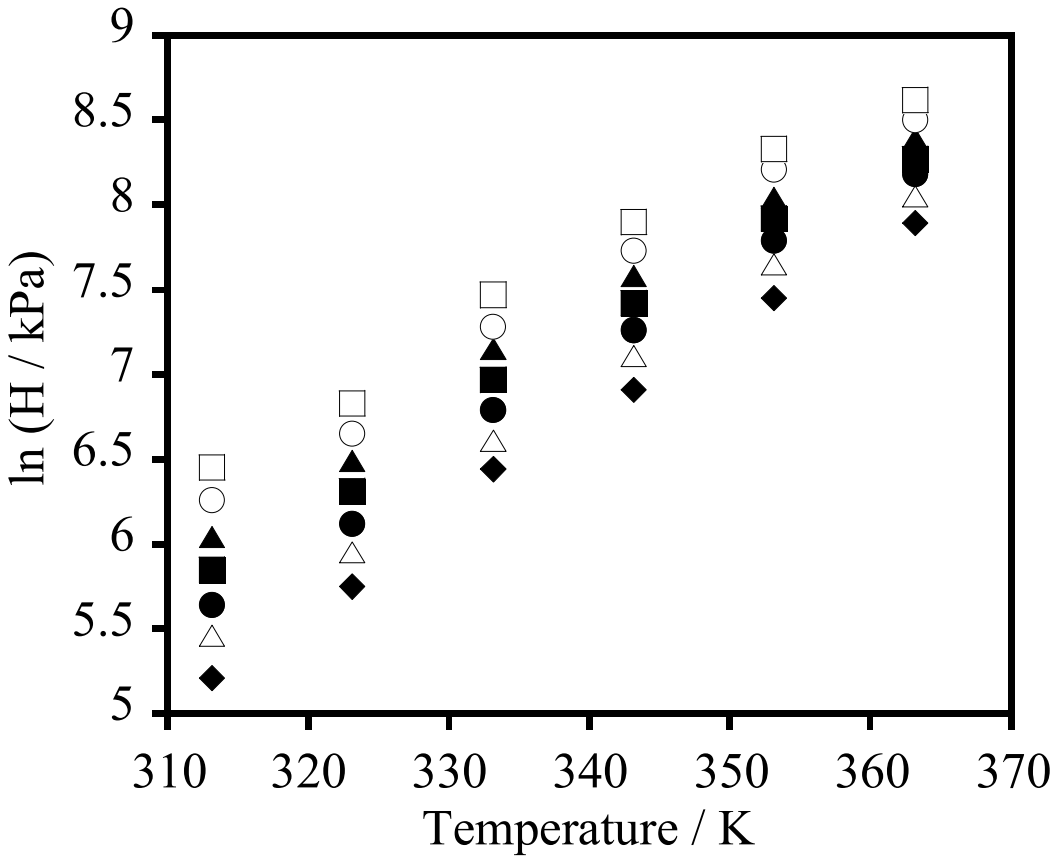

Figure 12. Henry's constants for 1-butanol [151] in (◆) pure water and in aqueous Na_2SO_4 solutions: (△) 0.2 m, (●) 0.4 m, (■) 0.6 m, (▲) 0.8 m, (○) 1.0 m, and (□) 1.2 m.

Table 13. Henry's constants for 2-ketones in aqueous NaCl solutions [151].

	T / K	pure water		0.2 molal		0.4		0.6		0.8		1.0		1.2	
		H/kPa	err*/kPa	H	err	H	err	H	err	H	SD	H	err	H	err
	313	454	18	629	62	497	29	523	45	542	34	569	54	600	53
	323	686	16	892	97	718	38	763	36	789	46	824	33	866	41
	333	1016	22	1310	130	1089	86	1090	24	1150	40	1250	31	1301	37
2-propanone	343	1489	40	1500	120	1570	130	1600	130	1680	120	1830	130	1880	130
	353	2086	23	2207	54	2295	71	2420	120	2496	96	2660	130	2790	140
	363	2910	160	3180	260	3320	290	3500	270	3560	240	3900	280	4090	340
	313	721	3	767	4	794	41	842	72	883	52	940	70	1006	73
	323	1167	26	1301	52	1252	46	1362	44	1436	61	1520	41	1614	53
	333	1775	30	1982	34	1906	36	1965	49	2114	48	2359	44	2480	42
2-butanone	343	2670	100	2740	230	2920	240	3010	250	3170	240	3510	260	3660	270
	353	3733	73	3906	145	4120	200	4400	290	4590	240	4910	260	5250	310
	363	4960	480	5030	580	5300	630	5640	640	5820	620	6410	700	6800	790
	313	1149	32	1243	37	1321	65	1420	98	1508	75	1619	86	1759	86
	323	1819	42	1950	60	1991	54	2214	56	2371	77	2538	60	2721	71
	333	2826	42	3063	67	3124	71	3207	108	3510	58	4013	98	4251	80
2-pentanone	343	4300	130	4630	180	5020	180	5228	194	5556	196	6217	198	6580	220
	353	6290	180	6640	320	7090	440	7636	571	8050	500	6640	380	7170	450
	363	8690	440	9440	800	10070	880	10780	880	11240	790	12490	940	13410	1140
	313	1497	90	1630	108	1770	120	1930	160	2070	140	2240	150	2460	160
	323	2429	16	2602	29	2704	25	3056	21	3322	57	3589	27	3874	31
	333	3822	117	4160	220	4320	180	4440	210	4930	153	5740	220	6130	210
2-hexanone	343	5740	570	6280	630	6900	680	7260	720	7780	780	8790	870	9420	930
	353	9370	860	10020	1070	10840	1250	11800	1440	12590	1450	10440	1150	11390	1290
	363	11900	1330	12930	1660	13830	1850	14910	1950	15800	1940	17760	2240	19170	2530
	313	2220	45	2340	130	2583	96	2845	81	3080	111	3340	150	3690	170
	323	3630	150	3910	170	3960	180	4635	199	5120	240	5610	240	6010	260
	333	5680	510	6330	590	6500	570	6417	585	7270	650	8910	780	9430	820
2-heptanone	343	9510	1040	10510	1200	11670	1380	12385	1416	13370	1490	15250	1750	16470	1880
	353	15830	1670	16660	1840	18240	1980	20019	2189	21660	2350	17950	1960	19720	2140
	363	21730	1530	23310	2120	25270	2310	27396	2481	29360	2670	33250	3010	36140	3280

*err = experimental error determined with Eq. 157

Table 14. Henry's constants for 1-alkanols in aqueous Na_2SO_4 solutions [151].

	T / K	Pure water		0.2 molal		0.4		0.6		0.8		1.0		1.2	
		H/kPa	err*/kPa	H	err	H	err	H	err	H	err	H	err	H	err
	313	68	4	81	9	91	11	110	10	120	10	140	10	160	10
	323	144	17	167	20	180	20	210	30	240	30	260	30	300	40
	333	251	23	280	30	320	30	360	30	400	40	430	40	490	50
ethanol	343	382	24	430	30	460	30	520	40	570	40	620	50	700	50
	353	613	97	690	110	760	120	800	130	850	140	950	150	1020	170
	363	950	130	1020	150	1120	160	1170	170	1230	170	1300	180	1400	190
	313	126	8	150	20	180	20	220	30	250	30	310	30	360	30
	323	220	20	270	26	310	30	360	40	420	40	480	50	560	60
	333	382	16	440	20	515	23	599	25	690	30	770	30	910	40
1-propanol	343	626	16	739	21	835	27	950	50	1090	50	1230	50	1410	70
	353	1070	100	1270	130	1430	140	1570	160	1720	180	1980	210	2180	240
	363	2030	220	2300	250	2570	290	2760	320	2990	350	3250	360	3580	400
	313	184	6	230	20	280	20	350	30	420	40	520	30	631	36
	323	310	30	380	40	450	40	550	50	660	60	780	80	920	100
	333	624	22	742	29	888	33	1064	38	1275	47	1460	50	1760	60
1-butanol	343	1000	30	1221	37	1428	48	1665	80	1960	90	2284	100	2690	130
	353	1730	140	2100	180	2430	200	2760	260	3110	290	3680	350	4160	400
	363	2680	280	3120	330	3570	380	3910	440	4400	480	4900	510	5560	580
	313	160	10	210	20	260	20	330	30	410	40	523	39	650	50
	323	369	98	455	32	550	40	690	50	850	60	1030	90	1270	110
	333	683	63	830	23	1017	26	1250	30	1549	39	1820	45	2256	53
1-pentanol	343	1180	130	1479	44	1784	62	2130	109	2570	127	3072	157	3700	200
	353	2000	400	2510	180	2970	200	3480	280	4030	330	4890	390	5700	460
	363	3410	580	4080	400	4780	480	5360	570	6250	623	7140	690	8380	810
	313	360	20	520	50	675	57	890	80	1130	90	1486	94	1910	120
	323	620	50	768	58	945	71	1210	100	1520	120	1905	167	2400	230
	333	1137	22	1374	28	1721	43	2162	43	2760	60	3340	70	4230	90
1-hexanol	343	1840	32	2336	74	2905	110	3553	196	4291	221	5460	320	6740	390
	353	3140	180	4010	265	4850	290	5890	450	7010	526	8740	630	10490	780
	363	4510	400	5520	510	6660	620	7680	790	9290	860	10900	990	13210	1180

*err = experimental error determined with Eq. 157

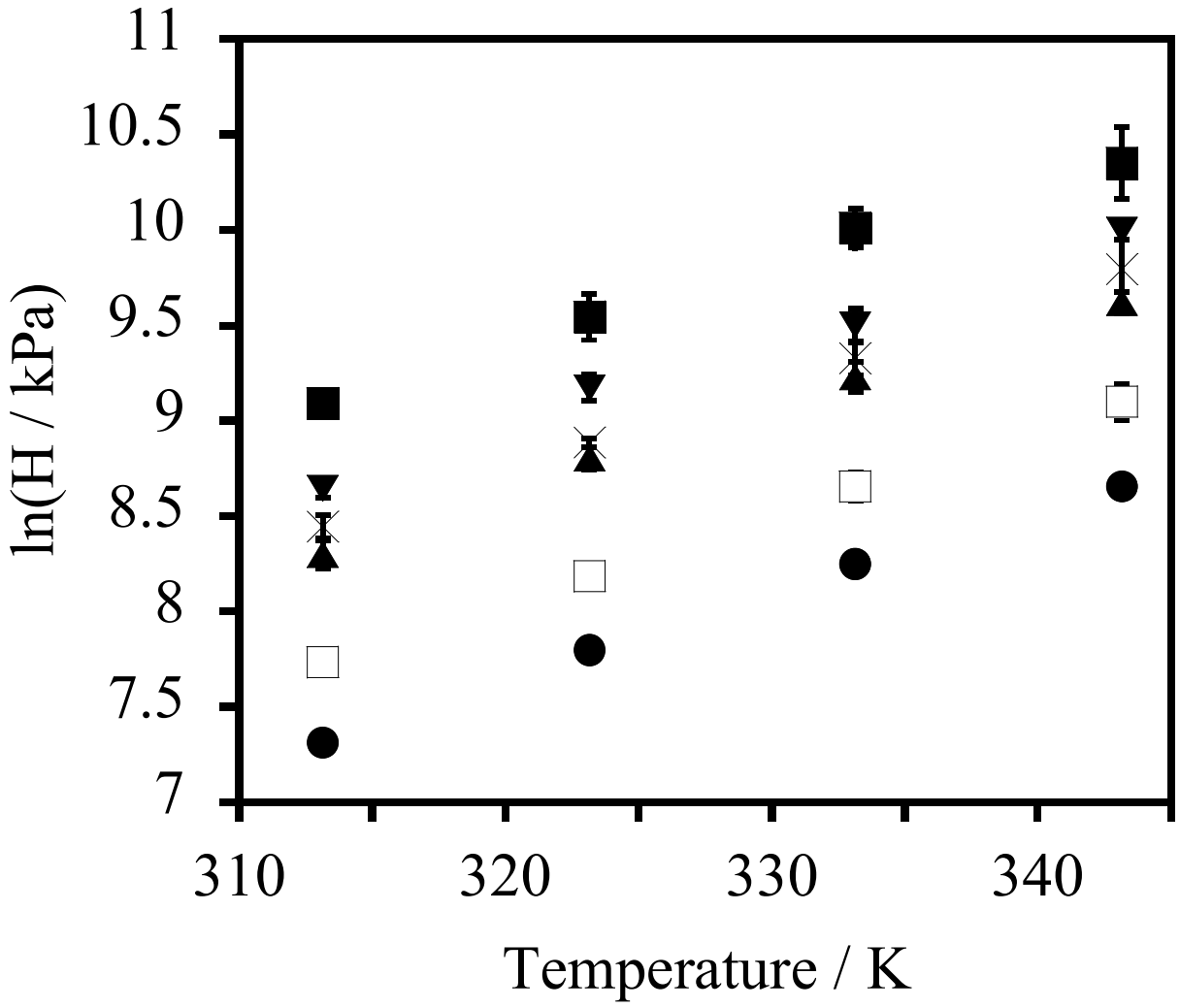

Figure 13. 2-hexanone in (●) pure water [157] and with NaCl and Na_2SO_4: (□) 1.0 m NaCl (I = 1.0) [157], (▲) 75 mole % NaCl : 25% Na_2SO_4 (I = 3.0) [157], (×) 1.0 m Na_2SO_4 (I = 3.0) [157], (▼) 50 % NaCl : 50 % Na_2SO_4 (I = 4) [157], (■) 25 % NaCl : 75 % Na_2SO_4 (I = 5) [157].

Table 15. Henry's constants of 2-ketones with mixtures of NaCl and Na_2SO_4 [157].

	T / K	0.50 : 1.50[a] NaCl : Na_2SO_4		1.00 : 1.00[a] NaCl : Na_2SO_4		1.50 : 0.50[a] NaCl : Na_2SO_4	
		H / kPa	err[b] / kPa	H	err	H	err
2-propanone	323	1380	47	1000	46	800	51
	333	2020	160	1610	63	1280	114
	343	3100	203	2150	144	1830	129
	353	4180	688	3340	98	2500	158
2-butanone	323	2840	140	1980	103	1510	105
	333	4360	4363	3240	168	2410	169
	343	6670	495	4410	293	3560	243
	353	9130	1559	6990	247	4990	309
2-pentanone	323	5410	340	3650	194	2680	196
	333	8490	8494	6050	363	4320	262
	343	13210	1140	8350	606	6510	468
	353	18340	3302	13430	559	9280	523
2-hexanone	323	8850	499	5700	306	4030	307
	333	14010	14010	9630	669	6660	390
	343	22310	2294	13420	1133	10220	821
	353	31630	6132	21980	1043	15020	814
2-heptanone	323	14970	950	9160	491	6330	499
	333	23830	23829	15960	1346	10750	641
	343	39040	5205	22200	2278	16620	1500
	353	56140	13387	37010	1853	25140	1952

[a]Moles of salt
[b]standard deviation

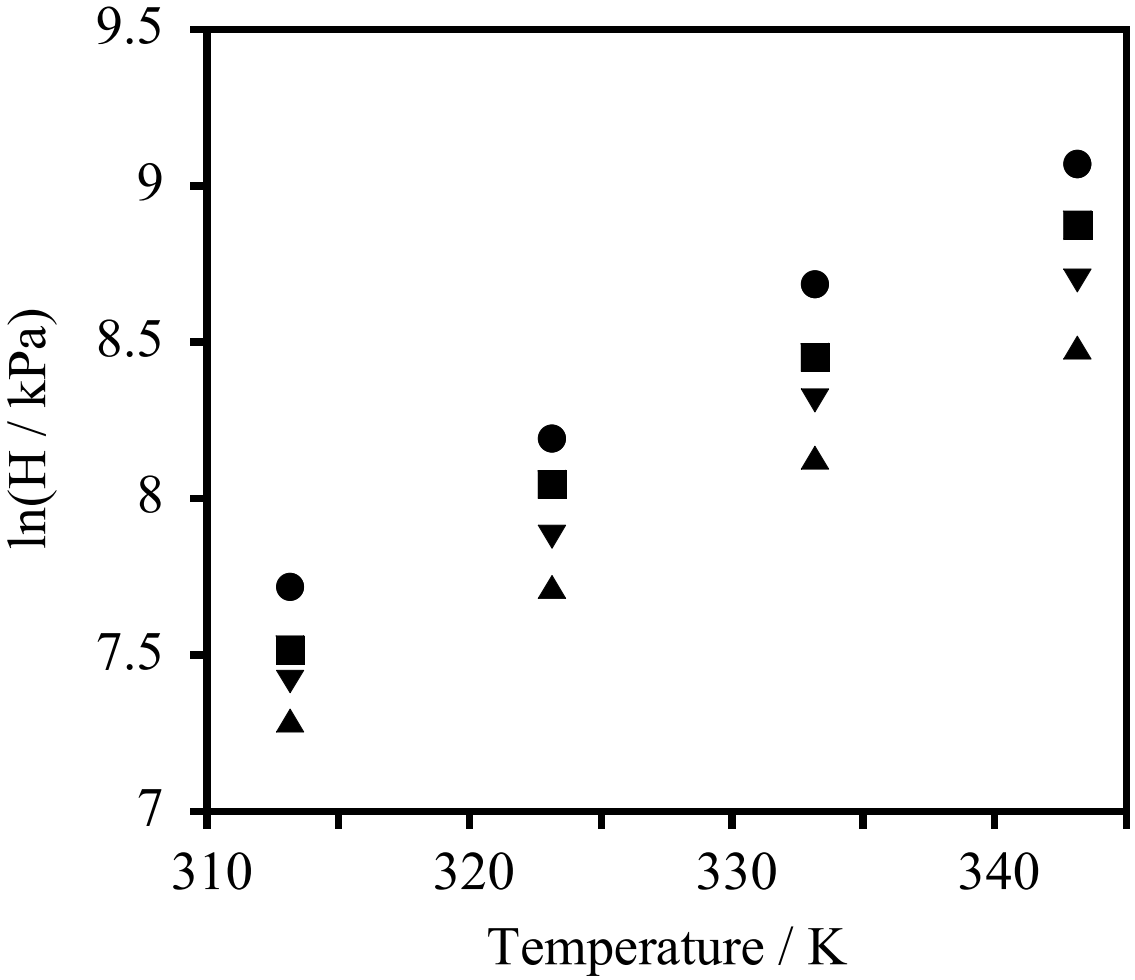

Figure 14. 2-heptanone in (●) pure water [151], (■) with 0.5 m tetraethylammonium bromide (TEA-Br) [157], (▼) with 1.0 m TEA-Br [157], (▲) with 3.0 m TEA-Br [157].

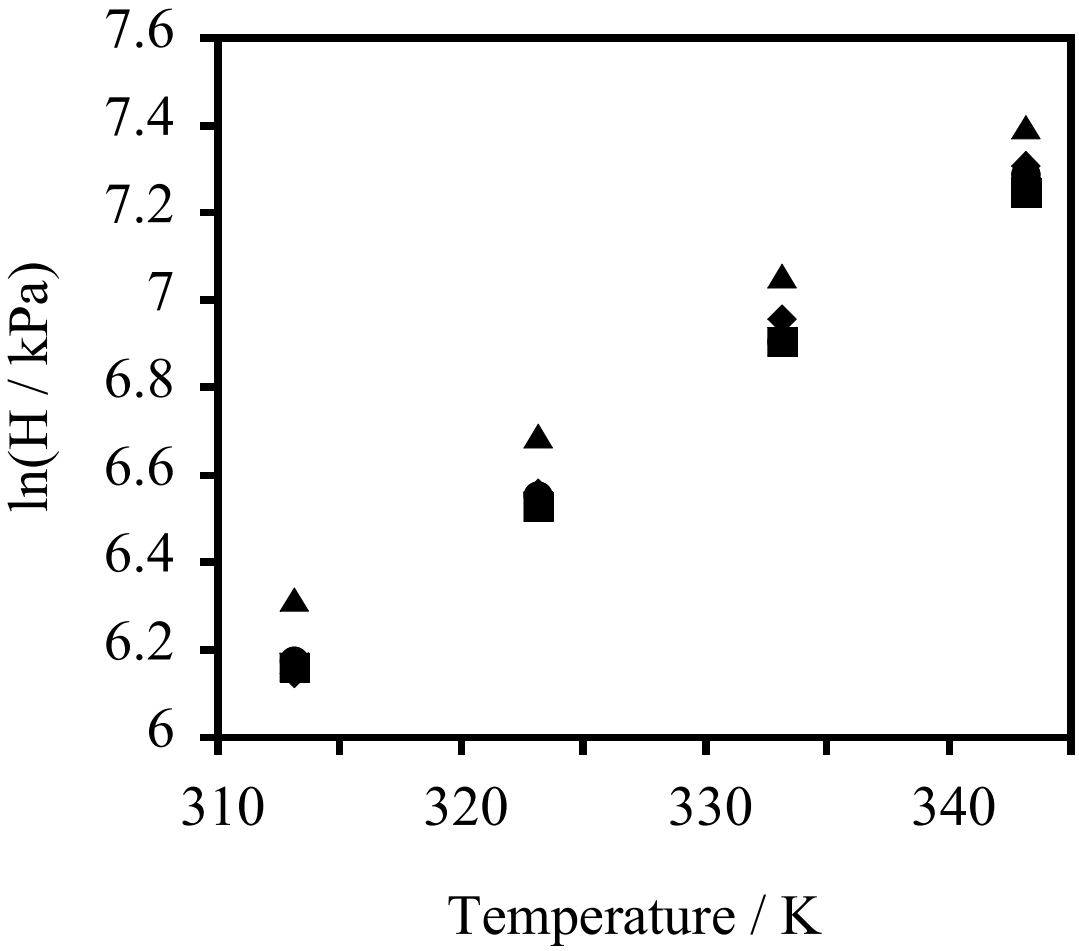

Figure 15. 2-propanone in (●) pure water [151], (■) with 0.5 m tetraethylammonium bromide (TEA-Br) [157], (▼) with 1.0 m TEA-Br [157], (▲) with 3.0 m TEA-Br [157].

Table 16. Henry's constants of 2-ketones with tetraethylammonium bromide.

	T / K	0.5 m		1.0 m		3.0 m	
		H / kPa	err[b] / kPa	H	err	H	err
2-propanone	323	480	47	480	53	550	37
	333	700	76	690	54	800	65
	343	1000	82	1000	15	1160	56
	353	1460	68	1370	82	1630	93
2-butanone	323	N/A	N/A	N/A	N/A	N/A	N/A
	333	N/A	N/A	N/A	N/A	N/A	N/A
	343	N/A	N/A	N/A	N/A	N/A	N/A
	353	N/A	N/A	N/A	N/A	N/A	N/A
2-pentanone	323	1070	99	990	86	1020	55
	333	1760	59	1540	131	1540	116
	343	2490	233	2310	74	2280	93
	353	3750	261	3270	246	3190	132
2-hexanone	323	1360	127	1230	108	1190	65
	333	2240	163	1960	172	1900	207
	343	3330	329	3000	124	2720	113
	353	5080	418	4270	318	3840	134
2-heptanone	323	1850	181	1670	108	1470	75
	333	3130	238	2650	172	2250	170
	343	4710	517	4090	124	3400	146
	353	7180	705	5820	318	4840	157

[a]Standard deviation

N/A = Data signal obscured by impurity peak

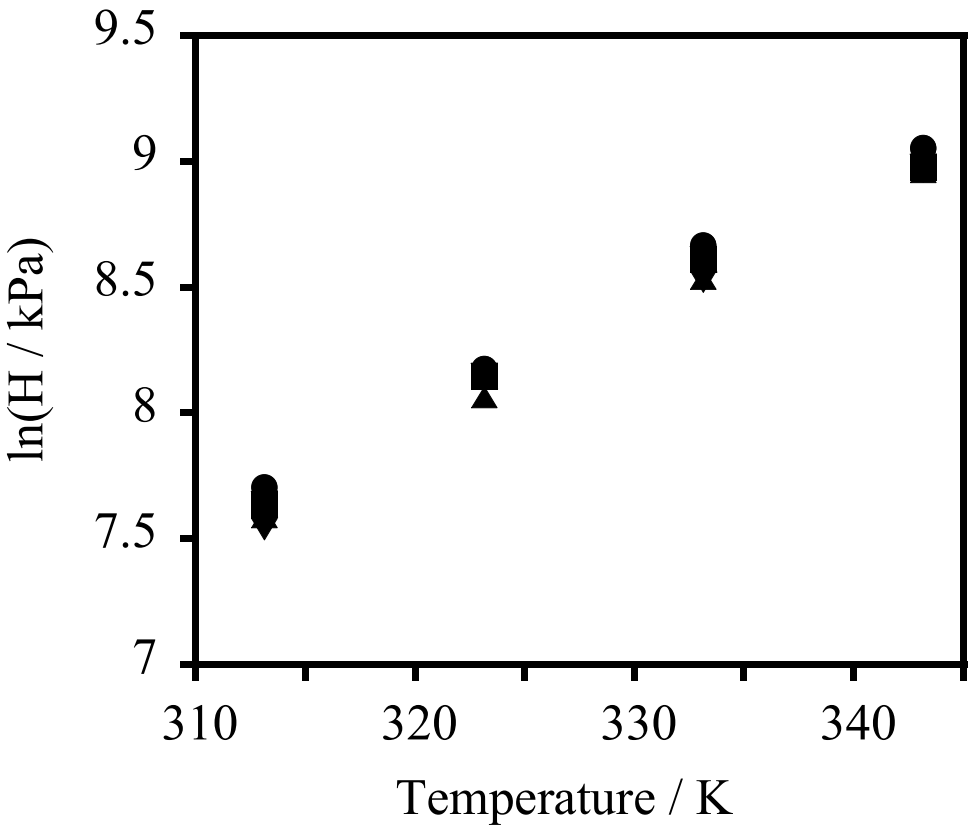

Figure 16. 2-heptanone in (●) pure water [151], (■) with 0.5 m tetramethylammonium bromide (TMA-Br) [157], (▼) with 1.0 m TMA-Br [157], (▲) with 3.0 m TMA-Br [157].

Table 17. Henry's constants of 2-ketones with tetramethylammonium bromide.

	T / K	0.5 m		1.0 m		3.0 m	
		H / kPa	err[b] / kPa	H	err	H	err
2-propanone	323	N/A	N/A	N/A	N/A	N/A	N/A
	333	N/A	N/A	N/A	N/A	N/A	N/A
	343	N/A	N/A	N/A	N/A	N/A	N/A
	353	N/A	N/A	N/A	N/A	N/A	N/A
2-butanone	323	N/A	N/A	N/A	N/A	N/A	N/A
	333	N/A	N/A	N/A	N/A	N/A	N/A
	343	N/A	N/A	N/A	N/A	N/A	N/A
	353	N/A	N/A	N/A	N/A	N/A	N/A
2-pentanone	323	1140	102	1080	44	1230	128
	333	1760	172	1760	140	1830	192
	343	2680	353	2680	254	2790	353
	353	3790	258	3980	305	4020	840
2-hexanone	323	1480	119	1370	37	1370	292
	333	2410	243	2310	187	2120	209
	343	3790	568	3540	297	3660	459
	353	5410	419	5400	447	5500	390
2-heptanone	323	2080	171	1880	45	1980	173
	333	3460	355	3440	336	3180	340
	343	5540	842	5040	412	5110	655
	353	7950	648	7790	680	7760	546

[a]Standard deviation
N/A = Data signal obscured by impurity peak

4.4.2 Transportation fuel components and organic sulfides.

Measured Henry's constants of aromatic gasoline components including toluene, ethylbenzene, and o-xylene are listed in Table 18. A representative plot of data for o-xylene in sodium chloride solutions is shown in Figure 17. The solubility was the lowest when the ethyl group was present, somewhat higher when one methyl group was present and highest when two methyl groups were present. The ethyl group enhances the dipole moment of ethylbenzene over toluene, however it is bulkier which prevents it from having stronger interactions with salts and water. The addition of a second methyl group enhances the dipole moment of the o-xylene over that of toluene and ethylbenzene while maintaining the overall compactness of toluene.

A comparison of the Henry's constants of common gasoline combustion enhancers methyl *tert*butyl ether (MTBE) and ethyl tertbutyl ether (ETBE) in Table 18 shows that the extension of the methyl group to an ethyl group reduces its solubility just as going from toluene to ethylbenzene results in reduced solubility. The average experimental uncertainty for the gasoline components was 6 % in pure water and 10 % for solutions with 0.5 and 1.0 molal NaCl.

An investigation of the two organic sulfur compounds dimethyl sulfide (DMS) and dimethyl disulfide (DMDS) summarized in Table 19 reveals that the additional sulfur in DMDS serves to increase the solubility of DMDS over that of DMS. The additional sulfur serves to increase the dipole of DMDS over DMS by pulling electrons towards the center of the molecule where the sulfur atoms are located. The stronger dipole without the addition of a bulky group increases the dipole-dipole interactions, which help DMDS to partition into the liquid phase more so than DMS. The measurements of pure water and

DMS and DMDS had an average experimental uncertainty of 4 % and the average uncertainty with 0.6 molal sodium sulfate was 5 %.

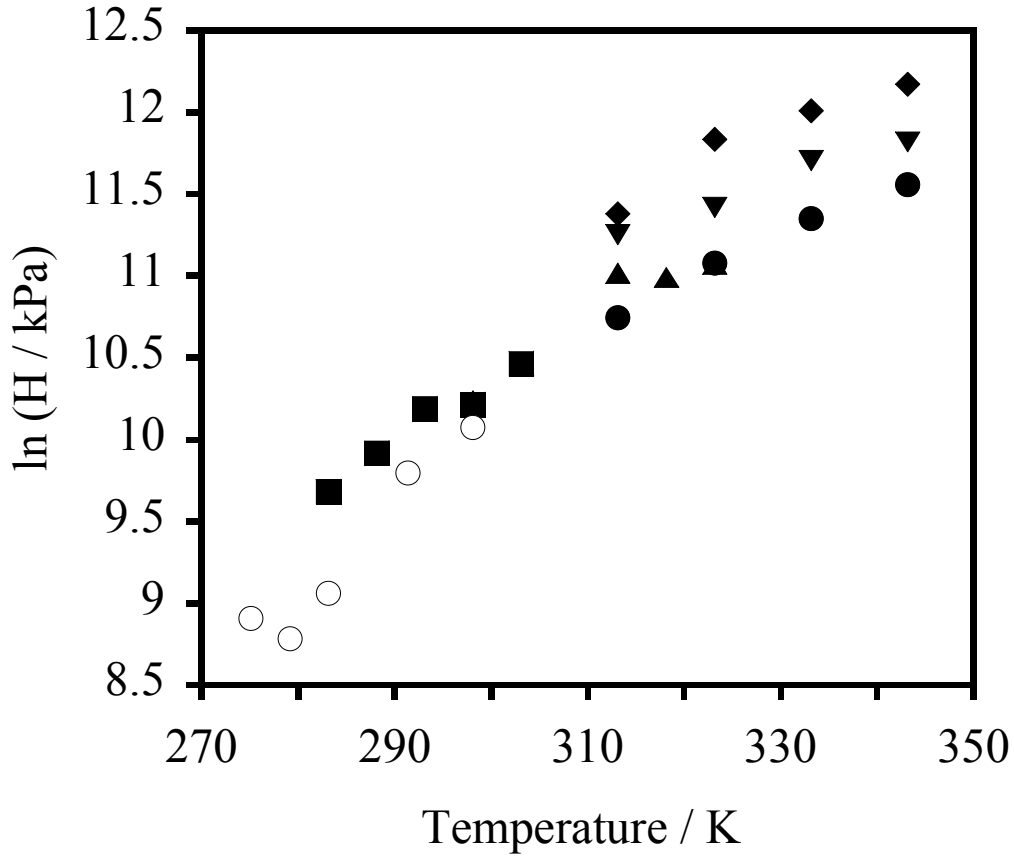

Figure 17. Henry's constants for o-xylene in pure water: (◆), (▲) [158], (■) [15], (○) [16] and in aqueous sodium chloride solutions: (●) 0.5 m, (■) 1.0 m.

Table 18. Henry's constants of transportation fuel components in aqueous sodium chloride solution.

	T / K	pure water		0.5 molal		1.0 molal	
		H/kPa	SD*/kPa	H	SD	H	SD
MTBE	313	10040	164	15290	304	16910	269
	323	15620	345	21670	865	32050	1623
	333	23860	955	32260	1259	43870	3164
	343	34000	776	44120	1805	60520	2559
ETBE	313	23150	742	28150	859	33300	2002
	323	41700	2776	47900	1354	66100	7104
	333	59500	6139	67900	8194	93800	7711
	343	78700	9465	116000	31749	164400	26645
toluene	313	58810	4221	90120	5585	92310	7482
	323	74400	6631	102800	8073	163100	26943
	333	90200	3491	122700	9113	179400	24115
	343	107000	5338	147100	24914	195400	20904
o-xylene	313	47760	2484	73600	2815	83630	5179
	323	64800	4054	90900	5255	137900	18330
	333	84800	4151	121100	8166	164200	20519
	343	95800	4030	135700	26112	192800	10844
ethylbenzene	313	72140	1941	128570	3614	138700	10903
	323	92600	7255	144700	10325	270000	82576
	333	124400	6883	183000	37206	269000	50502
	343	149200	10364	218000	58124	359000	84549

* Standard deviation

Table 19. Henry's constants for sulfides in water and sodium sulfate solutions.

	T / K	pure water		0.6 molal	
		H/kPa	SD*/kPa	H	SD
dimethyl sulfide	313	17610	448	32910	858
	323	24400	1367	40180	1479
	333	31000	1602	49800	2552
	343	38510	821	58400	2955
dimethyl disulfide	313	13880	604	26150	923
	323	19830	936	34750	920
	333	25500	1435	43200	4345
	343	34100	2719	56500	5727

* Standard deviation

4.5 Error analysis

Error analysis techniques for the relative and differential methods can be found in Appendix B.

5. THERMODYNAMIC MODELING

The limited quantity of experimental data for dilute VOCs in aqueous electrolyte systems coupled with the difficulty of measuring their air-water partitioning behavior has created a great need for models that can interpolate and extrapolate available data. Therefore, a model based on dilute solution theory [4] was evaluated for correlating and extrapolating Henry's constants over wide ranges of temperatures, and salt concentrations. In addition, the model was extended to higher pressures in this work.

5.1 Henry's constants at different pressures.

The extension of Eq. 69 to different pressures follows from the thermodynamic relationship between the fugacity of the solute in the liquid phase, f_i^L, and its partial molar volume in the liquid phase, $\bar{v}_i$.

$$\left(\frac{\partial ln\, f_i^L}{\partial P}\right)_{T,x} = \frac{\bar{v}_i}{RT} \qquad (141)$$

We can substitute the thermodynamic definition of Henry's constant since at thermodynamic equilibrium $f_i^L = f_i^V$,

$$H_{i,j} = \lim_{x_i \to 0} \left(\frac{f_i^V}{x_i}\right), \qquad (142)$$

where f_i^V is the vapor phase fugacity of solute *i*. the following expression is obtained:

$$\left(\frac{\partial\left(ln\, H_{i,j} + ln\, x_i\right)}{\partial P}\right)_{T,x} = \frac{\bar{v}_i^{\infty}}{RT} \qquad (143)$$

since the system is dilute $\bar{v}_i$ turns into $\bar{v}_i^{\infty}$, the partial molar volume of solute *i* at infinite dilution. The derivative of x_i with respect to *P* in Eq. 143 is zero since the partial derivative is taken at constant composition.

$$\left(\frac{\partial ln H_{i,j}}{\partial P}\right)_T = \frac{\bar{v}_i^{\infty}}{RT}, \qquad (144)$$

If Eq. 144 is integrated with respect to *P* at constant *T*.

$$ln H_{i,j}[P] - ln H_{i,j}[P^r] = \int_{P^r}^{P} \frac{\bar{v}_i^{\infty}}{RT} dP \qquad (145)$$

Where $H_{i,j}[P^r]$ is Henry's constant evaluated at an arbitrary reference pressure, P^r. If the temperature of the system is well below the critical temperature of the solvent, it is possible to assume that $\bar{v}_i^{\infty}$ is independent of pressure, and Eq. 145 becomes:

$$ln H_{i,j}[T,P] = ln H_{i,j}[T,P^r] + \bar{v}_i^{\infty} \frac{(P - P^r)}{RT} \qquad (146)$$

In the case of an electrolyte solution, the solvent *j* is a mixture of water and salt and can be represented by the subscript, *m*.

$$ln H_{i,m}[T,P] = ln H_{i,m}[T,P^r] + \bar{v}_i^{\infty} \frac{(P - P^r)}{RT} \qquad (147)$$

When added to Eq. 69, we obtain the following general expression for Henry's constant of solute *i* in a solvent *m* as a function of temperature, pressure, and salt concentration.

$$lnH_{i,m}[T,P] = lnP_j^{sat} + \frac{A_{ij}}{T_r} + B_{ij}\frac{(1-T_r)^{0.355}}{T_r} + C_{ij}\frac{exp(1-T_r)}{T_r^{0.41}} + D\,x_k + \bar{v}_i^{\infty}\frac{(P - P_{ref})}{RT}. \qquad (148)$$

5.1.1 Error analysis for the parameters of Eq. 148.

According to Halpern [76] the uncertainty in the parameters of an equation such as Eq. 148 can be determined by solving for the parameter of interest and taking the partial derivative of each term with respect to the experimentally measured quantities that contain uncertainties. The specific equations for calculating the uncertainty in each of the parameters can be found in Appendix C. The uncertainty for each parameter was computed and tabulated in Table 20.

Table 20. Uncertainty of the parameters in Eq. 148.

	Salt	$\varepsilon_{A_{ij}}$ %	$\varepsilon_{B_{ij}}$ %	$\varepsilon_{C_{ij}}$ %	ε_D %	$\varepsilon_{v_i^{-\infty}}$ %	Data Range (K)*	(molal)	Ref
Alkanols									
methanol	NaCl	0.05	0.08	0.6	3.1		313 - 343	0.97 – 2.71	
	KCl	0.05	0.08	0.6	2.5		313 - 343	0.34 – 2.72	
	Na_2SO_4	0.05	0.08	0.6	1.6		313 - 343	0.4. 0.8	
	Na_2CO_3	0.05	0.08	0.6	0.8		313 - 343	0.5, 1.0, 1.5	
ethanol	Na_2SO_4	0.003	0.12	0.007	2.3		313 - 363	0.2 – 1.2	[6, 151]
1-propanol	Na_2SO_4	0.04	0.07	0.08	1.9		313 - 363	0.2 – 1.2	[6, 151]
1-butanol	Na_2SO_4	0.07	0.06	0.7	1.2		313 - 363	0.2 – 1.2	[6, 151]
1-pentanol	Na_2SO_4	0.03	0.02	0.5	2.5		313 - 363	0.2 – 1.2	[6, 151]
1-hexanol	Na_2SO_4	4	8	6	1.2		313 - 363	0.2 – 1.2	[6, 151]
Ketones									
2-propanone	NaCl	0.1	0.2	0.4	2.5		313 - 363	0.2 – 1.2	[151]
	Na_2SO_4	0.1	0.2	0.4	1.4		323 - 353	0.2 - 1	[155]
	NaCl + Na_2SO_4	0.1	0.2	0.4	0.8		313 - 363	2.0	[157]
	TEAB	0.1	0.2	0.4	3.2		313 - 363	0.5, 1.0, 3.0	[157]
2-butanone	NaCl	0.1	0.2	0.4	1.9		313 - 363	0.2 – 1.2	[151]

Table 20 Continued

	Na_2SO_4	0.1	0.2	0.4	0.6	323 - 353	0.2 - 1	[155]
	NaCl + Na_2SO_4	0.1	0.2	0.4	0.7	313 - 363	2.0	[157]
2-pentanone	NaCl	0.1	0.2	0.4	0.9	313 - 363	0.2 – 1.2	[151]
	Na_2SO_4	0.1	0.2	0.4	0.4	323 - 353	0.2 - 1	[155]
	NaCl + Na_2SO_4	0.1	0.2	0.4	0.7	313 - 363	2.0	[157]
	TMAB	0.1	0.2	0.4	2.6	313 - 363	0.5, 1.0, 3.0	[157]
	TEAB	0.1	0.2	0.4	2.2	313 - 363	0.5, 1.0, 3.0	[157]
2-hexanone	NaCl	0.1	0.2	0.4	0.7	313 - 363	0.2 – 1.2	[151]
	Na_2SO_4	0.1	0.2	0.4	0.3	323 - 353	0.2 - 1	[155]
	NaCl + Na_2SO_4	0.1	0.2	0.4	0.2	313 - 363	2.0	[157]
	TMAB	0.1	0.2	0.4	2.3	313 - 363	0.5, 1.0, 3.0	[157]
	TEAB	0.1	0.2	0.4	3.5	313 - 363	0.5, 1.0, 3.0	[157]
2-heptanone	NaCl	0.1	0.2	0.4	1.3	313 - 363	0.2 – 1.2	[151]
	Na_2SO_4	0.1	0.2	0.4	0.5	323 - 353	0.2 - 1	[155]
	NaCl + Na_2SO_4	0.1	0.2	0.4	0.7	313 - 363	2.0	[157]
	TMAB	0.1	0.2	0.4	4.5	313 - 363	0.5, 1.0, 3.0	[157]
	TEAB	0.1	0.2	0.4	3.2	313 - 363	0.5, 1.0, 3.0	[157]

Table 20 Continued

Sulfides									
dimethyl sulfide	Na_2SO_4	0.02	0.05	0.24	0.3		275 - 343	0.33 – 1.3	[26, 30, 157]
dimethyl disulfide	Na_2SO_4	0.03	0.06	1.12	0.4		313 - 343	0.33 – 1.3	[30, 157]
***Tert*butyl Ethers**									
methyl *tert*butyl ether	NaCl	0.001	0.006	0.005	2.4		298 - 343	0.5, 1	[157, 158]
ethyl *tert*butyl ether	NaCl	0.04	0.05	0.68	4.1		298 - 343	0.5, 1	[157]
Aromatic Hydrocarbons									
toluene	NaCl	0.01	0.05	0.04	2.2		275 - 333	0.5, 1	[15, 157] [16, 158, 159]
o-xylene	NaCl	0.02	0.06	0.04	2.0		275 - 343	0.5, 1	[15, 16, 157, 158]
ethylbenzene	NaCl	0.004	0.02	0.02	2.4		275 - 343	0.5, 1	[15, 16, 157, 158]
Light Gases									
methane	NaCl	0.02	0.6	0.01	1.5	0.7	324 - 523	1, 4	[81, 160]
methane	$CaCl_2$	0.02	0.6	0.01	1.8	0.7	324 - 523	1	[160, 161]
nitrogen	NaCl	0.09	0.10	1.2	1.3	0.9	324 - 398	1, 4	[81, 160]

5.1.2 Results for high-pressure ternary systems.

Eq. 148 was tested at high pressures in the case of methane + water. The reference pressure was chosen to be 300 atm, and methane + water data at this pressure were regressed to obtain A_{ij}, B_{ij}, and C_{ij} in Eq. 148. Data at 600 atm were then regressed to yield an estimate of the partial molar volume $\bar{v}_i^{\infty}$ of methane at infinite dilution in water. The value of $\bar{v}_i^{\infty}$ determined by regression was 38.9 cm^3 mol^{-1}, which compares well with a value of 34.5 cm^3 mol^{-1} reported by Moore et al. [162]. Different data sets yield slightly different values of $\bar{v}_i^{\infty}$ as shown in Table 21. However, agreement between different estimates of $\bar{v}_i^{\infty}$ and the reported experimental value is reasonable. Table 21 also presents values of D, in units of molality, obtained from methane + water + $CaCl_2$ and methane + water + NaCl data at 300 atm. Fugacity coefficients of methane were calculated using the Lee-Kesler equation of state [100] assuming a pure methane headspace above the salt solutions. Duan et al. [163] have noted that this assumption produces excellent estimates of the fugacity coefficient of methane using the Lee-Kesler equation below 523 K and 1600 atm. "Effective" Henry's constants of methane were calculated from the ratio of the fugacity of pure methane in the vapor phase to its mole fraction in the liquid phase ($H_{CH4,w} = \phi_{CH4} P / x_{CH4}$). The resulting parameters in

Table 21 were used to demonstrate the extrapolation capability of the model as follows. In Figure 18, the parameters for methane + water obtained from published data at 300 and 600 atm and over a 200-Kelvin temperature range were used to obtain Henry's constants at pressures ranging from 100 atm to 1065 atm. In Figure 19, parameters obtained by regressing low temperature data (324 K – 473 K) were used to calculate Henry's constants at temperatures up to 523 K. Again, excellent agreement between calculation and experiment was obtained. In Figure 20, the value of *D* obtained using methane + water + 1.0 molal $CaCl_2$ data was used to calculate Henry's constants in this ternary system from 100 atm to 600 atm, with good success.

Henry's constants for water + nitrogen from 100 – 600 atm and over a 74 K temperature range were also regressed a reference pressure of 300 atm and the results are presented in Figure 21. Henry's constants for water + NaCl + nitrogen from 100 – 600 atm and over a 74 K temperature range were regressed with a single value of *D* listed in Figure 21 and the results are shown in Figure 22.

Table 21. Constants of Eq. 148 for gases + water + salt at 300 atm.

Compound	methane [164]	methane [164]	nitrogen
Temp. Range of Data / K	324 - 523	324 - 473	324 - 398
Pressure Range / atm	97 - 1065	97 - 1065	100 - 600
P_{ref} / atm	300	300	300
A_{ij}	-11.06	-14.86	5.35
B_{ij}	5.81	5.93	3.35
C_{ij}	12.20	15.57	-0.64
D (NaCl)	0.16	0.146	0.26
NaCl Conc. / m	1.0, 4.0	1.0, 4.0	1.0, 4.0
D ($CaCl_2$)	0.33	0.341	
$CaCl_2$ Conc. / m	1.0	1.0	
$\bar{v}_i^{\infty}$ (cm^3 mol^{-1})	38.9	37.5	59.2
[a]AAD / %	0.3	0.3	0.2
[b]MAD / %	0.8	0.9	0.6

[a] Average Absolute Deviation = Σ [| ln (H_{expt}) – ln (H_{calc})| / ln (H_{expt})] / n * 100.
[b] Maximum Absolute Deviation = Max | ln (H_{expt}) – ln (H_{calc})| / H_{expt} * 100.

Table 22. Comparison of partial molar volumes for methane and nitrogen in pure water.

T / K	ΔP / bar	(CH_4) $\bar{v}^{\infty}$ / cm^3 mol^{-1}	(N_2) $\bar{v}^{\infty}$ / cm^3 mol^{-1}
324 - 523	300	38.9	59.2
298	1	34.5 [162]	35.7 [162]
375	400	41.4 [81]	37.7 [81]
398	400	46.6 [81]	38.9 [81]

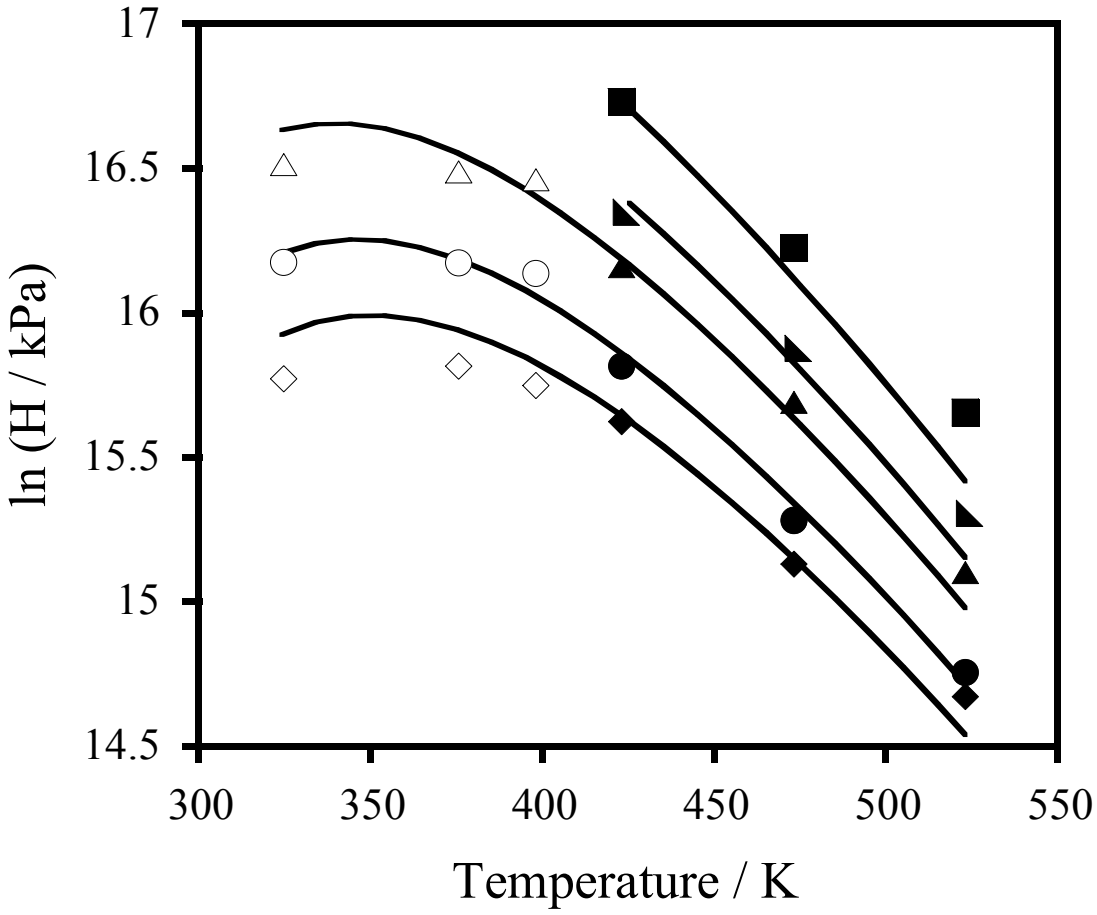

Figure 18. Calculated Henry's constants for methane in pure water (lines). Experimental data of ref [81] at (◇) 100 atm, (○) 300 atm and (△) 600 atm. Data of ref [160] at (◆) 97 atm, (●) 290 atm, (▲) 581 atm, (◣) 774 atm, and (■) 1065 atm.

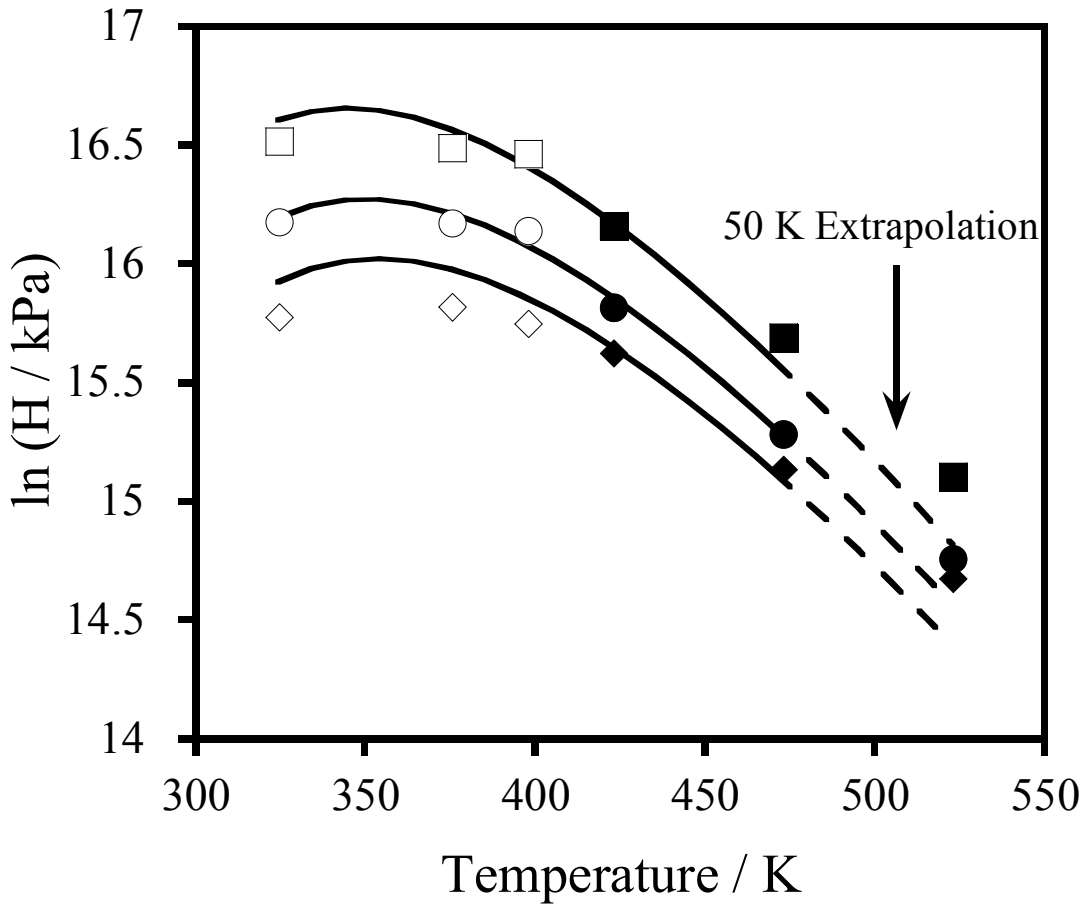

Figure 19. Extrapolation of Henry's constants of methane in pure water. Data of ref. [81] at: (◇) 100 atm, (○) 300 atm and (□) 600 atm. Data of ref. [160] at: (◆) 97 atm, (●) 290 atm, and (■) 581 atm.

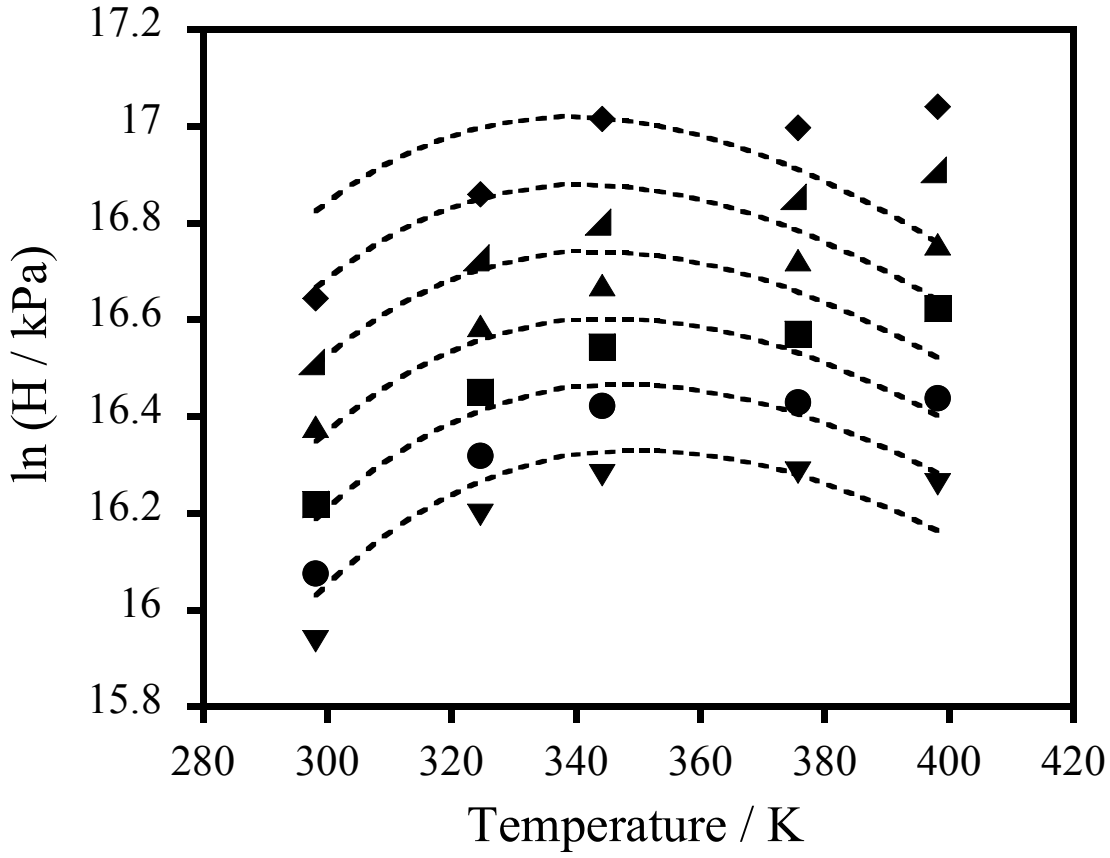

Figure 20. Calculated Henry's constants for methane in 1 molal aqueous $CaCl_2$ solutions at (▼) 100 atm, (●) 200 atm, (■) 300 atm, (▲) 400 atm, (◢) 500 atm, (◆) 600 atm. Data of ref. [161] and *D* determined from data at 300 atm (solid line).

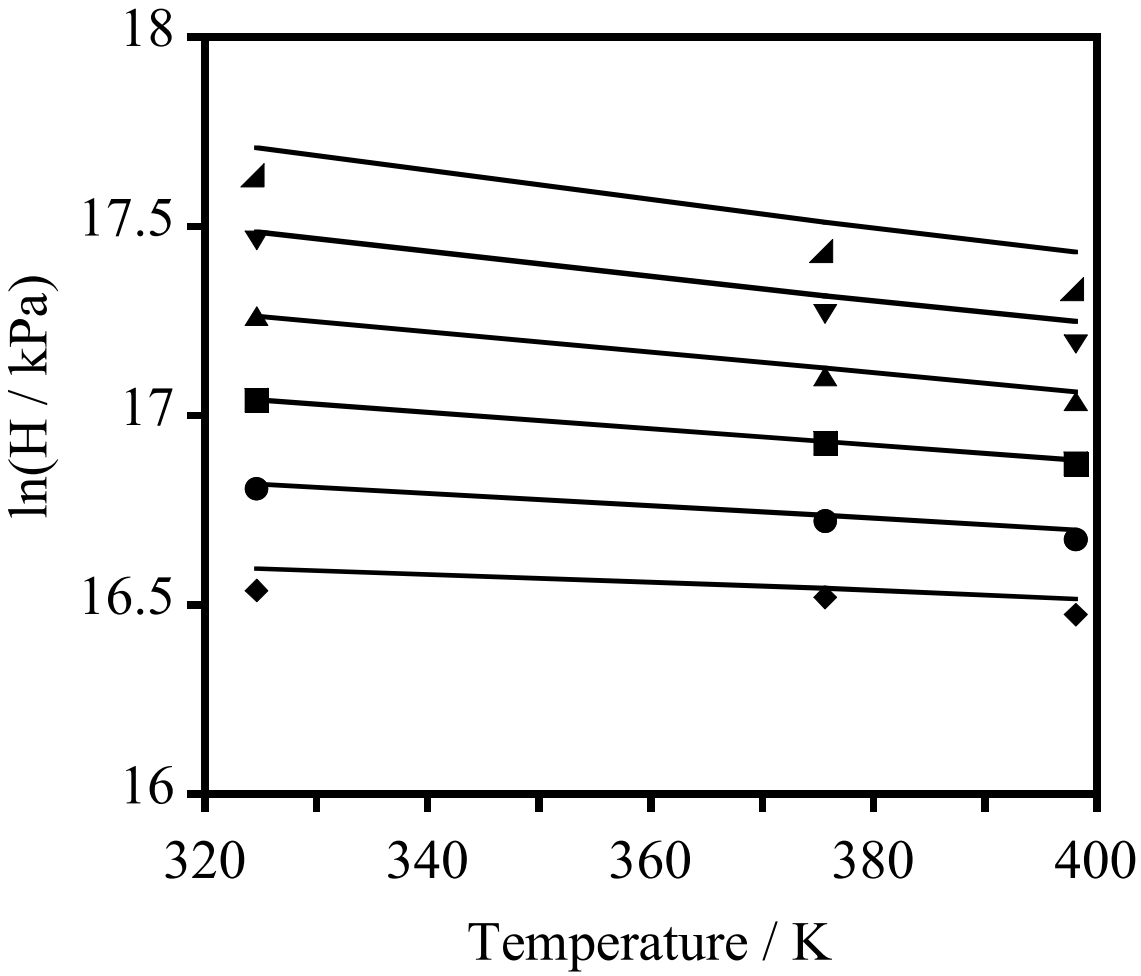

Figure 21. Henry's constants of nitrogen gas in pure water at (◆) 100 atm total pressure, (●) 200 atm, (■) 300 atm, (▲) 400 atm, (▼)500 atm, (◢) 600 atm fit with (—) Eq. 148.

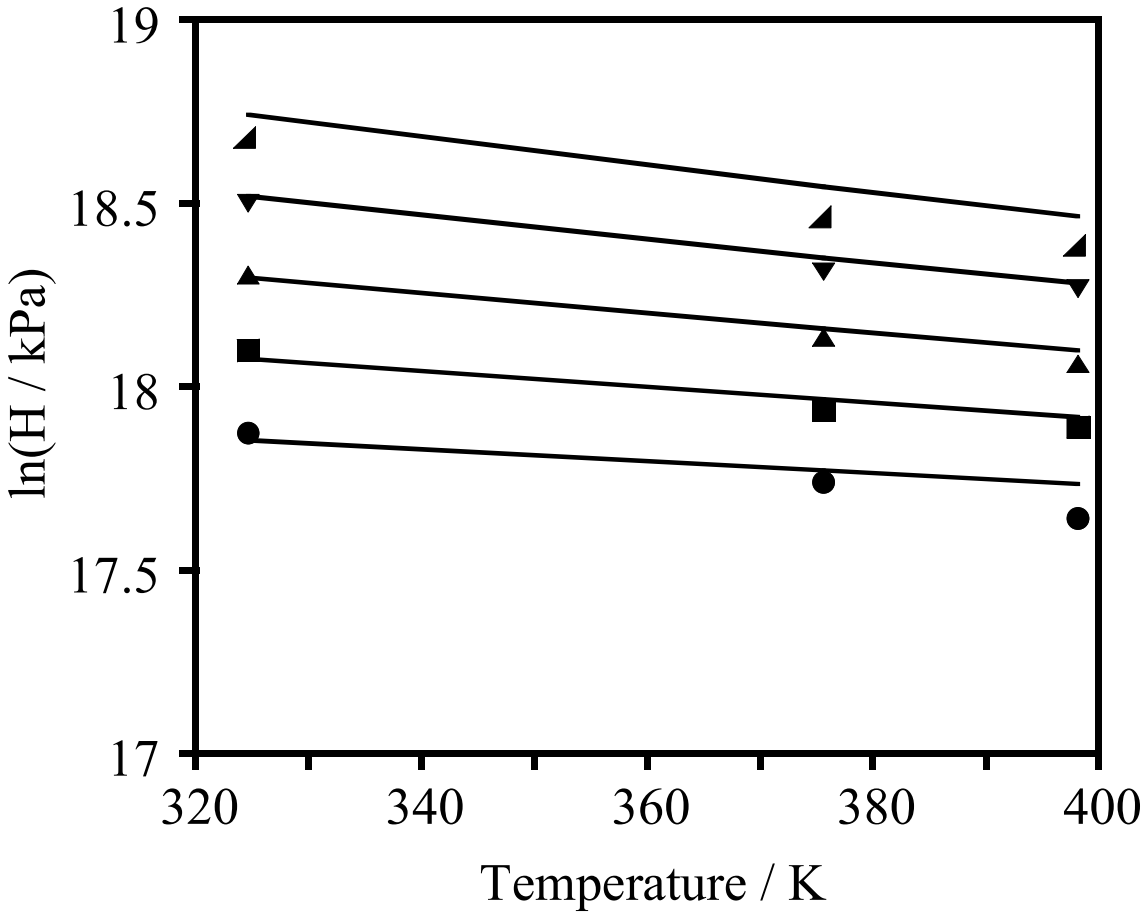

Figure 22. Henry's constants of nitrogen gas in 4.0 m aqueous NaCl solutions at: (●) 200 atm, (■) 300 atm, (▲) 400 atm, (▼) 500 atm, (◢) 600 atm fit with (—) Eq. 148.

5.2 Estimation of methane emissions from produced water.

The utility of Eq. 148 can be seen when predicting methane emissions in natural gas production from deepwater reservoirs. It is of interest to know the amount of methane emission since it is a GHG that plays a role in the global climate change. The natural gas industry produces 497 million barrels of salt water annually [165]. This solution contains from 2 to 20 wt. % salt and exits the well at pressures ranging from 1 to 68 atm. The produced water with entrained methane gas is fed into a high-pressure separator that allows the methane to disengage from the produced water. Most of the produced water is re-injected back into the reservoir and 30 % of the total volume is held in an atmospheric pressure tank for re-injection at a later time. In the atmospheric pressure tank, methane that was dissolved at high pressures in the separator partitions into the tank headspace and escapes into the atmosphere through the tank vent. When Eq. 148 was applied to calculate methane emissions with parameters in Table 21, estimates were between 50 and 57 % lower than those calculated by Shires and Harrison [165] with ASPEN Plus [166]. This indicates that the ASPEN Plus simulation calculated a larger solubility for the methane in the high-pressure separator than the calculations outlined in this report. The difference of approximately 50 % over the entire range of pressures and salt concentrations in Table 23 is probably caused by the default ASPEN interaction parameters for methane and the salt ion. Data regressions are usually necessary to determine the specific electrolyte / nonelectrolyte parameters and if not performed, lead to offsets from literature data.

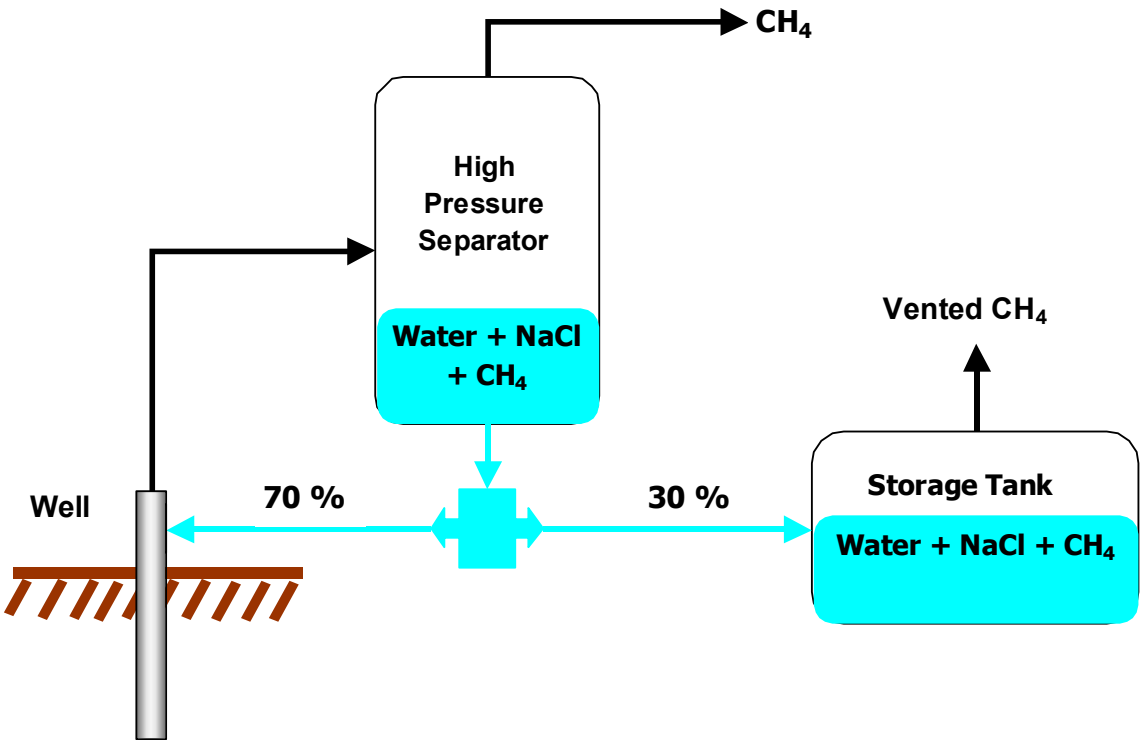

Figure 23. Schematic of high-pressure methane separator and ambient pressure storage tank.

Table 23. Methane emission from produced water at 323 K.

Salt , Wt %	Pressure, psi	Methane Emissions, 10^6 lb / yr (**API [165]**)	Methane Emissions, 10^6 lb / yr (**this work**)	% difference
NaCl				
20	50	1.6	0.8	50
	250	10.8	5.1	53
	1000	38.8	18.7	52
10	250	16.4	7.5	55
	1000	58.7	27.3	54
2	250	19.4	9.5	51
	1000	69.5	34.8	50
$CaCl_2$				
20	50	1.6	0.7	56
	250	10.8	4.5	58
	1000	38.8	16.6	57
10	250	16.4	7.1	57
	1000	58.7	25.8	56
2	250	19.4	9.4	51
	1000	69.5	34.5	50

5.3 Correlation of ambient pressure ternary systems

Very few values of Henry's constants of VOCs have been reported in the literature, especially at temperatures other than 298 K. Published data were compiled on all systems for which measurements were available at more than one temperature and salt concentration. Binary data (VOC + water) were then regressed using a nonlinear least squares method and the constants A_{ij}, B_{ij}, and C_{ij} in Eq. 69 were obtained for each system. The D parameter in Eq. 69 was then obtained by regression of ternary (VOC + water + salt) data at one salt concentration. Two scales of concentration were used in these correlations - the molality scale and the ionic strength defined by:

$$I = 1/2 \cdot \sum m_s \cdot z_s^2 , \qquad (149)$$

where m_s is the molality of a salt ion, and z_s is the charge number of the ion.

Most data sources listed in Table 24 report values of dimensionless Henry's constants. Dimensionless Henry's constants were converted to thermodynamic Henry's constants for comparison to other literature sources as follows:

$$H_{i,j} = \left(H_c \; R\, T\right) / \; \bar{v}_j \qquad (150)$$

where $\bar{v}_j$ is the molar volume of the solvent (water). Some data sources, for example [35], reported values of activity coefficients at infinite dilution. These were also converted to thermodynamic Henry's constants by combining Eqs. 6 and 150 to yield the following relationship:

$$H_{i,j} = \gamma_i^{\infty} P_i^{sat} . \qquad (151)$$

Table 24 summarizes the results of the regression of thermodynamic Henry's constants for the available ternary systems. Note that parameters A_{ij}, B_{ij}, and C_{ij} were

obtained from binary data and therefore do not change with the salt in Table 24 for the same VOC. Also, there was negligible change in the fit of the data when salt concentration was converted from a molality scale to the ionic strength scale. This is clear from values of the *D* parameter in Table 24 for VOCs + water + NaCl or KCl using the two scales. Therefore, the molality scale was employed in most calculations. The overall average absolute deviation between calculated and experimental values for all 56 systems was 0.8 %, which is less than the error in the data. The maximum error was 5.3 %, which is also within the experimental uncertainty. Eq. 69 is therefore an excellent expression for correlating Henry's constants of VOCs in salt solutions at constant pressure.

Table 24. Constants of Eq. 69 for VOCs in aqueous salt solutions at 1 atm.

	Salt	A_{ij}	B_{ij}	C_{ij}	D (molal)	D (Ionic Str.)	Data Range (K)*	Data Range (molal)	AAD[a]	MAD[b]	Ref
Alkanols											
methanol	NaCl	9.16	-10.05	-0.15	0.11	0.11	313 - 343	0.97 – 2.71	1.9	3.1	[6, 132]
	KCl	9.16	-10.05	-0.15	0.11	0.11	313 – 343	0.34 – 2.72	2.0	5.1	[6, 132]
	Na_2SO_4	9.16	-10.05	-0.15	0.47	0.24	313 - 343	0.4, 0.8	1.3	2.8	[4, 6]
	Na_2CO_3	9.16	-10.05	-0.15	0.21	0.19	313 - 343	0.5, 1, 1.5	1.5	4.0	[4, 6]
ethanol	Na_2SO_4	-38.24	0.93	35.35	0.52	0.18	313 - 363	0.2 – 1.2	1.3	3.9	[6, 151]
1-propanol	Na_2SO_4	13.62	-11.72	-2.74	0.68	0.24	313 - 363	0.2 – 1.2	1.2	4.6	[6, 151]
1-butanol	Na_2SO_4	9.58	-11.28	0.81	0.84	0.29	313 - 363	0.2 – 1.2	1.0	3.8	[6, 151]
1-pentanol	Na_2SO_4	10.04	-14.51	2.72	0.97	0.33	313 - 363	0.2 – 1.2	1.2	3.3	[6, 151]
1-hexanol	Na_2SO_4	9.57	-10.61	0.64	1.11	0.37	313 - 363	0.2 – 1.2	1.0	4.5	[6, 151]
Ketones											
2-propanone	NaCl	8.03	-3.06	-3.31	0.22	0.22	313 - 363	0.2 – 1.2	0.4	4.2	[151]
	Na_2SO_4	8.03	-3.06	-3.31	0.68	0.23	323 - 353	0.2 - 1	0.2	0.7	[155]
	NaCl + Na_2SO_4	8.03	-3.06	-3.31		0.21	313 - 363	2.0	0.3	0.8	[157]
	TEAB	8.03	-3.06	-3.31	0.05	0.05	313 - 363	0.5, 1.0, 3.0	0.6	0.9	[157]
2-butanone	NaCl	-19.81	0.91	19.51	0.26	0.26	313 - 363	0.2 – 1.2	0.3	1.0	[151]

Table 24 Continued

	Na_2SO_4	-19.81	0.91	19.51	0.86	0.29	323 - 353	0.2 - 1	0.2	0.6	[155]
	NaCl + Na_2SO_4	-19.81	0.91	19.51		0.25	313 - 363	2.0	0.3	0.9	[157]
2-pentanone	NaCl	8.58	-6.42	-0.97	0.34	0.34	313 - 363	0.2 – 1.2	0.2	1.0	[151]
	Na_2SO_4	8.58	-6.42	-0.97	1.03	0.34	323 - 353	0.2 - 1	0.2	0.6	[155]
	NaCl + Na_2SO_4	8.58	-6.42	-0.97		0.30	313 - 363	2.0	0.4	.08	[157]
	TMAB	8.58	-6.42	-0.97	-0.03	-0.03	313 - 363	0.5, 1.0, 3.0	0.5	0.9	[157]
	TEAB	8.58	-6.42	-0.97	-0.08	-0.08	313 - 363	0.5, 1.0, 3.0	0.7	1.1	[157]
2-hexanone	NaCl	9.19	-7.77	-0.43	0.40	0.40	313 - 363	0.2 – 1.2	0.4	0.9	[151]
	Na_2SO_4	9.19	-7.77	-0.43	1.22	0.40	323 - 353	0.2 - 1	0.4	1.0	[155]
	NaCl + Na_2SO_4	9.19	-7.77	-0.43		0.35	313 - 363	2.0	0.5	0.9	[157]
	TMAB	9.19	-7.77	-0.43	-0.03	-0.03	313 - 363	0.5, 1.0, 3.0	0.4	0.7	[157]
	TEAB	9.19	-7.77	-0.43	-0.13	-0.13	313 - 363	0.5, 1.0, 3.0	1.0	1.3	[157]
2-heptanone	NaCl	9.97	-10.70	1.14	0.42	0.42	313 - 363	0.2 – 1.2	0.4	0.9	[151]
	Na_2SO_4	9.97	-10.70	1.14	1.30	0.43	323 - 353	0.2 - 1	0.4	0.8	[155]
	NaCl + Na_2SO_4	9.97	-10.70	1.14		0.37	313 - 363	2.0	0.3	0.9	[157]
	TMAB	9.97	-10.70	1.14	-0.05	-0.05	313 - 363	0.5, 1.0, 3.0	0.4	0.8	[157]
	TEAB	9.97	-10.70	1.14	-0.19	-0.19	313 - 363	0.5, 1.0, 3.0	1.0	1.5	[157]

Table 24 Continued

Sulfides											
dimethyl sulfide	Na_2SO_4	10.55	-5.22	-2.43	0.76	0.25	275 - 343	0.33 – 1.3	0.6	2.1	[26, 30, 157]
dimethyl disulfide	Na_2SO_4	9.49	-6.40	-0.77	0.91	0.30	313 - 343	0.33 – 1.3	0.8	2.3	[30, 157]
***Tert*butyl Ethers**											
methyl *tert*butyl ether	NaCl	-172.14	39.99	131.96	0.50	0.50	298 - 343	0.5, 1	1.1	2.6	[157, 158]
ethyl *tert*butyl ether	NaCl	10.3	-10.3	1.7	0.49	0.49	298 - 343	0.5, 1	0.7	1.1	[157]
Aromatic Hydrocarbons											
toluene	NaCl	-31.28	8.70	26.34	0.80	0.80	275 - 333	0.5, 1	1.0	1.7	[15, 157] [16, 158, 159]
	SW [d]	-31.28	8.70	26.34	0.0082 [c,d]		275 - 333	17.5, 35 [c,d]	0.9	2.7	[15, 16, 158, 159]
o-xylene	NaCl	-24.69	7.38	21.17	0.87	0.87	275 - 343	0.5, 1	1.2	2.1	[15, 16, 157, 158]
	SW	-24.69	7.38	21.17	0.0119 [c,d]		275 - 343	17.5, 35 [c,d]	0.9	2.3	[15, 16, 158]
m-xylene	SW	10.43	-10.03	1.75	0.0090 [c,d]		275 - 298	17.5, 35 [c,d]	0.8	1.6	[16, 132]
p-xylene	SW	10.45	-12.59	3.62	0.0120 [c,d]		275 - 298	17.5, 35 [c,d]	0.9	2.4	[16, 132]
ethylbenzene	NaCl	-76.69	20.90	59.23	0.94	0.94	275 - 343	0.5, 1	1.2	1.6	[15, 16, 157, 158]
	SW	-76.69	20.90	59.23	0.0110 [c,d]		275 - 343	17.5, 35 [c,d]	1.2	1.7	[15, 16, 132, 158]
benzene	NaCl	-68.81	22.13	50.95	0.43	0.43	275 - 333	0.2 – 1.5	0.7	2.9	[15, 16, 35, 159]
	SW	-68.81	22.13	50.95	0.0077 [c,d]		275 - 333	17.5, 35 [c,d]	0.9	2.9	[15, 16, 35, 159]

Table 24 Continued

Chlorinated Hydrocarbons

trichloroethylene	NaCl	-33.05	5.21	30.73	0.39	0.39	275 - 333	0.2 – 1.5	0.7	2.5	[15, 16, 19, 35, 158, 159]
	SW	-33.05	5.21	30.73	0.0086 [c,d]		275 - 333	17.5, 35 [c,d]	0.6	2.5	[15, 16, 19, 35, 158, 159]
chloroform	NaCl	-23.85	3.10	23.45	0.35	0.35	275 - 333	0.5 – 2.5	0.5	1.9	[15, 16, 19, 35, 159]
	SW	-23.85	3.10	23.45	0.0057 [c,d]		275 - 333	17.5, 35 [c,d]	0.5	1.9	[15, 16, 19, 35, 159]
tetrachloromethane	SW	15.14	-13.72	0.77	0.0089 [c,d]		275 - 298	17.5, 35 [c,d]	0.4	1.1	[16, 19, 132]
dichloromethane	NaCl	-40.64	12.33	31.93	0.28	0.28	283 - 313	0.5 – 2.5	0.2	0.8	[15, 19, 35]
tetrachloroethylene	SW	10.62	-13.99	4.88	0.0112 [c,d]		275 - 298	17.5, 35 [c,d]	0.4	2.3	[16, 132]
1,1-dichloroethane	SW	10.40	-10.18	1.81	0.0081 [c,d]		275 - 298	17.5, 35 [c,d]	0.5	1.8	[16, 132]
1,2-dichloroethane	NaCl	-2.63	-3.97	8.59	0.32	0.32	275 - 313	0.2 – 1.5	0.5	3.5	[16, 35]
	SW	-2.63	-3.97	8.59	0.0049 [c,d]		275 - 313	17.5, 35 [c,d]	1.2	5.3	[16, 35]
1,1,1-trichloroethane	SW	10.57	-11.02	2.74	0.0092 [c,d]		275 - 298	17.5, 35 [c,d]	0.5	2.1	[16, 132]

* Temperature range of binary data.

[a] Average Absolute Deviation = Σ [| ln (H_{expt}) – ln (H_{calc})| / ln (H_{expt})] / n * 100 .

[b] Maximum Absolute Deviation = Max | ln (H_{expt}) – ln (H_{calc})| / H_{expt} * 100 .

[c] salt concentration in kg salt / kg pure water.

[d] Artificial seawater consisting of: 54.93 wt.% chloride, 30.53 % sodium, 7.67 % sulfate, 3.68 % magnesium, 1.18 % cadmium, and 1.11 % potassium in deionized water [16].

5.4 Regression of Henry's constants of o-xylene + water + NaCl

Correlation of data for MTBE, ETBE, ethylbenzene, toluene, and o-xylene was accomplished with a single value of *D* for each compound. In general, maximum absolute deviations (MAD) between calculated and experimental values for gasoline components did not exceed 2.6 % and average absolute deviations (AAD) did not exceed 1.2 %. When available, Henry's constants from the literature mostly agreed with the data from this work, as can be seen in Figure 24, and they were correlated along with data from this work.

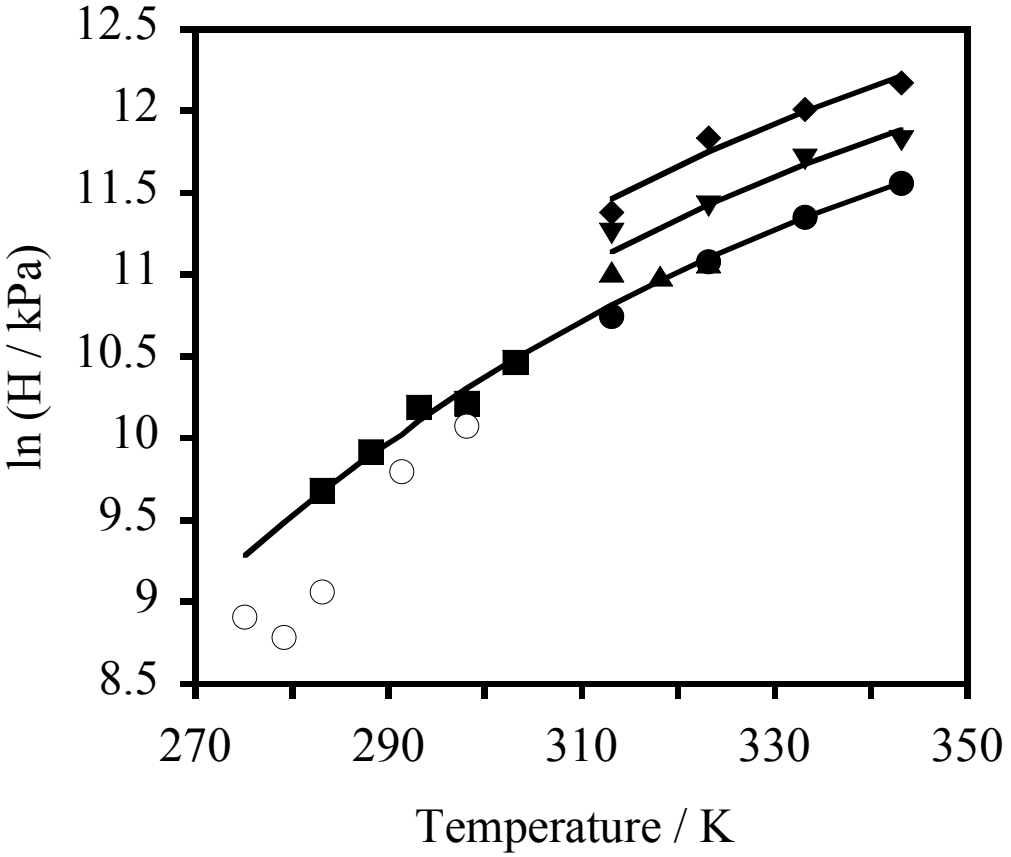

Figure 24. Henry's constants for o-xylene in pure water: (◆), (▲) [158], (■) [15], (○) [16] and in aqueous sodium chloride solutions: (●) 0.5 m, (■) 1.0 m. Correlated with Eq. 69.

5.5 Regression of Henry's constants of organic sulfides + water + Na_2SO_4

Henry's constants for dimethyl sulfide and dimethyl disulfide in sodium sulfate solutions were also correlated using a single salt effect parameter per VOC. The MAD and AAD for dimethyl sulfide and dimethyl disulfide did not exceed 1.0 % and 0.5 %. Literature data for dimethyl sulfide in pure water from Dacey et al. [26] and dimethyl sulfide + water + sodium sulfate from Przyjazny et al. [30] were incorporated into the correlation to span temperatures ranging from 274 to 343 K and salt concentrations up to 3 molal. In the case of dimethyl sulfide in water, the data of Dacey et al. extended the temperature range, as shown in Figure 25. In correlating the data for DMDS the Henry's constants at $I = 4.0$ in Przyjazny et al. were not used to obtain D since they fall atop the next lowest salt concentration of $I = 3.0$. Przyjazny et al. gave no explanation for the overlap indicating that there may be an error in the equation that they reported.

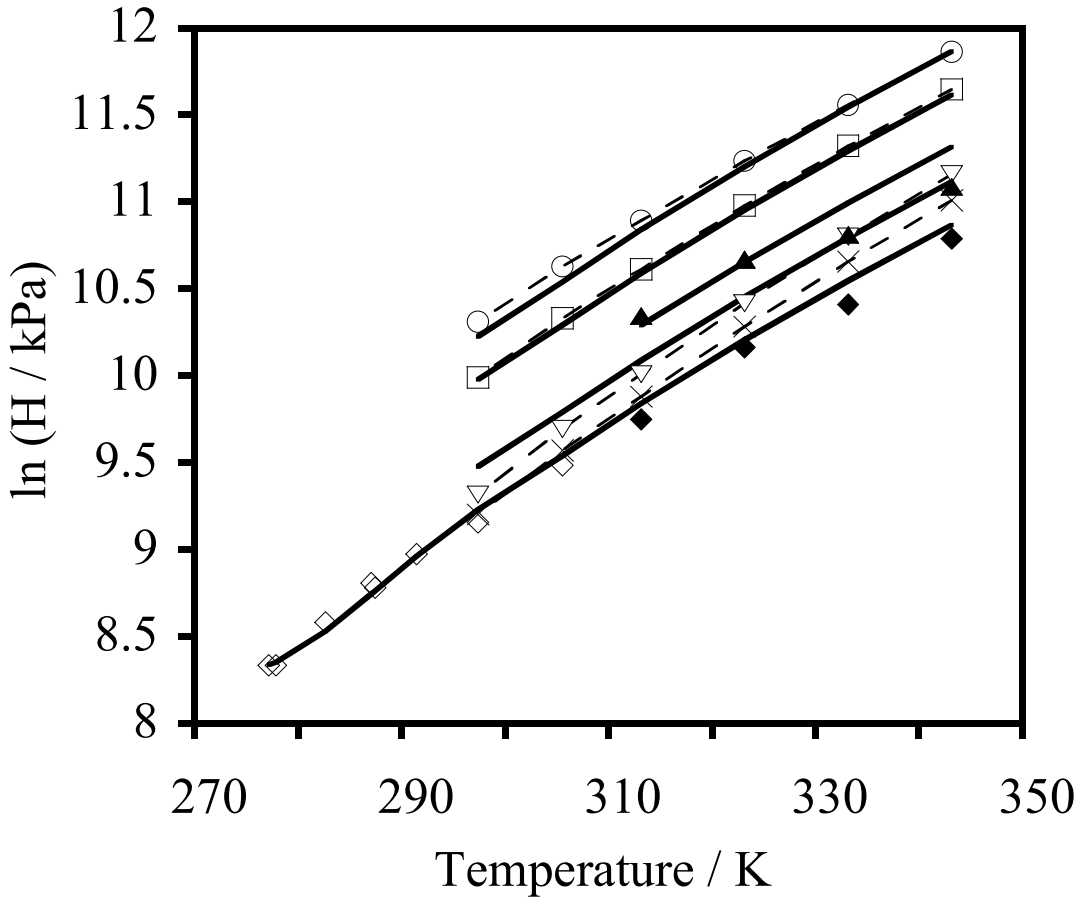

Figure 25. Henry's constants of dimethyl sulfide + water from (◇) Dacey et al. [26], (◆) this work, (-×-) Przyjazny [30]. Also with Na_2SO_4: (-▽-) I (molar) = 1.0 [30], (▲) I = 1.8 (this work), (-□-) I = 3.0 [30], (-○-) I = 4.0 [30]. Data were correlated with (━) Eq. 69.

5.6 Regression of Henry's constants of 2-ketones + water + tetraalkylammonium bromide salts.

Experimental error for all available data points did not exceed 11 %. Correlation with Eq. 69 yielded an AAD of no more than 1.0 % and a MAD not exceeding 1.5 %. Equation 69 over predicted Henry's constants of 2-heptanone, 2-hexanone, and 2-pentanone in 0.5 and 1.0 molal tetraethylammonium bromide (TEA-Br) solutions, while adequately correlating Henry's constants of 2-heptanone in 3.0 molal TEA-Br as shown in Figure 26. This non-linear behavior in the Henry's constants is probably due to disruption of the hydrogen-bonding network caused by ethyl groups on the cation of TEA-Br, as well as the effect of stronger dispersion forces between the cation and VOC. Salting out of 2-propanone was observed in 3.0 molal TEA-Br as shown in Figure 27. The changeover in the salt effect as the hydrocarbon backbone becomes shorter suggests that dispersion forces between the hydrocarbon groups in 2-propanone and the organic cation are not sufficient to overcome the effects of the disruption of the hydrogen bonded network of water [5] by the large organic cation of TEA-Br.

Correlation of systems of 2-ketones + water + tetramethylammonium bromide (TMA-Br) with Eq. 69 yielded an AAD of no more than 0.4 % and a MAD of no more than 0.9 %. As shown in Figure 28, Eq. 69 was also better able to correlate the Henry's constants of 2-heptanone with TMA-Br where weak salting in occurred. It is probable that the weaker dispersion forces from the methyl groups of the cation were the reason for the significantly lower degree of salting in.

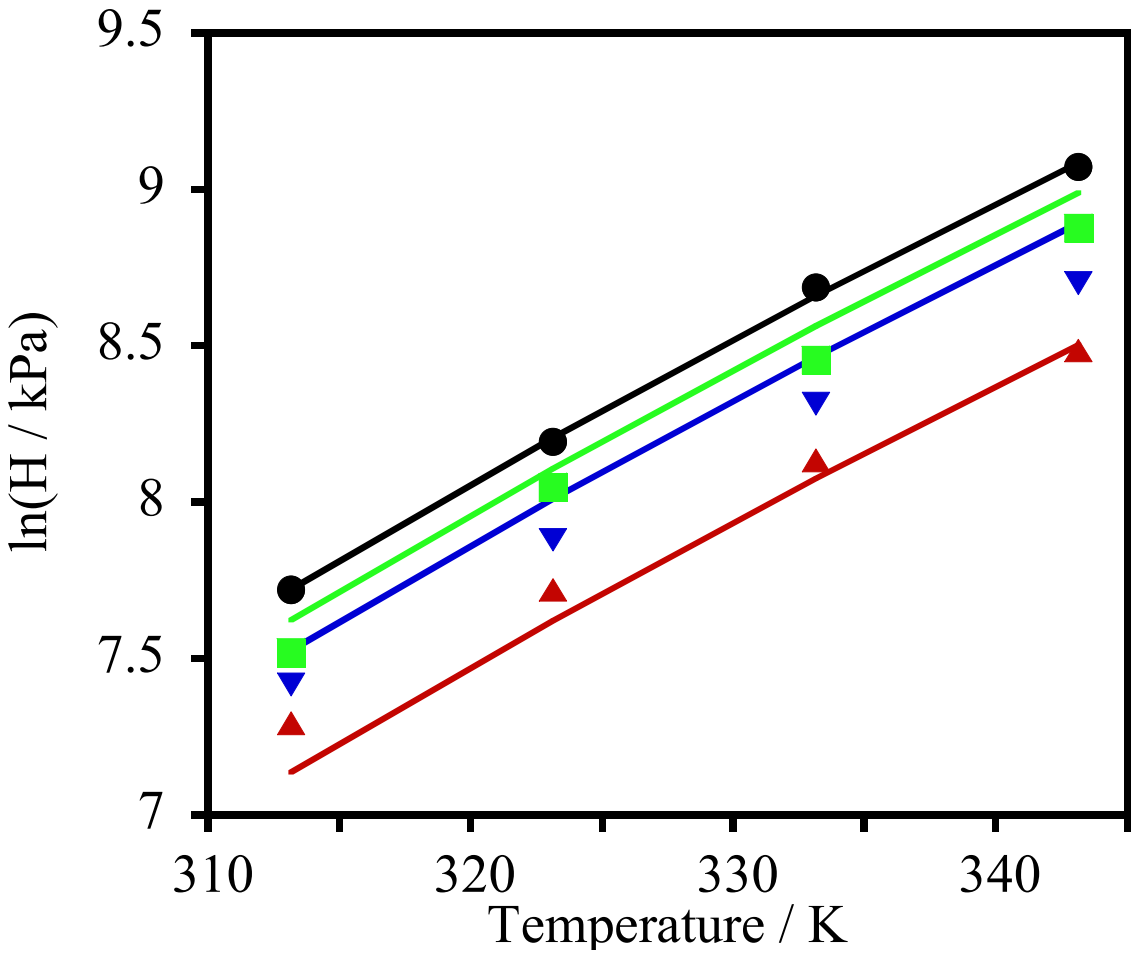

Figure 26. 2-heptanone in (●) pure water [151], (■) with 0.5 m TEA-Br [157], (▼) with 1.0 m TEA-Br [157], (▲) with 3.0 m TEA-Br [157]. Correlated with Eq. 69.

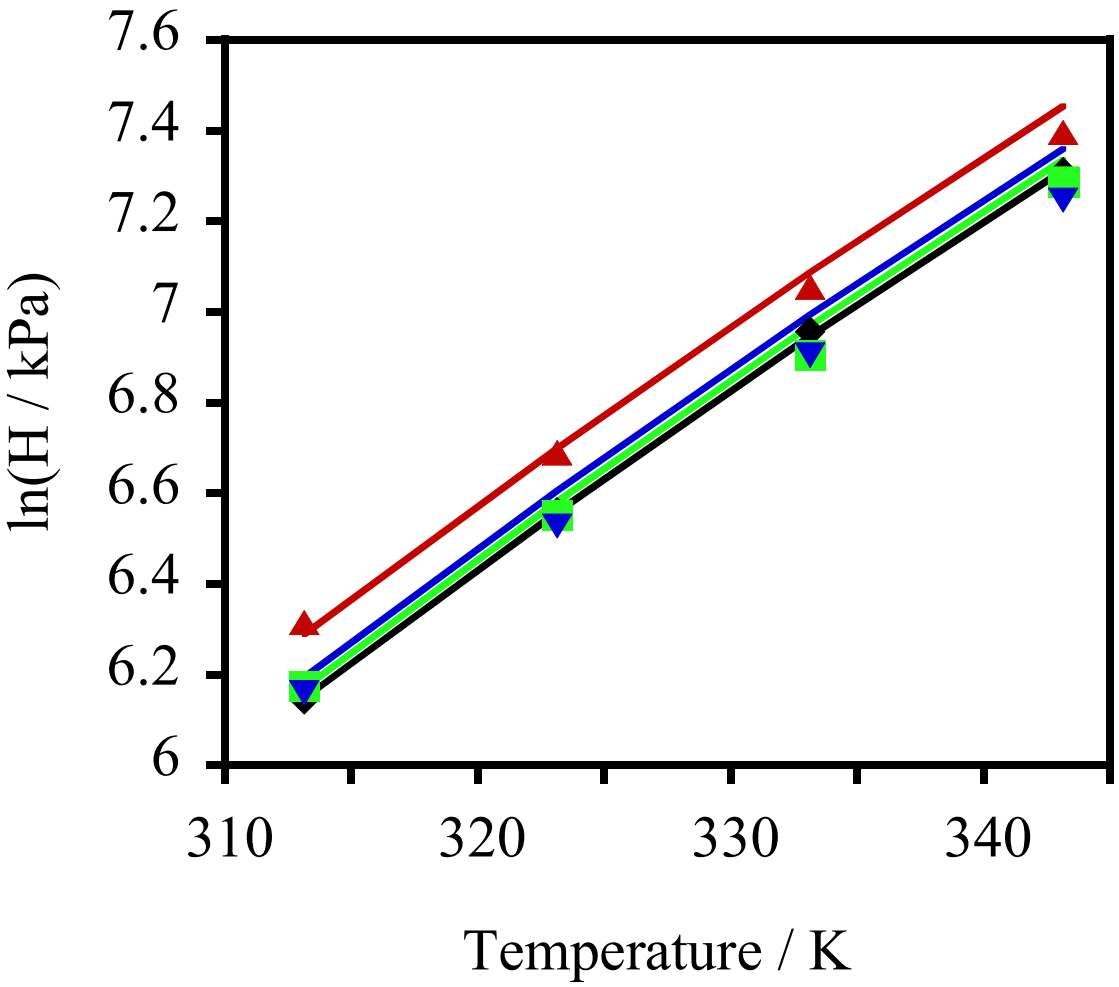

Figure 27. 2-propanone in (●) pure water [151], (■) with 0.5 m TEA-Br [157], (▼) with 1.0 m TEA-Br [157], (▲) with 3.0 m TEA-Br [157]. Correlated with Eq. 69.

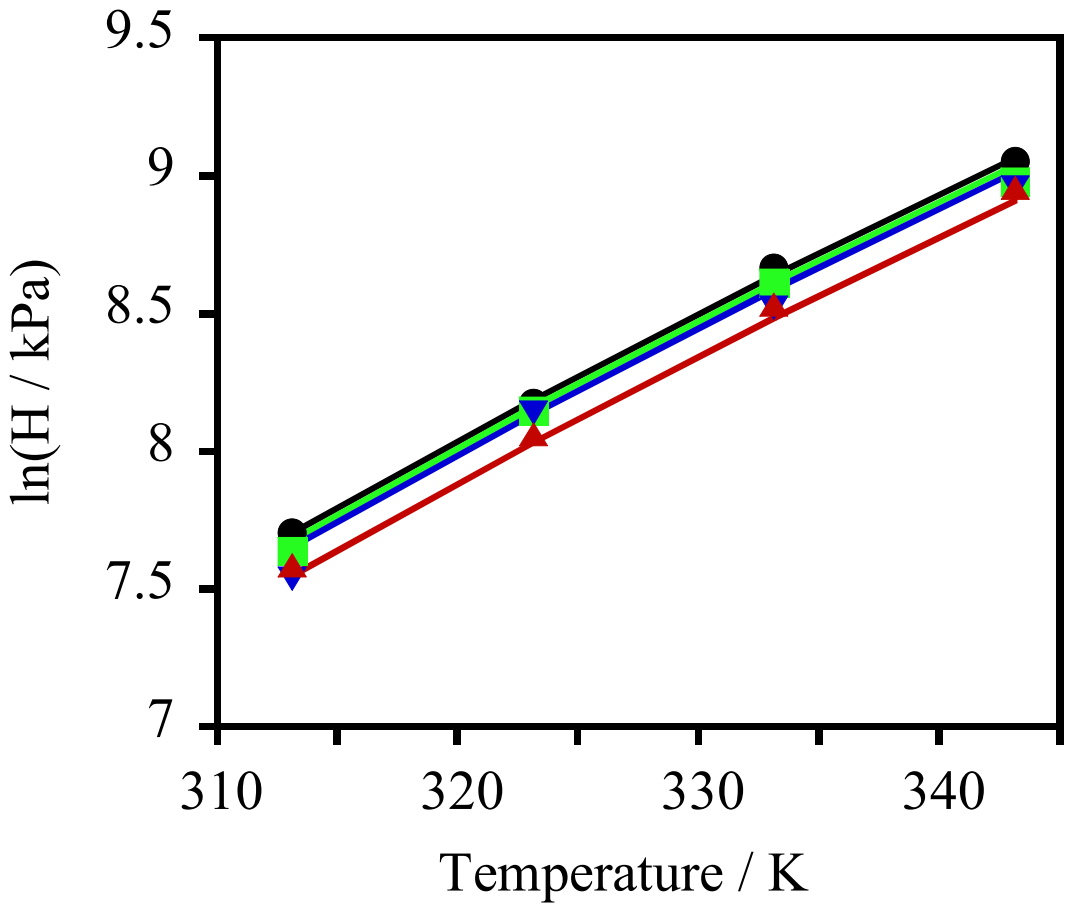

Figure 28. 2-heptanone in (●) pure water [151], (■) with 0.5 m TMA-Br [157], (▼) with 1.0 m TMA-Br [157], (▲) with 3.0 m TMA-Br [157]. Correlated with Eq. 69.

5.7 Regression of Henry's constants of 2-ketones + water + Na_2SO_4.

Eq. 69 was used to correlate Henry's constants of the 2-ketones in sodium sulfate solutions, using a single parameter *D*. The entire range of salt concentrations could be correlated with an AAD of no more than 0.4 % and a MAD of 1.0 %. The results for 2-propanone are shown in Figure 29. Similar results were observed in the case of the other 2-ketones studied in this work.

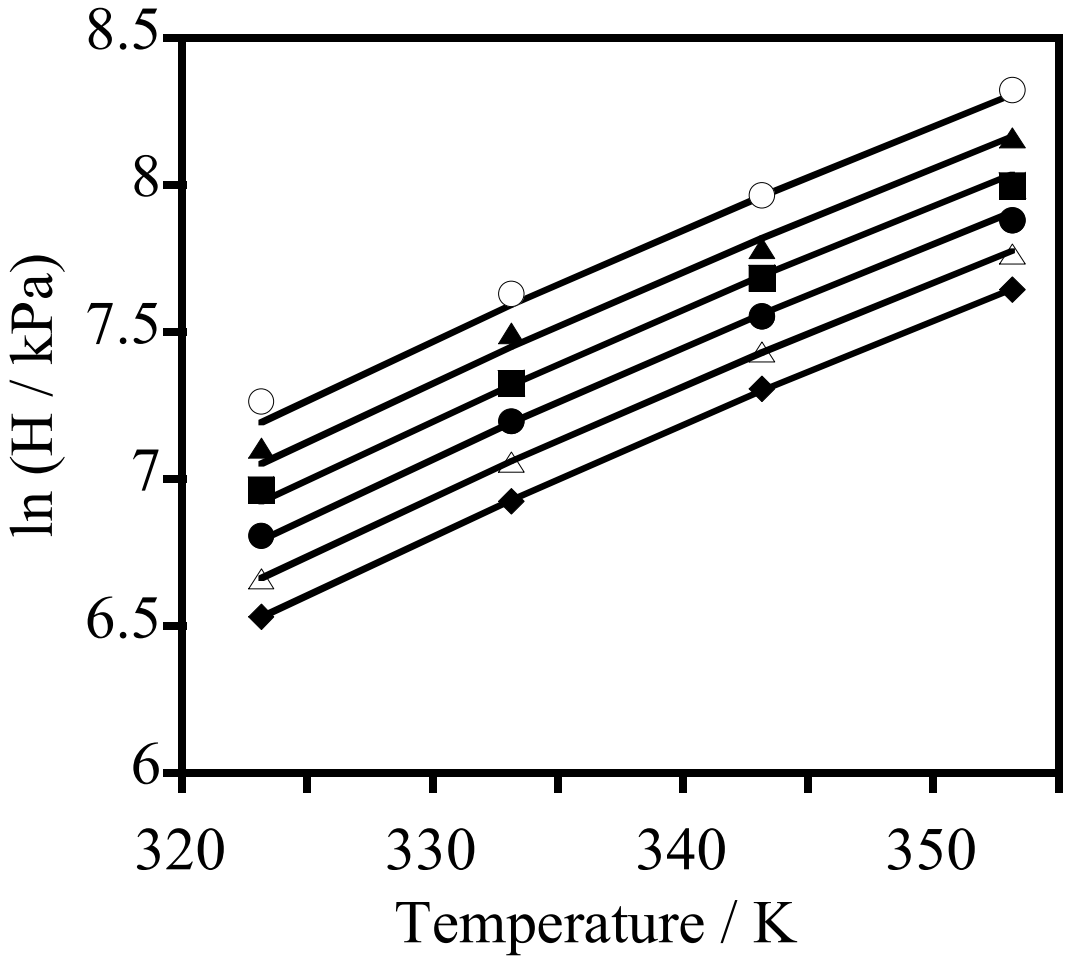

Figure 29. Henry's constants of 2-propanone + water: (◆). Also with Na_2SO_4 from this work at (△) 0.2 molal, (●) 0.4 m, (■) 0.6 m, (▲) 0.8 m, (○) 1.0 m. Data were correlated using Eq. 69.

5.8 Regression of Henry's constants of 2-ketones + water + NaCl.

Equation 69 proved sufficient to correlate Henry's constants of the VOCs at all salt concentrations. A representative plot of Henry's constants of 2-hexanone in sodium chloride solutions is presented in Figure 30. The AAD for the 2-ketone + NaCl + water data was 0.4 % and the MAD did not exceed 4.2 %. The MAD for the data was no more than 4.2 %.

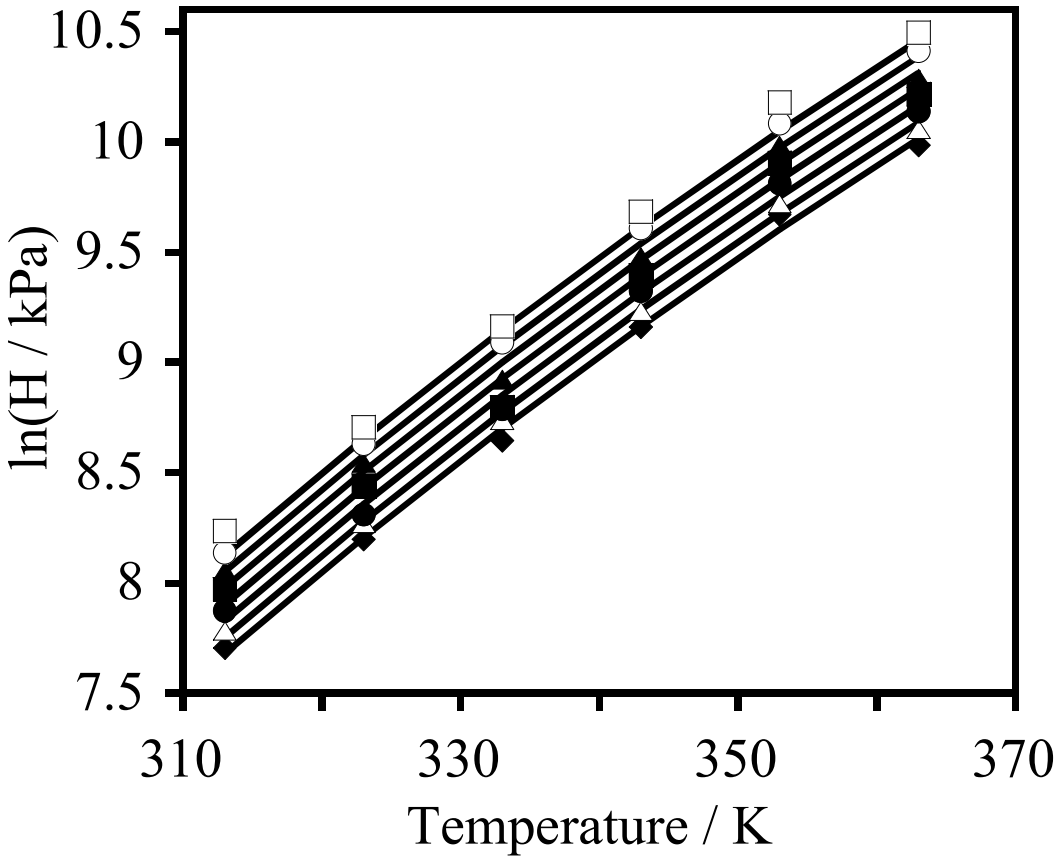

Figure 30. Henry's constants for 2-hexanone from this work in (◆) pure water and in aqueous NaCl solutions: (△) 0.2 m, (●) 0.4 m, (■) 0.6 m, (▲) 0.8 m, (○) 1.0 m, and (□) 1.2 m. The data are correlated with Eq. 69.

5.9 Regression of Henry's constants of 2-ketones + water + NaCl / Na_2SO_4 mixtures.

Henry's constants of 2-ketones in sodium chloride + sodium sulfate solutions were correlated successfully with Eq. 69 showing a full spectrum of composition. The salt effects were successfully predicted by the single temperature-independent parameter, *D*, in Eq. 69 as shown in Figure 13. The total concentration of salt in the solution was maintained at 2.0 molal while the total ionic strength on a molality basis, *I*, was calculated as follows,

$$I = 1/2 \sum_{i=1}^{n} m_i z_i^2 \,, \qquad (152)$$

where, *n* is the number of unique ionic species and *z* is the charge on an ionic species. Total ionic strength of the sodium chloride and sodium sulfate mixtures, as calculated with Eq. 152 varied from 3.0 to 5.0 as the molar proportions of sodium chloride and sodium sulfate was varied from 0.5 : 1.5 to 1.5 : 0.5. The data for sodium chloride solutions and sodium sulfate solutions shown in Figure 13 were both at a salt concentration of 1.0 molal, yielding an ionic strength of 1.0 for sodium chloride and 3.0 for sodium sulfate.

The close correlation of salt mixtures offers an alternative to continuum models (Eqs. 20 through 22) that fail to describe the salting out quantitatively and also fail to even qualitatively describe the salting in of a volatile solute. This inability to predict salt effects stems from the fact that the models assume the dielectric constant of the solvent to be homogeneous when it is not in practice. Water, for example, will have a single-digit dielectric constant in the vicinity of a salt ion and a dielectric constant of 78 near room temperature several water molecules away from the salt ion. Dilute solution theory based

models such as Eqs. 69 and 148 allow one to navigate around the shortcomings of continuum models and correlate air/water partitioning coefficients (Henry's constants) of VOCs and GHGs with a single temperature independent parameter. Using the molal ionic strength scales the effects of different ions appropriately so that a single parameter, *D*, will accomplish the entire correlation task over wide temperature ranges as shown in Figure 31.

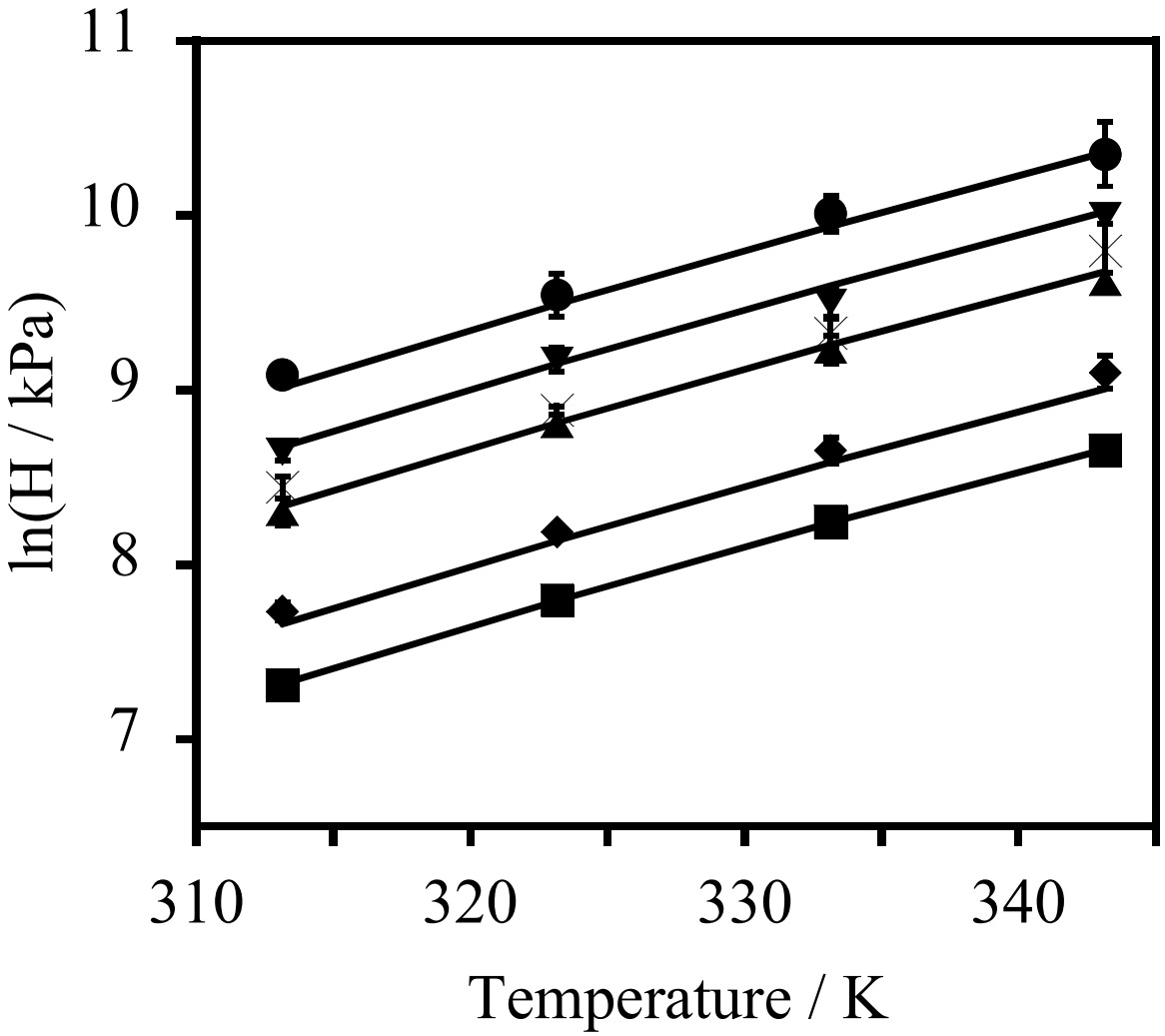

Figure 31. 2-hexanone in (■) pure water [157] and with NaCl and Na_2SO_4: (◆) 1.0 m NaCl (I = 1.0) [157], (▲) 75 mole % NaCl : 25% Na_2SO_4 (I = 3.0) [157], (×) 1.0 m Na_2SO_4 (I = 3.0) [157], (▼) 50 % NaCl : 50 % Na_2SO_4 (I = 4) [157], (●) 25 % NaCl : 75 % Na_2SO_4 (I = 5) [157]. Correlated with (━) Eq. 69.

5.10 Regression of Henry's constants of 1-alkanols + water + Na_2SO_4.

Equation 69 worked well in correlating the data for this system with units of ionic strength or molality. An example fit of Henry's constants for 1-butanol in Figure 32 showed close agreement between the data and model. The AAD for the fit of the data was 1.3 % and the average absolute deviation (AAD) did not exceed 4.6 %.

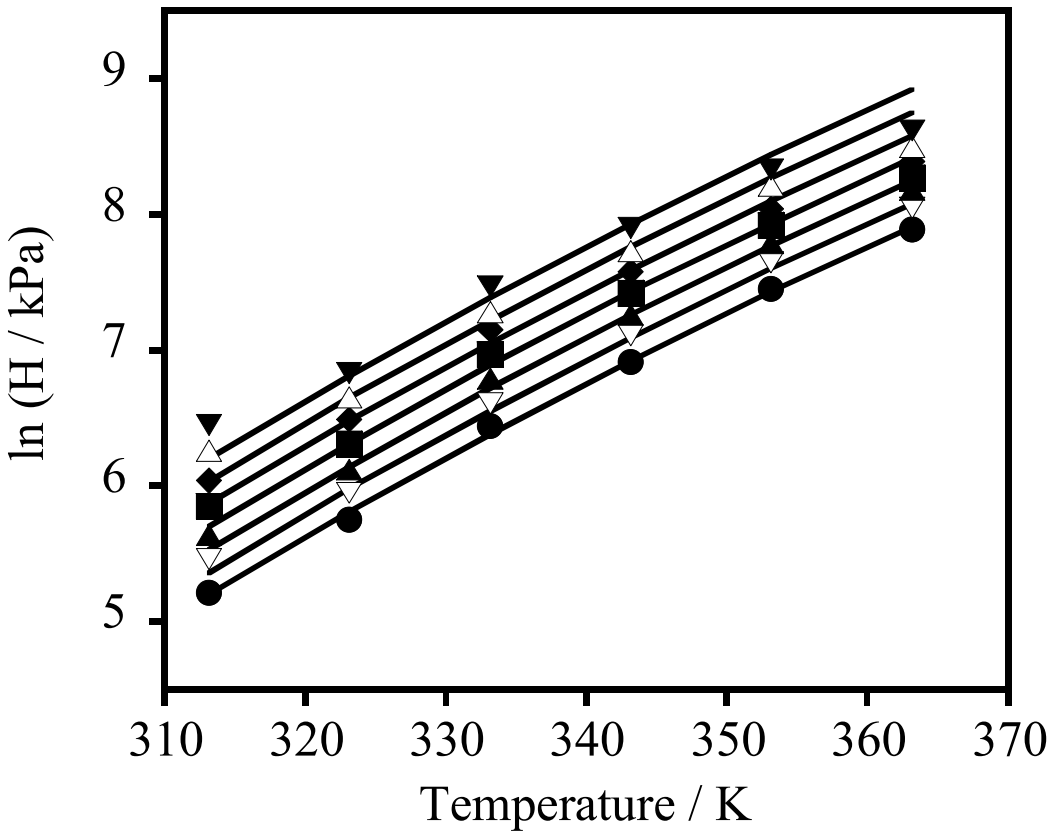

Figure 32. Henry's constants for 1-butanol [151] in (●) pure water and in aqueous Na_2SO_4 solutions: (▽) 0.2 m, (▲) 0.4 m, (■) 0.6 m, (◆) 0.8 m, (△) 1.0 m, and (▼) 1.2 m. Correlated with (━) Eq. 69.

5.11 Trends in regression parameters.

Regressed values of D also compared well with temperature-averaged values of Setchenov constants k_s obtained from the literature, as can be seen in Figure 33. It is possible to see from this Figure that when exposed to sodium sulfate, 2-ketones have greater salt effect parameters and Setchenov constants than 1-alkanols due to the 1-alkanol's hydrogen bonding capability.

Since Setchenov constants are generally available only at 298 K, regressed values of D were also compared with calculated k_s at 298 K. One such comparison is shown in Figure 35 where D values obtained by regression of experimental data of Brendel and Sandler [35] for five VOCs in NaCl solutions are compared with k_s values at 298 K. There is excellent agreement between the two sets of constants and therefore, it is possible to use k_s values at 298 K directly in Eq. 69. This is demonstrated in Figure 35 where experimental values of Henry's constants of benzene in NaCl solutions over a 30 K temperature range are correlated using the ks determined at 298 K in Eq. 69. Good agreement between calculation and experiment is seen.

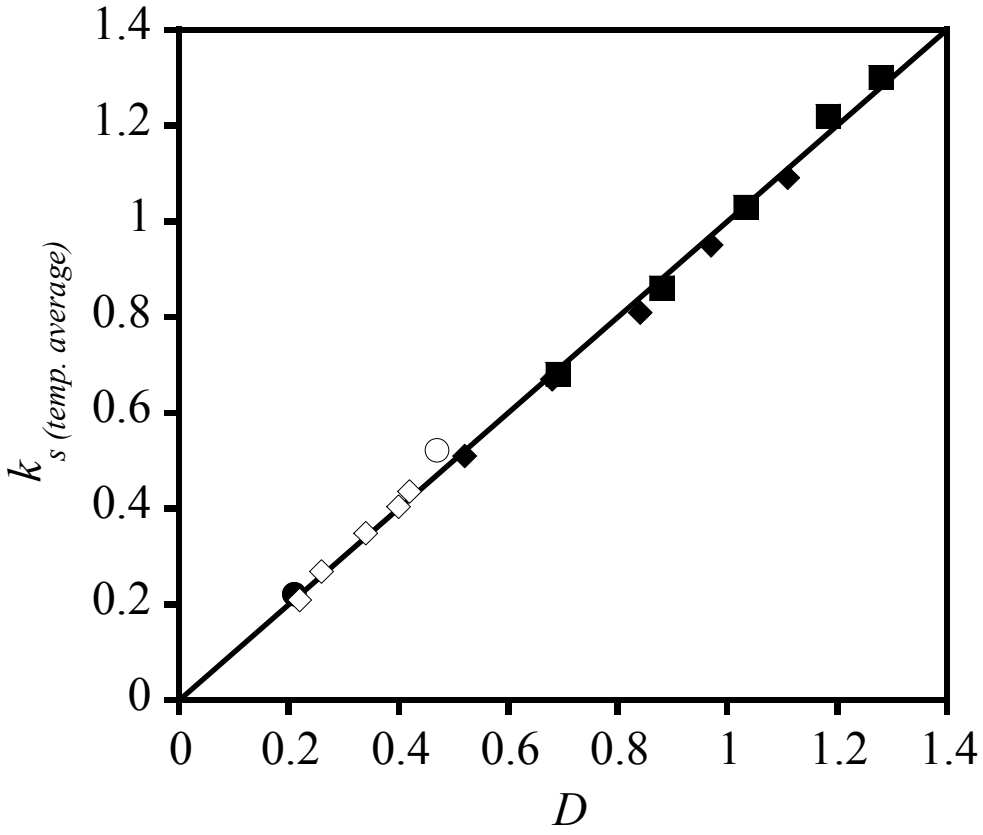

Figure 33. Comparison between temperature averaged Setchenov constants and *D* on a molality basis in the system: 2-ketones + Na_2SO_4 + water (■), 2-ketones + NaCl + water (◇),1-alkanols (excluding methanol) + Na_2SO_4 + water (◆), methanol + Na_2SO_4 (○) [4], and methanol + Na_2CO_3 (●) [4].

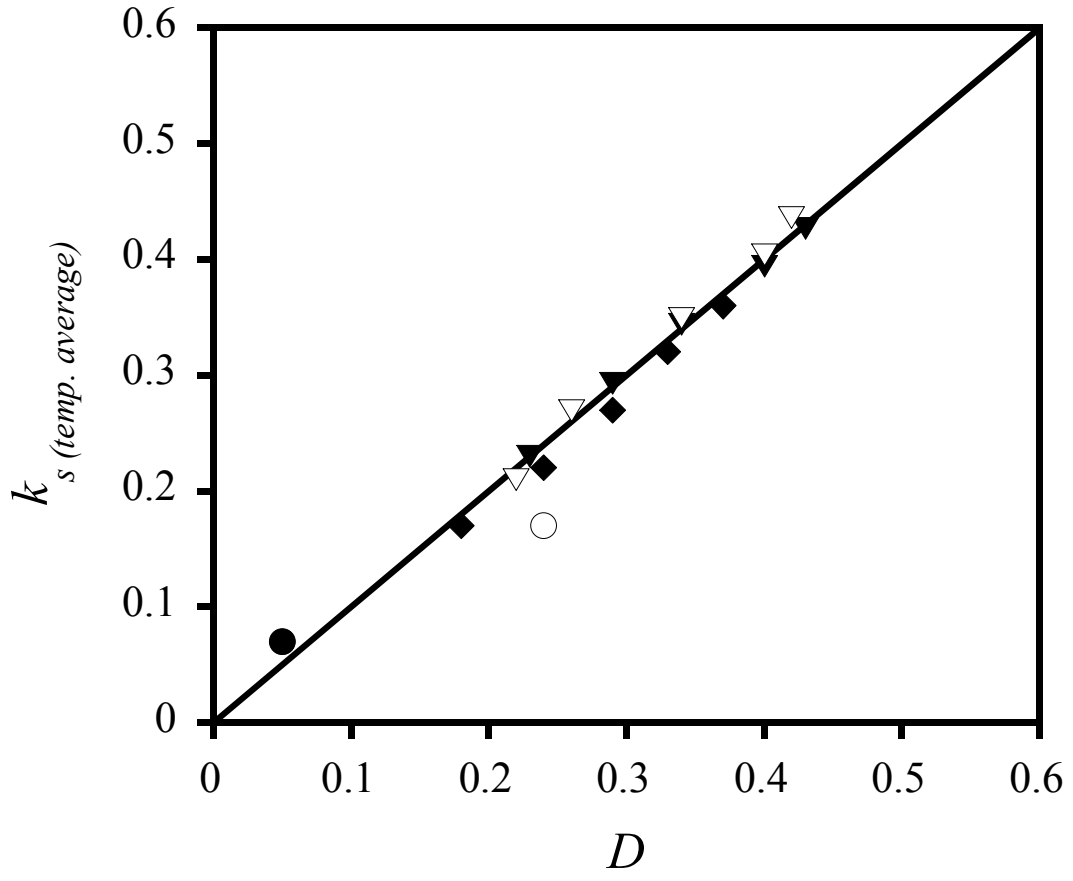

Figure 34. Comparison between temperature averaged Setchenov constant and *D,* on an ionic strength basis in the system: 2-ketones + Na_2SO_4 + water (■), 2-ketones + NaCl + water (▽), 1-alkanols (excluding methanol) + Na_2SO_4 + water (▼), methanol + Na_2SO_4 + water (○) [4], and methanol + Na_2CO_3 + water (●) [4].

Table 25. Comparison of *D* with the Setchenov constant at 298 K [164].

VOC	NaCl conc. Range (m)	D*	k_s**
trichloroethylene	0.2 - 1.5	0.391	0.367
dichloromethane	0.5 - 2.5	0.279	0.278
chloroform	0.5 - 2.5	0.347	0.309
1,2-dichloroethane	0.2 - 2.5	0.318	0.304
benzene	0.2 - 1.5	0.433	0.420

* D calculated using VOC + water + NaCl data of Brendel and Sandler [35].
** k_s calculated using VOC + water + NaCl data at 25 C from Brendel and Sandler [35]

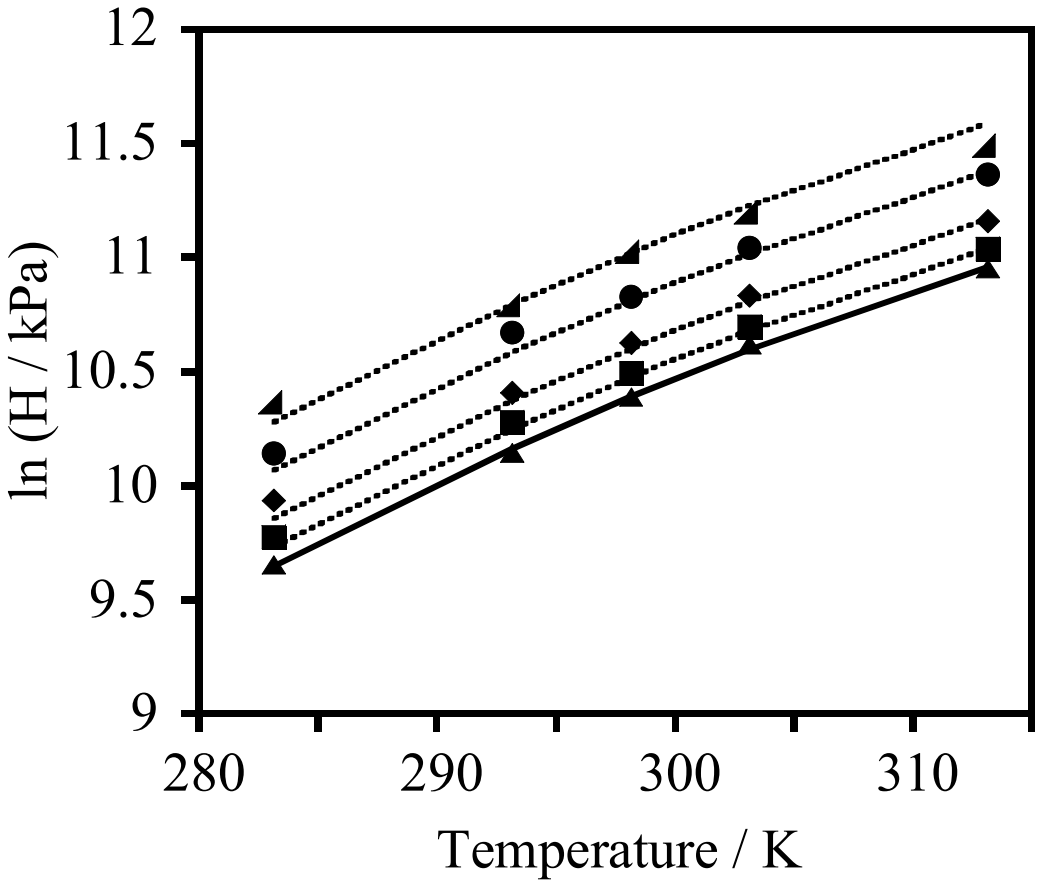

Figure 35. Henry's constants of benzene [35] in (▲) pure water (■) 0.2 m NaCl, (◆) 0.5 m NaCl, (●) 1.0 m NaCl, and (◢) 1.5 m NaCl solutions using k_s at 298 K in Eq. 69.

5.12 Trends of *D* with molecular size for homologous series of 1-alkanols and 2-ketones.

Figure 36 shows that *D* for a homologous series of 1-alkanols and 2-ketones follows a linear trend with the critical molar volume, V_{crit} of the VOC. All salt effect parameters for homologous compounds with inorganic salts can be predicted with a single trend line. This trend in *D* vs. V_{crit} supports the finding of Debye and Macaulay whose electrostatic model (Eq. 20) shows that the Setchenov constant is directly proportional to the molar volume of the solute. Linear trends could be found for 2-ketones and TEA-Br and TMA-Br, however, they did not pass through the origin. The reason for the different salt effect parameter trends is due to the higher dispersion forces from the tetraalkylammonium cation in solution where the simple inorganic salts are very compact and the electrons in the valence cannot arrange themselves into temporary dipoles as easily. Figure 37 shows that the salt effect parameters in Figure 36 can be generalized to other salts on the ionic strength basis.

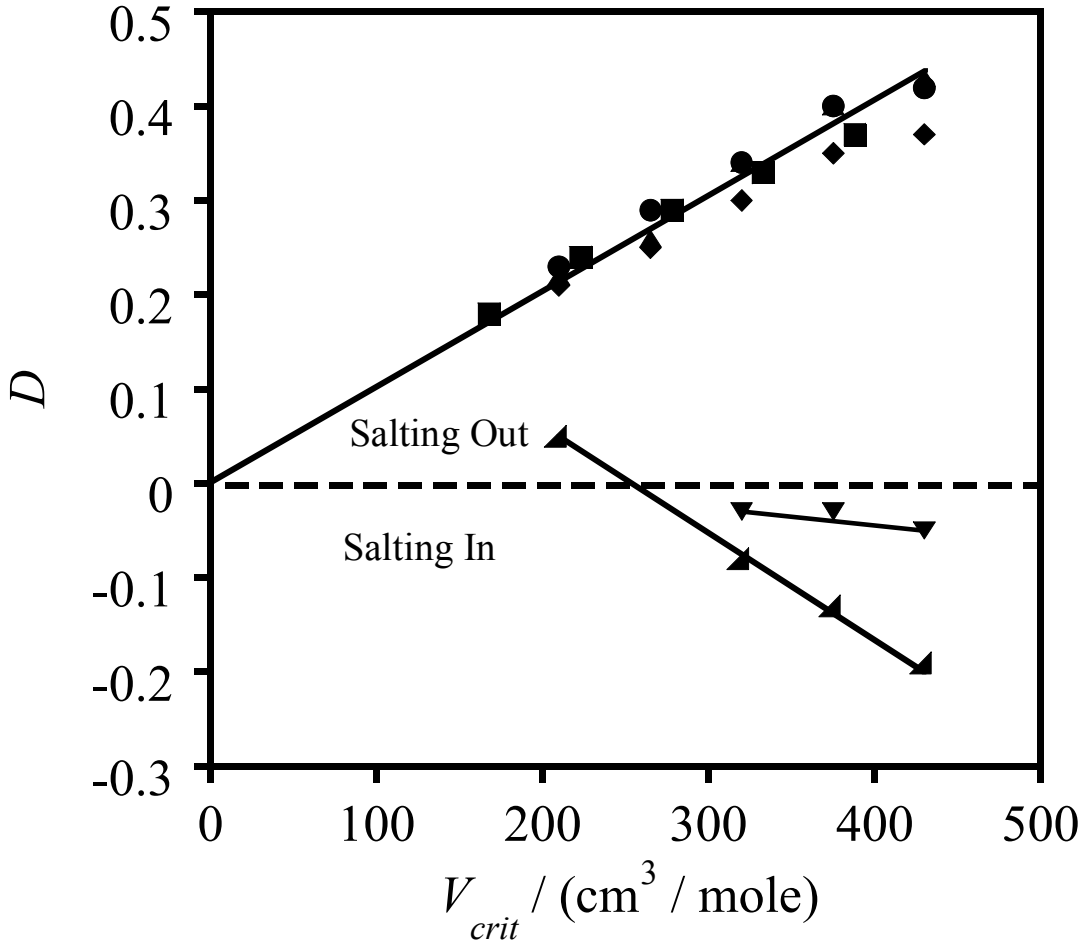

Figure 36. Parameter *D* from Eq. 69 on an ionic strength basis as a function of critical molar volume for: (◆) 2-ketones + NaCl + Na_2SO_4, (▲) 2-ketones + NaCl [151], (●) 2-ketones + Na_2SO_4 [155], (▼) 2-ketones + TMA-Br, (◢) 2-ketones + TEA-Br, (■) 1-alkanols + Na_2SO_4 [151]. (—) least squares fit.

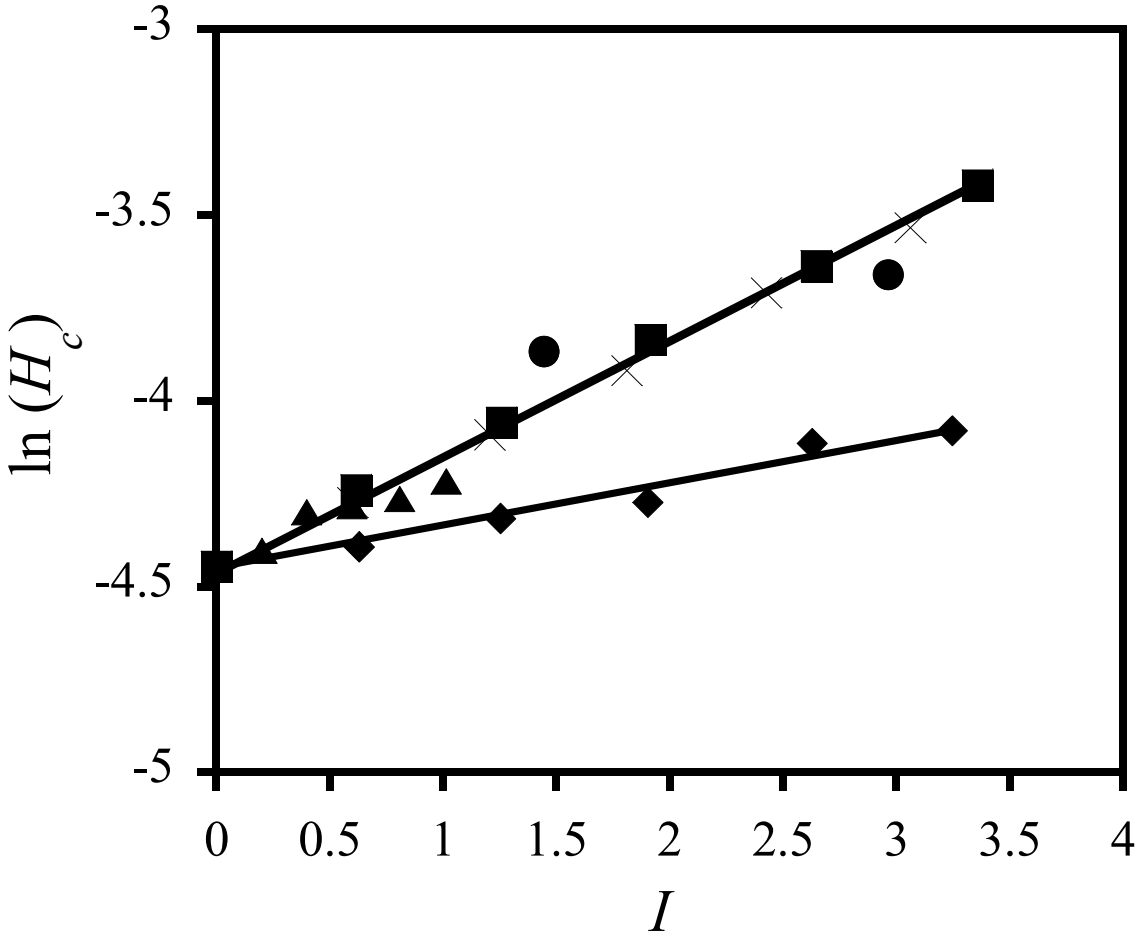

Figure 37. Salt effects for 2-propanone with (◆) sodium sulfate [151], (●) potassium sulfate [151], (×) sodium carbonate [151], (▲) sodium chloride [151], and (■) calcium chloride [151].

Trends in all of the parameters of Eq. 69 provide a means to obtain constants for VOCs and GHGs in a homologous series even if there are no prior Henry's constants tabulated in the literature. Trends in the salt effect parameter *D* as a function of critical molar volume have been shown in Figure 36. Henry's constants for homologous series of 2-ketones and 1-alkanols regressed from 313 to 343 K generated clear linear trends in *A*, *B*, and *C* as a function of molecular size in Figure 38 for 2-ketones and Figure 39 for 1-alkanols.

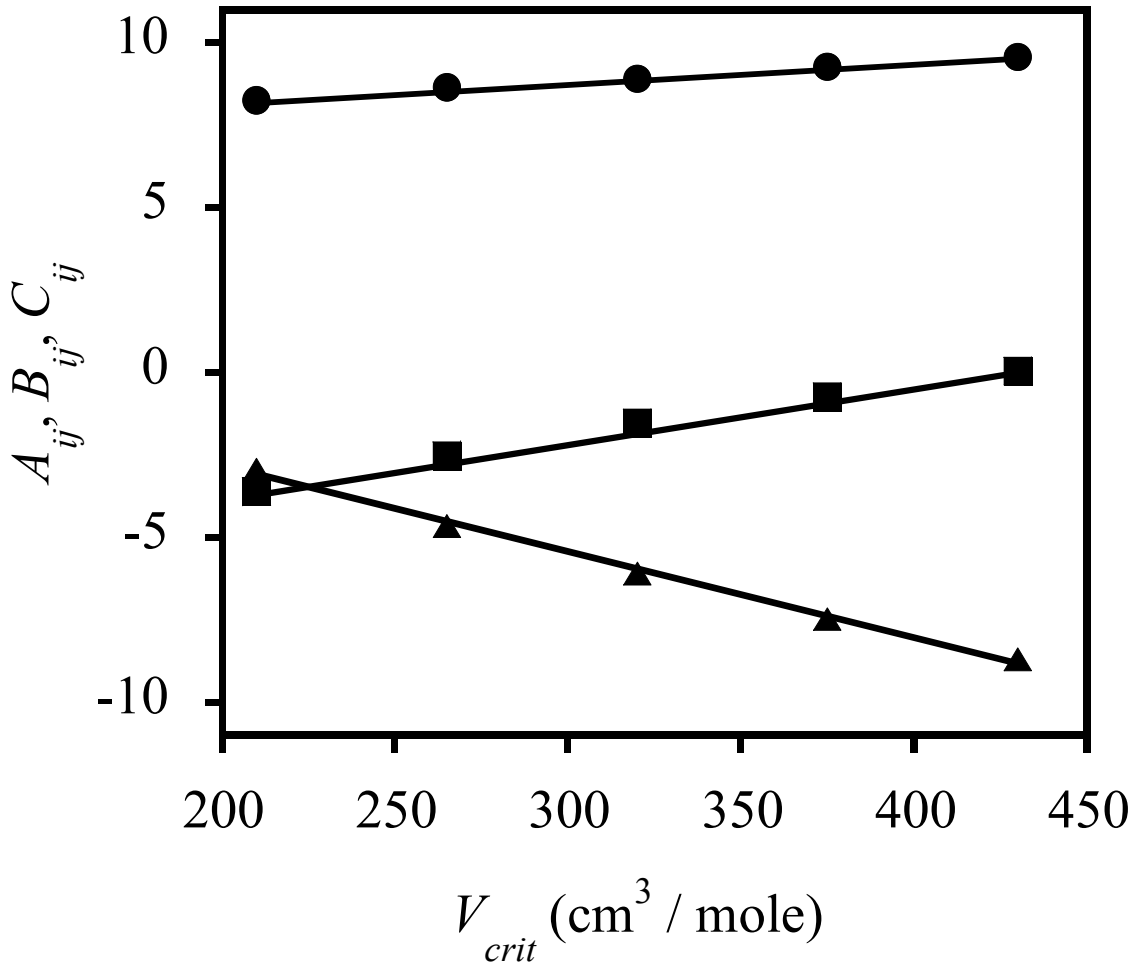

Figure 38. Trends in the binary parameters of Eq. 69 with a homologous series of 2-ketones (2-propanone to 2-heptanone) (●) A_{ij}, (▲) B_{ij}, (■) C_{ij}.

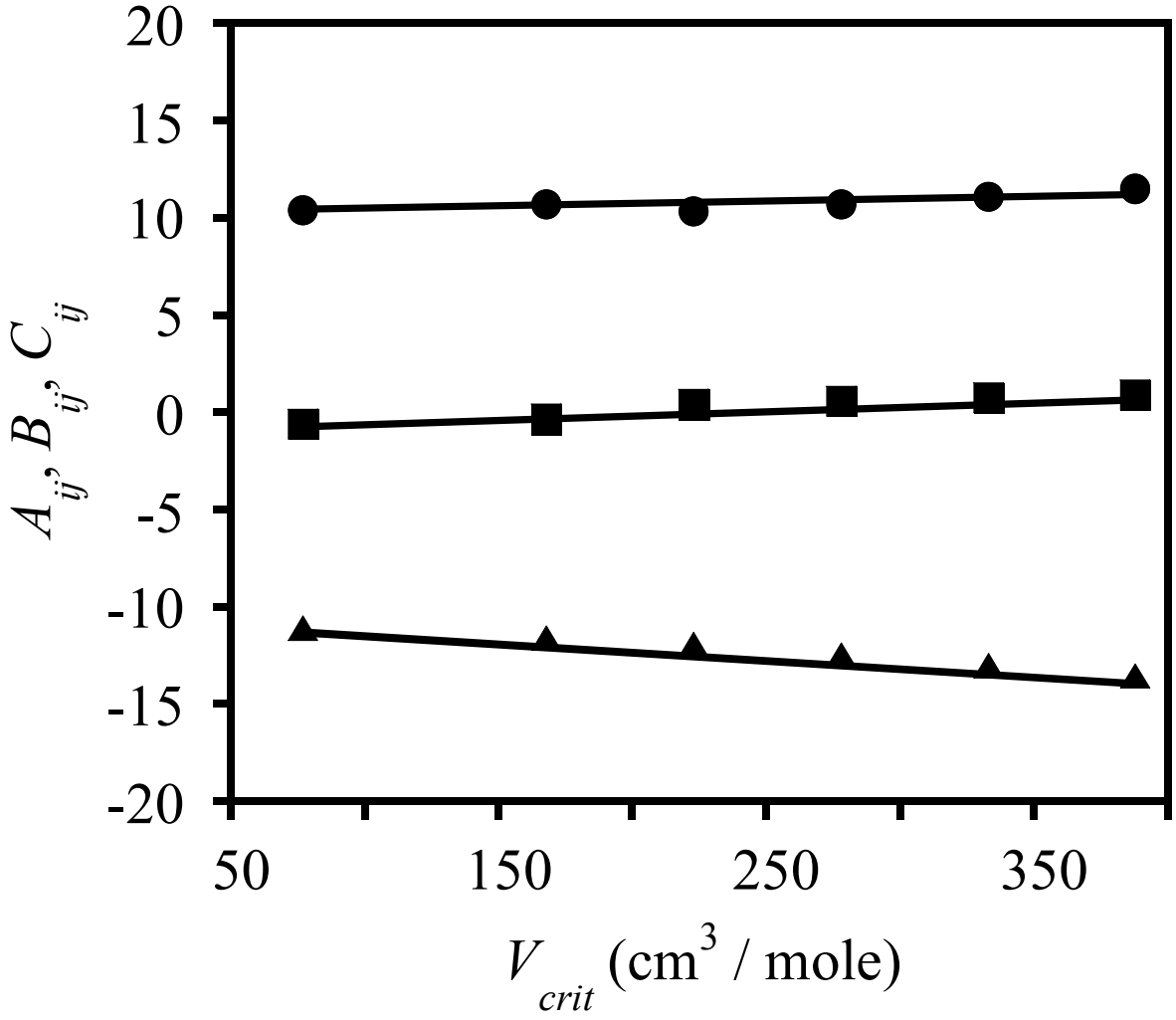

Figure 39. Trends in the binary parameters of Eq. 69 with a homologous series of 1-alkanols (methanol to 1-hexanol) (●) A_{ij}, (▲) B_{ij}, (■) C_{ij}.

6. CONCLUSIONS AND RECOMMENDATIONS

In this work Henry's constants in 39 systems containing a VOC, water, and salt were determined from 313 to 363 K using headspace gas chromatography. An additional 19 systems were used to supplement the data obtained in this work. The systems measured have relevance to the paper industry and the energy industry.

A new relative headspace gas chromatography method was developed for rapid determination of Henry's constants of moderately volatile VOCs such as 1-alkanols and 2-ketones. The method rests upon the fact that the VOC concentration in the liquid phase does not change measurably if samples are withdrawn from a very small vapor space above the liquid at equilibrium. The new relative method was checked against the differential method of Chai and Zhu [1, 67] and was found to agree within experimental error. The new relative method is unsuitable for highly volatile solutes such as aromatic hydrocarbons since they partition mostly into the headspace. Partial molar excess enthalpies at infinite dilution were obtained by differentiation of Henry's constant data for methanol, ethanol, 1-propanol, and 2-butanone and compared with calorimetrically determined values. The 50 % agreement between the two sets was considered satisfactory because differentiation represents a very severe test of the validity of the data.

The dilute solution theory-based model of Teja et al. [4] was extended to high pressures using the Krichevsky-Kasarnovsky type approach. The parameter in this pressure term is the partial molar volume of the volatile solute at infinite dilution.

The salt effect parameter, D, was found to be equal to the temperature-average Setchenov constant through a parity plot. This gives the ability to use any existing literature data since spacing between the curves is nearly identical for salts that exhibit

salting out behavior. All of the simple salts examined (NaCl, $CaCl_2$, Na_2SO_4, Na_2CO_3, K_2SO_4) reduce VOC and GHG solubility. The degree to which they influence the Henry's constant was successfully predicted by a Setchenov-like term using units of ionic strength and units of molality consistent with the electrostatic model Debye and McAulay [90]. This allows one to generalize the salting out parameter in Eqs. 69 or 148 to other simple inorganic salts not used in this work on the basis of ionic strength.

Correlation of Henry's constants for VOCs and GHGs in the presence of salt mixtures can be accomplished using the total ionic strength. Use of molal ionic strength scales the salt effects appropriately so that salts that induce more salting out have proportionally higher ionic strengths. As a result, a single factor, *D*, can be used to correlate Henry's constants in aqueous solutions containing salt mixtures.

The new model is capable of correlating water + salt + VOC systems from ambient conditions to near the critical point of water.

Two salts that enhance VOC solubility were used with a homologous series of 2-ketones. TEA-Br interacted strongly with the higher molecular weight 2-ketones resulting in salting in for most compounds. 2-propanone was salted out by TEA-Br. TMA-Br tended to exhibit a slight salting in effect on 2-ketones heavier than 2-propanone. Salting out was observed for 2-propanone as well in the presence of TMA-Br. This behavior can be explained by molecular modeling results [5] where the organic cation breaks up the hydrogen bonded structure and allows hydrophobic solutes such as higher 2-ketones. The lower molecular weight 2-propanone is very hydrophilic and does not increase its solubility when the water molecules are disordered. Upon exposure to the bromide ion, 2-

propanone salts out and its Henry's constants are readily predicted by Setchenov's relationship.

The atmosphere contains a wide variety of salts that enhance or inhibit the solubility of VOCs. It would be a logical next step to determine Henry's constants for mixtures consisting of one salt that enhances the solubility of VOCs (salts in) and one that reduces VOC solubility (salts out). This data could be used to develop a model that will predict the salt effects of these mixtures.

Having measured the Henry's constants of 2-ketones (2-propanone to 2-heptanone) with sodium sulfate and sodium chloride in addition to tetraalkylammonium salts, a logical follow-up to this would be to investigate the partitioning of 2-alkanols (2-propanol to 2-hexanol) with the same salts to examine the predictability of their air-water partitioning.

To further address global warming, VLE data for carbon dioxide should be modeled with Eq. 148. The aqueous CO_2 - salt systems is more involved since the liquid phase divides into two phases with different amounts of CO_2 at high pressure and temperatures below 373 K.

Future modeling work should be focused on the interactions between salt ions such as TMA-Br and TEA-Br and VOCs. As stated earlier, predicting salt effect parameters for a homologous series of alkanols or ketones with the functional group at different positions along the structure can help to further generalize the model and enable more *a priori* predictions. Predicting the behavior of salts that enhance the solubility of VOCs will be of use for environmental modeling and in the development of separations

processes for removal of heavy organic vapor from a light gas stream such as methane as typically occurs in the extraction of methane from wells.

APPENDIX A: PROCEDURE FOR HEADSPACE GAS CHROMATOGRAPHY.

Equipment Preparation

1. Open the valves so that the handle will not turn on 3 compressed gas cylinders: hydrogen, helium (open this valve slowly since the impurity trap must be pressurized over the course of 10 seconds to avoid damage to the adsorbent inside), and ultra zero air.

2. Turn the equipment in the following order:
   - Computer (requires floppy disk to boot (NT username: *administrator*; leave the password box blank; select the domain: *MUFASA*).
   - Headspace Sampler (HS): power switch is on the back near the counter top. Make certain that the temperatures are set to the lowest temperature in your set of runs. If the sampler says that the RAM values are lost, press the Clear button until the message stops flashing and re-enter the desired starting oven temperatures that are typically a 40 C oven temp., 50 C valve temp, and 200 C transfer line temp.
   - Gas Chromatograph (GC): press the power switch on the front lower left corner completely inward and release somewhat slowly. If the ground fault protector on the outlet pops, turn off the GC and reset the ground fault protected outlet that it is plugged into.

3. When the FID temperature reaches 150 C, you should hear a pop from the flame ionization detector (FID) atop the GC. Several minutes later open the hatch on top of the GC and position a mirror or glass headspace vial over the open hole in the FID—the surface should fog when the water vapor from the FID contacts the surface.

Software Settings

4. Select the programs for Headspace and GC.

   - Headspace sampler: **Start → All Programs → Headspace Control → HP7694 Link**

   - GC: **Start → All Programs → HP ChemStation → Instrument 1 Online**

5. The HP ChemStation software for the GC will open the routine that was running when the computer was shut down.

6. The GC run time which determines how long FID sensor output is logged is set in the **Oven** section of HP ChemStation. The oven settings can be accessed by pressing the oven button in the workspace. In this dialog box, an oven temperature program can be specified and the length of time that the sensor logs the data by changing the **Oven Hold Time**. The oven hold time will control how long sensor data is logged for each injection.

7. Typical GC settings categorized according to their place in the software for 2-ketones are as follow:

Oven:

Hold Time: 6.5 min

Oven Temperature: 60 C

Inlets:

Mode: Splitless

Temperature: 250 C

Total Flow Rate: 10.9 ml / min

Pressure: 3.32 psi (will be set by the linear velocity in the next section)

Column:

Type: HP INNOWAX 0.53 mm column with 1 μm thick immobile phase.

Carrier Gas Velocity: 62 cm / s

Detector:

Hydrogen Gas Flow Rate: 40 ml / min

Air Flow Rate: 400 ml / min

Makeup Flow Rate: 40 (unitless)

Lit Offset: 0.3 (tells the GC when the flame is out and must be relit. Set this lower if the FID tries to relight even though it is already working.)

If the FID is not producing a continuous flame, reignite the detector until the flame stays on by using the “Reignite” button in the FID dialog box.

Signals:

Data Rate: 20 Hz

Minimum Peak Width: 0.01 min

8. Open a headspace sampler routine and enter the typical headspace sampler software settings are as follow for 2-ketones equilibrating at 40 C:

   Oven Temperature: *40 C*
   Valve Temperature: *50 C*
   Transfer Line Temperature: *200 C*
   GC Cycle Time: *7.5 min*
   Vial Equilibration Time: *45 min (for 15 ml in 21.6 ml vial)*
   Vial Pressurization Time: *0.70 min*
   Sample Loop Fill Time: *0.05 min*
   Loop Equilibration Time: *0.05 min*
   Sample Injection Time: *1.00 min*
   Shaker Setting: *high*

9. To export the GC data to the clip board so that it can be deposited in MS Excel Switch to the view of the integrated data in the GC monitoring program and follow these menu commands:
   - File => Export File => CSV File
     x Write to Clipboard
     Select the content, press OK.

Shut Down Procedure

10. To Shut down the Headspace Sampler, first ensure that the oven temperature is set back to 40 C and the valve temperature is set back to 50 C so that it can be preheated the next day. Second, flip the power switch off on the back of the unit.

11. To shut down the GC, first shut down the HP ChemStation software. Second, power down the GC by pressing the power button in the lower left corner and releasing it slowly.

12. Close the valves on the three high-pressure gas cylinders supplying the equipment.

Equipment Operating Parameter File Locations

The location of the HP ChemStation files for GC operation is:

c:/HPChem/I

The location of the headspace sampler files is:

c:/HP7694/methods.

Backup of Data

The data from the computer drives will be located in the Teja Group Network folder under “lab computer backups”

APPENDIX B: ERROR ANALYSIS FOR THE RELATIVE AND DIFFERENTIAL METHODS.

Error analysis for the relative method

According to Chai et al. [155], Henry's constants of a volatile compound *i* in water with and without salt are related to measured chromatographic peak areas as follows:

$$H_{i,m} = H_{i,0}\frac{A_m}{A_0} \qquad (153)$$

where $H_{i,0}$ and $H_{i,m}$ are Henry's constants of the VOC in water and in the salt solution; and A_0, A_m are peak areas obtained from a chromatographic analysis of the headspace above water and the salt solution, respectively. Thus Henry's constant of the VOC in the salt solution $H_{i,m}$ can be obtained from two peak areas and a reference value of the Henry's constant.

According to Halpern [76], the overall uncertainty $\sigma_{Hi,m}$ in Henry's constant $H_{i,m}$ can be obtained by taking the total differential of Eq. 153,

$$dH_{i,m} = \left[\left(\frac{\partial H_{i,m}}{\partial H_{i,0}}\right)_{A_m,A_0} dH_{i,0} + \left(\frac{\partial H_{i,m}}{\partial A_m}\right)_{H_{i,0},A_0} dA_m + \left(\frac{\partial H_{i,m}}{\partial A_0}\right)_{H_{i,0},A_m} dA_0\right] \qquad (154)$$

Inserting Eq. 154 to obtain and expression for the variance of the Henry's constant in our sample,

$$\sigma^2_{H_{i,m}} = \frac{1}{N-1}\sum_{i=1}^{N} dH^2_{i,m}\,, \qquad (155)$$

where N is the number of replicates. The derivatives are converted to variances and we obtain the following expression for the variance in the Henry's constant:

$$\sigma^2_{H_{i,m}} = \left[\left(\frac{\partial H_{i,m}}{\partial H_{i,0}} \right)^2 \sigma^2_{H_{i,0}} + \left(\frac{\partial H_{i,m}}{\partial A_m} \right)^2 \sigma^2_{A_m} + \left(\frac{\partial H_{i,m}}{\partial A_0} \right)^2 \sigma^2_{A_0} \right] \quad (156)$$

dividing both sides by Eq. 153 and taking the square root of both sides yields an expression for the uncertainty in the Henry's constant of the sample expressed in terms of the uncertainty in the reference Henry's constant $\sigma_{Hi,0}$ and the uncertainties in the peak areas σ_{Am} and σ_{A0} as follows:

$$\frac{\sigma_{H_{i,m}}}{H_{i,m}} = \sqrt{\left(\frac{\sigma_{H_{i,0}}}{H_{i,0}} \right)^2 + \left(\frac{\sigma_{A_m}}{A_m} \right)^2 + \left(\frac{\sigma_{A_0}}{A_0} \right)^2} \quad (157)$$

The uncertainties were estimated from the standard deviations from 3 separate runs and Eq. 157.

Error analysis for the differential method.

Each Henry's constant is the average of three replicate runs performed on different days. The error in the measurement is reported as the relative standard deviation of the three replicate runs with the exception of the aromatics that were measured six times since they were included with methyl *tert*butyl ether and ethyl *tert*butyl ether.

APPENDIX C: ERROR ANALYSIS FOR DILUTE SOLUTION THEORY

In this work, the Henry's constant possesses the greatest uncertainty and will be solely used to compute the uncertainty in all of the parameters in Eq. 148. The error for binary parameter A_{ij} in Eq. 148 is calculated as follows:

$$A_{ij} = T_r\, ln\left(H_{i,m}\right) - T_r\, ln\, P_j^{sat} - B_{ij}\left(1-T_r\right)^{0.355} - C_{ij}\, exp\left(1-T_r\right)T^{0.59} - Dx_k T_r - \bar{v}_i^{\infty}\frac{\left(P-P_{ref}\right)T_r}{RT} \quad (158)$$

Taking the partial derivative of Eq. 158 with respect to the Henry's constant, $H_{i,m}$ and inserting into Halpern's formula for uncertainty yields:

$$\varepsilon_{A_{ij}} = \sqrt{\left(\frac{T_r}{ln\left(H_{i,j}\right)}\right)^2 \varepsilon^2_{ln\left(H_{i,j}\right)}} \quad (159)$$

Where $\varepsilon_{A_{ij}}$ is the uncertainty in parameter A_{ij} in Eq. 159 and $\varepsilon^2_{ln\left(H_{i,j}\right)}$ is the calculated standard deviation in the Henry's constant. The expressions for the uncertainties in the other two binary parameters $\varepsilon_{B_{ij}}$ and $\varepsilon_{C_{ij}}$ plus the salt effect parameter D and the molar volume at infinite dilution $\bar{v}_i^{\infty}$ are,

$$\varepsilon_{B_{ij}} = \sqrt{\left(\frac{T_r}{ln\left(H_{i,j}\right)\left(1-T_r\right)^{0.355}}\right)^2 \varepsilon^2_{ln\left(H_{i,j}\right)}}, \quad (160)$$

$$\varepsilon_{C_{ij}} = \sqrt{\left(\frac{T_r^{0.41}}{ln\left(H_{i,j}\right)\left(1-T_r\right)}\right)^2 \varepsilon^2_{ln\left(H_{i,j}\right)}}, \quad (161)$$

$$\varepsilon_D = \sqrt{\left(\frac{1}{ln\left(H_{i,m}\right)x_k}\right)^2 \varepsilon^2_{ln\left(H_{i,m}\right)}}\,, \tag{162}$$

and

$$\varepsilon_{\frac{-\infty}{v_i}} = \sqrt{\left(\frac{RT}{ln\left(H_{i,j}\right)\left(P - P^{ref}\right)}\right)^2 \varepsilon^2_{ln\left(H_{i,j}\right)}}\,. \tag{163}$$

REFERENCES

1. Chai, X. S. and Zhu, J. Y., Indirect headspace gas chromatographic method for vapor-liquid phase equilibrium study., Journal of Chromatography, A 1020 (2) (2003) 283-284.

2. Yaws, C. L., Sheth, S. D., and Han, M., Using solubility and Henry's law constant data for ketones in water, Pollution Engineering 30 (2) (1998) 44-46.

3. Gros, J. B., Dussap, C. G., and Catte, M., Estimation of O_2 and CO_2 Solubility in Microbial Culture Media, Biotechnology Progress 15 (5) (1999) 923-927.

4. Teja, A. S., Gupta, A. K., Bullock, K., Chai, X.-S., and Zhu, J., Henry's constants of methanol in aqueous systems containing salts, Fluid Phase Equilibria 185 (1-2) (2001) 265-274.

5. Slusher, J. T. and Cummings, P. T., Molecular Simulation Study of Tetraalkylammonium Halides. 1. Solvation Structure and Hydrogen Bonding in Aqueous Solutions, Journal of Physical Chemistry B 101 (19) (1997) 3818-3826.

6. Gupta, A. K., Teja, A. S., Chai, X. S., and Zhu, J. Y., Henry's constants of n-alkanols (methanol through n-hexanol) in water at temperatures between 40 ^{o}C and 90 ^{o}C, Fluid Phase Equilibria 170 (2) (2000) 183-192.

7. Staudinger, J. and Roberts, P. V., A critical review of Henry's law constants for environmental applications, Critical Reviews in Environmental Science and Technology 26 (3) (1996) 205-297.

8. Teja, A. S. and Patel, N. C., The Applications of a Generalized Equation of State to the Correlation and Prediction of Phase-Equilibria, Chemical Engineering Communications 13 (1-3) (1981) 39-53.

9. Wilding, W. V. and Wilson, L. C., Vapor-liquid and liquid-liquid equilibrium measurements on five binary mixtures, DIPPR Data Series 2 (Experimental Results for DIPPR 1990-91 Projects on Phase Equilibria and Pure Component Properties) (1994) 46-62.

10. Duan, Z., Moller, N., and Weare, J. H., Molecular dynamics simulation of PVT properties of geological fluids and a general equation of state of nonpolar and weakly polar gases up to 2000 K and 20,000 bar, Geochimica et Cosmochimica Acta 56 (10) (1992) 3839-45.

11. O'Sullivan, D. W., Lee, M., Noone, B. C., and Heikes, B. G., Henry's Law Constant Determinations for Hydrogen Peroxide, Methyl Hydroperoxide, Hydroxymethyl Hydroperoxide, Ethyl Hydroperoxide, and Peroxyacetic Acid, Journal of Physical Chemistry 100 (8) (1996) 3241-7.

12. Bowden, D. J., Clegg, S. L., and Brimblecombe, P., The Henry's law constants of the haloacetic acids, Journal of Atmospheric Chemistry 29 (1) (1998) 85-107.

13. Khan, I., Brimblecombe, P., and Clegg, S. L., Solubilities of pyruvic acid and the lower (C1-C6) carboxylic acids. Experimental determination of equilibrium vapor pressure above pure aqueous and salt solutions, Journal of Atmospheric Chemistry 22 (3) (1995) 285-302.

14. Zhou, X. and Mopper, K., Apparent partition coefficients of 15 carbonyl compounds between air and seawater and between air and freshwater; implications for air-sea exchange, Environmental Science and Technology 24 (12) (1990) 1864-9.

15. Ashworth, R. A., Howe, G. B., Mullins, M. E., and Rogers, T. N., Air-water partitioning coefficients of organics in dilute aqueous solutions, Journal of Hazardous Materials 18 (1) (1988) 25-36.

16. Dewulf, J., Drijvers, D., and van Langenhove, H., Measurement of Henry's law constant as function of temperature and salinity for the low temperature range, Atmospheric Environment 29 (3) (1995) 323-31.

17. Hine, J. and Mookerjee, P. K., Structural effects on rates and equilibriums. XIX. Intrinsic hydrophilic character of organic compounds. Correlations in terms of structural contributions, Journal of Organic Chemistry 40 (3) (1975) 292-8.

18. Clegg, S. L. and Brimblecombe, P., Solubility of volatile electrolytes in multicomponent solutions with atmospheric applications, ACS Symposium Series 416 (Chem. Model. Aqueous Syst. 2) (1990) 58-73 .

19. Gossett, J. M., Measurement of Henry's law constants for C1 and C2 chlorinated hydrocarbons, Environmental Science and Technology 21 (2) (1987) 202-8.

20. Bruyn, W. J. D., Swartz, E., Hu, J. H., Shorter, J. A., Davidovits, P., Worsnop, D. R., Zahniser, M. S., and Kolb, C. E., Henry's law solubilities and Setchenow coefficients for biogenic reduced sulfur species obtained from gas-liquid uptake measurements, Journal of Geophysical Research, [Atmospheres] 100 (D4) (1995) 7245-51.

21. Christie, A. O. and Crisp, D. J., Activity coefficients of the normal primary, secondary, and tertiary aliphatic amines in aqueous solutions, Journal of Applied Chemistry 17 (1) (1967) 11-14.

22. Bradley, R. S., Dew, M. J., and Munro, D. C., Solubility of benzene and toluene

in water and aqueous salt solutions under pressure, High Temperatures - High Pressures 5 (2) (1973) 169-76.

23. Wasik, S. P., Schwarz, F. P., Tewari, Y. B., Miller, M. M., and Purnell, J. H., A head-space method for measuring activity coefficients, partition coefficients, and solubilities of hydrocarbons in saline solutions, Journal of Research of the National Bureau of Standards (United States) 89 (3) (1984) 273-7.

24. Nicholson, B., Maguire, B. P., and Bursill, D. B., Henry's law constants for the trihalomethanes: effects of water composition and temperature, Environmental Science and Technology 18 (7) (1984) 518-21.

25. McGee, K. A., Susak, N. J., Sutton, A. J., and Haas, J. L. Jr., The solubility of methane in sodium chloride brines, Open-File Report - United States Geological Survey 81-1294 (1981) 42 pp.

26. Dacey, J. W. H., Wakeham, S. G., and Howes, B. L., Henry's law constants for dimethyl sulfide in fresh water and seawater, Geophysical Research Letters 11 (10) (1984) 991-4.

27. Kucklick, J. R., Hinckley, D. A., and Bidleman, T. F., Determination of Henry's law constants for hexachlorocyclohexanes in distilled water and artificial seawater as a function of temperature, Marine Chemistry 34 (3-4) (1991) 197-209.

28. Moore, R. M., Green, C. E., and Tait, V. K., Determination of Henry's law constants for a suite of naturally occurring halogenated methanes in seawater, Chemosphere 30 (6) (1995) 1183-91.

29. Keeley, D. F., Hoffpauir, M. A., and Meriwether, J. R., Solubility of aromatic hydrocarbons in water and sodium chloride solutions of different ionic strengths: C2-Substituted benzenes, Journal of Chemical and Engineering Data 36 (4) (1991) 456-9.

30. Przyjazny, A., Janicki, W., Chrzanowski, W., and Staszewski, R., Headspace gas chromatographic determination of distribution coefficients of selected organosulfur compounds and their dependence on some parameters, Journal of Chromatography 280 (2) (1983) 249-60.

31. McDevit, W. F. and Long, F. A. , The activity coefficient of benzene in aqueous salt solutions, Journal of the American Chemical Society 74 (1952) 1773-7.

32. Long, F. A. and McDevit, W. F. , Activity coefficients of nonelectrolyte solutes in aqueous salt solutions, Chemical Reviews (Washington, DC, United States) 51 (1952) 119-69.

33. Saylor, J. H., Whitten, A. I., Claiborne, I., and Gross, P. M., The solubilities of benzene, nitrobenzene, and ethylene chloride in aqueous salt solutions, Journal of the American Chemical Society 74 (1952) 1778-81.

34. Xie, W., Zheng, Z., Tang, M., Li, D., Shiu, W.-Y., and Mackay, D., Solubilities and Activity Coefficients of Chlorobenzenes and Chlorophenols in Aqueous Salt Solutions, Journal of Chemical and Engineering Data 39 (3) (1994) 568-71.

35. Brendel, M. L. and Sandler, S. I., The effect of salt and temperature on the infinite dilution activity coefficients of volatile organic chemicals in water, Fluid Phase Equilibria 165 (1) (1999) 87-97.

36. Burns, J. A. and Furter, W. F. , Effects of salts having large organic ions on vapor-liquid equilibrium, Advances in Chemistry Series 155 (Thermodyn. Behav. Electrolytes Mixed Solvents, Symp., 1975) (1976) 99-127.

37. Burns, J. A. and Furter, W. F. , Salt effect in vapor-liquid equilibrium at fixed liquid composition, Advances in Chemistry Series 177 (Thermodyn. Behav. Electrolytes Mixed Solvents 2) (1979) 11-26 .

38. Ohe, S. Vapor-Liquid Equilibrium Data: Salt Effect. 392 pp. 1991.

39. Eckert, C. A. and Schreiber, L. B., Use of infinite dilution activity coefficients with Wilson's equation, Industrial & Engineering Chemistry Process Design and Development 10 (4) (1971) 572-6.

40. Wilson, G. M., Vapor-liquid equilibrium. XI. A new expression for the excess free energy of mixing, Journal of the American Chemical Society 86 (2) (1964) 127-30.

41. Sun, T., Bullock, K. R., and Teja, A. S., Correlation and prediction of salt effects on vapor-liquid equilibrium in alcohol-water-salt systems, Fluid Phase Equilibria 219 (2) (2004) 257-264.

42. Yang, S.-O. and Lee, C. S., Vapor-Liquid Equilibria of Water + Methanol in the Presence of Mixed Salts, Journal of Chemical and Engineering Data 43 (4) (1998) 558-561.

43. Kumagae, Y., Mishima, K., Hongo, M., Kusunoki, M., and Arai, Y., Effect of calcium chloride on vapor-liquid equilibria of alcohol-alcohol and alcohol-water binary systems, Canadian Journal of Chemical Engineering 70 (6) (1992) 1180-5.

44. Banat, F. A., Abu Al-Rub, F. A., and Simandl, J., Experimental study of the salt effect in vapor/liquid equilibria using headspace gas chromatography, Chemical Engineering & Technology 22 (9) (1999) 761-765.

45. Pena, M. P., Vercher, E., and Martinez-Andreu, A., Isobaric Vapor-Liquid Equilibrium for Ethanol + Water + Strontium Chloride, Journal of Chemical and Engineering Data 40 (1) (1995) 311-14.

46. Abu Al-Rub, F. A., Banat, F. A., and Simandl, J., Isothermal vapour-liquid equilibria of 1-propanol-water-salt mixtures, Chemical Engineering Journal

(Lausanne) 74 (3) (1999) 205-210.

47. Sada, E., Morisue, T., and Yamaji, H., Salt effects on isobaric vapor-liquid equilibrium of isopropanol-water system, Canadian Journal of Chemical Engineering 53 (3) (1975) 350-3.

48. Rajendran, M., Renganarayanan, S., and Srinivasan, D., Salt effect in phase equilibria: effect of dissolved inorganic salts on the liquid-liquid equilibria of benzene-2-propanol-water system and the vapor-liquid equilibria of its constituent binaries, Fluid Phase Equilibria 50 (1-2) (1989) 133-64.

49. Slusher, J. T., Cummings, P. T., Hu, Y., Vega, C. A., and O'Connell, J. P., Vapor-Liquid Equilibrium and Density Measurements of Alkylammonium Bromide + Propanol + Water Systems, Journal of Chemical and Engineering Data 40 (4) (1995) 792-8.

50. Gironi, F. and Lamberti, L., Vapor-liquid equilibrium data for the water-2-propanol system in the presence of dissolved salts, Fluid Phase Equilibria 105 (2) (1995) 273-86.

51. Trampe, D. M. and Eckert, C. A., Limiting activity coefficients from an improved differential boiling point technique, Journal of Chemical and Engineering Data 35 (2) (1990) 156-62.

52. Thomas, E. R., Newman, B. A., Nicolaides, G. L., and Eckert, C. A., Limiting activity coefficients from differential ebulliometry, Journal of Chemical and Engineering Data 27 (3) (1982) 233-40.

53. Scott, L. S., Determination of activity coefficients by accurate measurement of boiling point diagram, Fluid Phase Equilibria 26 (2) (1986) 149-63.

54. Eckert, C. A., Wong, K. F., and Wong, K. F., Dilute solution behavior of two cyclic anhydrides, Industrial & Engineering Chemistry Fundamentals 10 (1) (1971) 20-3.

55. Sherman, S. R., Trampe, D. B., Bush, D. M., Schiller, M., Eckert, C. A., Dallas, A. J., Li, J., and Carr, P. W., Compilation and Correlation of Limiting Activity Coefficients of Nonelectrolytes in Water, Industrial & Engineering Chemistry Research 35 (4) (1996) 1044-58.

56. Trampe, D. B. and Eckert, C. A., A dew point technique for limiting activity coefficients in nonionic solutions, AIChE Journal 39 (6) (1993) 1045-50.

57. Pecsar, R. E. and Martin, J. J., Solution thermodynamics from gas-liquid chromatography, Analytical Chemistry 38 (12) (1966) 1661-9.

58. Shaffer, D. L. and Daubert, T. E., Gas-liquid chromatographic determination of solution properties of oxygenated compounds in water, Analytical Chemistry 41

(12) (1969) 1585-9.

59. Burnett, M. G., Determination of partition coefficients at infinite dilution by the gas chromatographic analysis of the vapor above dilute solutions, Anal. Chem. 35 (11) (1963) 1567-70.

60. Leroi, J. C., Masson, J. C., Renon, H., Fabries, J. F., and Sannier, H., Accurate measurement of activity coefficients at infinite dilution by inert gas stripping and gas chromatography, Industrial & Engineering Chemistry Process Design and Development 16 (1) (1977) 139-44.

61. Mackay, D., Shiu, W. Y., and Sutherland, R. P., Determination of air-water Henry's law constants for hydrophobic pollutants, Environmental Science and Technology 13 (3) (1979) 333-7.

62. Richon, D., Sorrentino, F., and Voilley, A., Infinite dilution activity coefficients by the inert gas stripping method: extension to the study of viscous and foaming mixtures, Industrial & Engineering Chemistry Process Design and Development 24 (4) (1985) 1160-5.

63. Wright, D. A., Sandler, S. I., and DeVoll, D., Infinite dilution activity coefficients and solubilities of halogenated hydrocarbons in water at ambient temperatures, Environmental Science and Technology 26 (9) (1992) 1828-31.

64. Yaws, C. L., Yang, H. C., Hopper, J. R., and Hansen, K. C., Organic chemicals: water solubility data, Chemical Engineering (New York, NY, United States) 97 (8) (1990) 115-16, 118.

65. Yaws, C. L., Yang, H. C., Hopper, J. R., and Hansen, K. C., Hydrocarbons: water solubility data, Chemical Engineering (New York, NY, United States) 97 (4) (1990) 177-8, 180, 182.

66. Hussam, A. and Carr, P. W., Rapid and precise method for the measurement of vapor/liquid equilibria by headspace gas chromatography, Analytical Chemistry 57 (4) (1985) 793-801.

67. Chai, X. S. and Zhu, J. Y., Indirect headspace gas chromatographic method for vapor-liquid phase equilibrium study, Journal of Chromatography, A 799 (1 + 2) (1998) 207-214.

68. USEPA . 63 Federal Register 18504, 15 Apr 1998.

69. Teja, A. S., Sandler, S. I., and Patel, N. C., A Generalization of the Corresponding States Principle Using 2 Nonspherical Reference Fluids, Chemical Engineering Journal and the Biochemical Engineering Journal 21 (1) (1981) 21-28.

70. Kolb, B., Welter, C., and Bichler, C., Determination of partition coefficients by automatic equilibrium headspace gas chromatography by vapor phase calibration,

Chromatographia 34 (5-8) (1992) 235-40.

71. McAullife, C., GC [gas-chromatographic] determination of solutes by multiple phase equilibration, Chemical Technology (Jan.) (1971) 46-51.

72. Ioffe, B. V.; Vitenberg, A. G. Head-space analysis and related methods in gas chromatography, Wiley, New York, 1984.

73. Guitart, R., Puigdemont, A., and Arboix, M., Rapid headspace gas chromatographic method for the determination of liquid/gas partition coefficients, Journal of Chromatography 491 (2) (1989) 271-80.

74. Ettre, L. S., Welter, C., and Kolb, B., Determination of gas-liquid partition coefficients by automatic equilibrium headspace-gas chromatography utilizing the phase ratio variation method, Chromatographia 35 (1-2) (1993) 73-84.

75. Chai, X. S. and Zhu, J. Y., Simultaneous measurements of solute concentration and Henry's constant using multiple headspace extraction gas chromatography, Analytical Chemistry 70 (16) (1998) 3481-3487.

76. Halpern, A. M. Experimental Physical Chemistry, Prentice Hall, Upper Saddle River, NJ, U.S.A., 1997.

77. Zhu, J. Y., Liu, P. H., Chai, X. S., Bullock, K. R., and Teja, A. S., Henry's Law Constant of Methanol in Pulping Spent Liquors, Environmental Science and Technology 34 (9) (2000) 1742-1746.

78. Eisert, R. and Levsen, K., Solid-phase microextraction coupled to gas chromatography: a new method for the analysis of organics in water, Journal of Chromatography, A 733 (1 + 2) (1996) 143-157.

79. Louch, D., Motlagh, S., and Pawliszyn, J., Dynamics of organic compound extraction from water using liquid-coated fused silica fibers, Analytical Chemistry 64 (10) (1992) 1187-99.

80. Nazarenko, A. Y., Liquid-Phase Headspace Micro-extraction Into a Single Drop, American Laboratory (August) (2004) 30-33.

81. O'Sullivan, T. D. and Smith, N. O., Solubility and partial molar volume of nitrogen and methane in water and in aqueous sodium chloride from 50 to 125 C and 100 to 600 atm, Journal of Physical Chemistry 74 (7) (1970) 1460-6.

82. Blount, C. W., Price, L. C., Wenger, L. M., and Tarullo, M., Methane solubility in aqueous sodium chloride solutions at elevated temperatures and pressures, Proceedings - United States Gulf Coast Geopressured-Geothermal Energy Conference 4 (3) (1980) 1225-62.

83. Clarke, E. C. W. and Glew, D. N., Evaluation of Thermodynamic Functions From

Equilibrium Constants, Transactions of the Faraday Society 62 (519P) (1966) 539-&.

84. Alvarez, J., Crovetto, R., and Fernandezprini, R., The Dissolution of N_2 and of H_2 in Water From Room-Temperature to 640-K, Berichte Der Bunsen-Gesellschaft-Physical Chemistry Chemical Physics 92 (8) (1988) 935-940.

85. Prini, R. F. and Crovetto, R., Evaluation of Data on Solubility of Simple Apolar Gases in Light and Heavy-Water at High-Temperature, Journal of Physical and Chemical Reference Data 18 (3) (1989) 1231-1243.

86. Krause, D. Jr. and Benson, B. B., The solubility and isotopic fractionation of gases in dilute aqueous solution. IIa. Solubilities of the noble gases, Journal of Solution Chemistry 18 (9) (1989) 823-73.

87. Clever, H. L. a. C. L. Y.; Editors . IUPAC Solubility Data Series, Vol. 27/28: Methane. 331 pp. 1987.

88. Setchenov, J., Über die Konstitution der Salzlösungen auf Grund ihres Verhaltens zu Kohlensäure, Z. Phys. Chem. 4 (1889) 117-125.

89. Pitzer, K. S. Activity coefficients in electrolyte solutions, CRC Press, Boca Raton : 1991.

90. Debye, P. and McAulay, J., The electric field of ions and the action of neutral salts, Physik. Z. 26 (1925) 22-9.

91. Duan, Z. and Weare, J. H., The Prediction of Methane Solubility in Natural-Waters to High Ionic-Strength From 0 - 250 ^{o}C and From 0 - 1600 Bar - Reply, Geochimica Et Cosmochimica Acta 56 (12) (1992) 4303.

92. Carroll, J. J., The Prediction of Methane Solubility in Natural-Waters to High Ionic-Strength From 0 ^{o}C to 250 ^{o}C and From 0 - 1600 Bar - Comment, Geochimica Et Cosmochimica Acta 56 (12) (1992) 4301-4302.

93. Haas, J. L. Jr. *Preliminary \"steam tables\" for sodium chloride solutions. Thermodynamic properties of the coexisting phases and thermochemical properties of the sodium chloride component*;USGS-OFR-75-675; 75.

94. Akinfiev, N. N. and Diamond, L. W., Thermodynamic description of aqueous nonelectrolytes at infinite dilution over a wide range of state parameters, Geochimica et Cosmochimica Acta 67 (4) (2003) 613-629.

95. Chemical Oceanography, Vol. 1. Riley, John. Price. and Skirrow, G. 1975. New York, NY, USA , Academic Press.

96. Pierotti, R. A., The solubility of gases in liquids, Journal of Physical Chemistry 67 (9) (1963) 1840-5.

97. Pierotti, R. A., Aqueous solutions of nonpolar gases, Journal of Physical Chemistry 69 (1) (1965) 281-8.

98. Reiss, H., Frisch, H. L., Helfand, E., and Lebowitz, J. L., Aspects of the statistical thermodynamics of real fluids, Journal of Chemical Physics 32 (1960) 119-24.

99. Reiss, H., Frisch, H. L., and Lebowitz, J. L., Statistical mechanics of rigid spheres, Journal of Chemical Physics 31 (1959) 369-80.

100. Lee, B. I. and Kesler, M. G., Generalized thermodynamic correlation based on three-parameter corresponding states, AIChE Journal 21 (3) (1975) 510-27.

101. Masterton, W. L. and Lee, T. P., Salting coefficients from scaled particle theory, Journal of Physical Chemistry 74 (8) (1970) 1776-82.

102. Xie, W. and Yang, W., Application of a scaled particle theory to polar solute system and calculation of the salt effect constant, Wuli Huaxue Xuebao 3 (3) (1987) 258-64.

103. Millero, F. J. Sea water as a multicomponent electrolyte solution. 1974; pp 3-80.

104. Spivey, J. P., Mccain, W. D., and North, R., Estimating Density, Formation Volume Factor, Compressibility, Methane Solubility, and Viscosity for Oilfield Brines at Temperatures From 0 to 275 Degrees C, Pressures to 200 Mpa, and Salinities to 5.7 Mole/Kg, Journal of Canadian Petroleum Technology 43 (7) (2004) 52-61.

105. Clegg, S. L.; Whitfield, M. Activity Coefficients in Natural Waters. Pitzer, Kenneth S. Activity Coefficients in Electrolyte Solutions. p 283. 1991. New York, NY, USA , Academic Press.

106. Tiepel, E. W. and Gubbins, K. E., Thermodynamic properties of gases dissolved in electrolyte solutions, Industrial & Engineering Chemistry Fundamentals 12 (1) (1973) 18-25.

107. Teja, A. S., Patel, N. C., and Ng, N. H., Vanderwaals One-Fluid Model for Mixtures and Generalized Equations of State, Chemical Engineering Science 33 (5) (1978) 624-625.

108. Reid, R. C.; Prausnitz, J. M.; Poling, B. E. The properties of gases and liquids, McGraw-Hill, New York : 1987.

109. Ni N, El-Sayed M M, Sanghvi T, and Yalkowsky S H, Estimation of the effect of NaCl on the solubility of organic compounds in aqueous solutions, Journal of pharmaceutical sciences 89 (12) (2000) 1620-5.

110. Ni, N. and Yalkowsky, S. H., Prediction of Setschenow constants, International Journal of Pharmaceutics 254 (2) (2003) 167-172.

111. Leo, A., Hansch, C., and Elkins, D., Partition coefficients and their uses, Chemical Reviews (Washington, DC, United States) 71 (6) (1971) 525-616.

112. Hansch, C., Maloney, P. P., Fujita, T., and Muir, R. M., Correlation of biological activity of phenoxyacetic acids with Hammett substituent constants and partition coefficients, Nature (London, United Kingdom) 194 (1962) 178-80.

113. Xie, W.-H., Shiu, W.-Y., and Mackay, D., A review of the effect of salts on the solubility of organic compounds in seawater, Marine Environmental Research 44 (4) (1997) 429-444.

114. Li, W., Xie, W., and Huang, Z., Activity coefficients of nonelectrolytes in aqueous salt solutions. Solubilities of n-hexanoic acid and n-heptanoic acid in aqueous solutions of salts with small ions, Gaodeng Xuexiao Huaxue Xuebao 6 (4) (1985) 351-6.

115. Xie, W., Su, J., and Xie, X., Studies on the activity coefficient of benzene and its derivatives in aqueous salt solutions, Thermochimica Acta 169 (1990) 271-86.

116. Schumpe, A., The estimation of gas solubilities in salt solutions, Chemical Engineering Science 48 (1) (1993) 153-8 .

117. van Krevelen, D. W. and Hoftijzer, P. J., Sur la solubilite des gas dans les solutions aqueuses, Chimie et Industrie Numero Speciale du XXIe Congres International de Chime Industrielle, Bruxelles (1950) 168-173.

118. Danckwerts, P. V. Gas-Liquid Reactions (McGraw-Hill Chemical Engineering Series). 276 pp. 1970.

119. Onda, K., Sada, E., Kobayashi, T., Kito, S., and Ito, K., Solubility of gases in aqueous solutions of mixed salts, Journal of Chemical Engineering of Japan 3 (2) (1970) 137-42.

120. Chang, R. F., Morrison, G., and Sengers, J. M. H. L., The critical dilemma of dilute mixtures, Journal of Physical Chemistry 88 (16) (1984) 3389-91.

121. Sengers, J. M. H. L., Dilute mixtures and solutions near critical points, Fluid Phase Equilibria 30 (1986) 31-9.

122. Morrison, G., Sengers, J. M. H. L., Chang, R. F., and Christensen, J. J., Thermodynamic anomalies in supercritical fluid mixtures, Process Technology Proceedings 3 (Supercrit. Fluid Technol.) (1985) 25-43.

123. Sengers, J. M. H. L., Solubility near the solvent's critical point, Journal of Supercritical Fluids 4 (4) (1991) 215-22.

124. Japas, M. L. and Levelt Sengers, J. M. H., Gas solubility and Henry's law near the solvent's critical point, AIChE Journal 35 (5) (1989) 705-13.

125. Harvey, A. H. and Levelt Sengers, J. M. H., Correlation of aqueous Henry's constants from 0 ^{o}C to the critical point, AIChE Journal 36 (4) (1990) 539-46.

126. Harvey, A. H., Levelt Sengers, J. M. H., and Tanger IV, J. C., Unified description of infinite-dilution thermodynamic properties for aqueous solutes, Journal of Physical Chemistry 95 (2) (1991) 932-7 .

127. Harvey, A. H., Supercritical solubility of solids from near-critical dilute-mixture theory, Journal of Physical Chemistry 94 (22) (1990) 8403-6.

128. Harvey, A. H., Semiempirical correlation for Henry's constants over large temperature ranges, AIChE Journal 42 (5) (1996) 1491-1494.

129. Harvey, A. H., Applications of Near-Critical Dilute-Solution Thermodynamics, Industrial & Engineering Chemistry Research 37 (8) (1998) 3080-3088.

130. Mendez-Santiago, J. and Teja, A. S., Solubility of Solids in Supercritical Fluids: Consistency of Data and a New Model for Cosolvent Systems, Industrial & Engineering Chemistry Research 39 (12) (2000) 4767-4771.

131. Prausnitz, J. M.; Lichtenthaler, R. N.; Azevedo, E. G. d. Molecular thermodynamics of fluid-phase equilibria, Prentice Hall PTR, Upper Saddle River, N.J. : 1999.

132. Bullock, K. R. and Teja, A. S., Henry's Constants of Volatile Organic Compounds in Aqueous Salt Solutions, Industrial & Engineering Chemistry Research 42 (25) (2003) 6494-6498.

133. Debye, P. and Huckel, E., The theory of electrolytes. I. Lowering of freezing point and related phenomena, Physik. Z. 24 (1923) 185-206.

134. Guggenheim, E. A., Specific thermodynamic properties of aqueous solutions of strong electrolytes, Philosophical Magazine (1798-1977) 19 (1935) 588-643.

135. Guggenheim, E. A. and Turgeon, J. C., Specific interaction of ions, Transactions of the Faraday Society 51 (1955) 747-61.

136. Pitzer, K. S. and Mayorga, G. , Thermodynamics of electrolytes. III. Activity and osmotic coefficients for 2-2 electrolytes, Journal of Solution Chemistry 3 (7) (1974) 539-46.

137. Pitzer, K. S. and Mayorga, G. , Thermodynamics of electrolytes. II. Activity and osmotic coefficients for strong electrolytes with one or both ions univalent, Journal of Physical Chemistry 77 (19) (1973) 2300-8.

138. Pitzer, K. S., Thermodynamics of electrolytes. I. Theoretical basis and general equations, Journal of Physical Chemistry 77 (2) (1973) 268-77.

139. Chen, C. C., Britt, H. I., Boston, J. F., and Evans, L. B., Local composition model for excess Gibbs energy of electrolyte systems. Part I: Single solvent, single completely dissociated electrolyte systems, AIChE Journal 28 (4) (1982) 588-96.

140. Chen, C. C. and Evans, L. B., A local composition model for the excess Gibbs energy of aqueous electrolyte systems, AIChE Journal 32 (3) (1986) 444-54.

141. Renon, H. and Prausnitz, J. M., Local compositions in thermodynamic excess functions for liquid mixtures, AIChE Journal 14 (1) (1968) 135-44.

142. Pitzer, K. S., Electrolytes. From dilute solutions to fused salts, Journal of the American Chemical Society 102 (9) (1980) 2902-6.

143. Chapman, W. G., Gubbins, K. E., Jackson, G., and Radosz, M., SAFT: equation-of-state solution model for associating fluids, Fluid Phase Equilibria 52 (1989) 31-8.

144. Chapman, W. G., Gubbins, K. E., Jackson, G., and Radosz, M., New reference equation of state for associating liquids, Industrial & Engineering Chemistry Research 29 (8) (1990) 1709-21.

145. Wertheim, M. S., Thermodynamic perturbation theory of polymerization, Journal of Chemical Physics 87 (12) (1987) 7323-31.

146. Wu, J. and Prausnitz, J. M., Phase Equilibria for Systems Containing Hydrocarbons, Water, and Salt: An Extended Peng-Robinson Equation of State, Industrial & Engineering Chemistry Research 37 (5) (1998) 1634-1643.

147. Blum, L. and Hoeye, J. S., Mean spherical model for asymmetric electrolytes. 2. Thermodynamic properties and the pair correlation function, Journal of Physical Chemistry 81 (13) (1977) 1311-16.

148. Li, J., Polka, H.-M., and Gmehling, J., A gE model for single and mixed solvent electrolyte systems. I. Model and results for strong electrolytes, Fluid Phase Equilibria 94 (1994) 89-114.

149. Guggenheim, E. A., The statistical mechanics of regular solutions, Proc. Roy. Soc. (London) A148 (1935) 304-12.

150. Abrams, D. S. and Prausnitz, J. M., Statistical thermodynamics of liquid mixtures. New expression for the excess Gibbs energy of partly or completely miscible systems, AIChE Journal 21 (1) (1975) 116-28.

151. Falabella, J. B., Nair, A., and Teja, A. S., Henry's Constants of 1-Alkanols and 2-Ketones in Salt Solutions, Journal of Chemical & Engineering Data 51 (5) (2006) 1940-1945.

152. Trampe, D. M. and Eckert, C. A., Calorimetric measurement of partial molar

excess enthalpies at infinite dilution, Journal of Chemical and Engineering Data 36 (1) (1991) 112-18.

153. Hovorka, S., Roux, A. H., Roux-Desgranges, G., and Dohnal, V., Limiting Partial Molar Excess Enthalpies of Selected Organic Compounds in Water at 298.15 K, Journal of Chemical and Engineering Data 47 (4) (2002) 954-959.

154. Korolev, V. P., Batov, D. V., and Krestov, G. A., Isotopic effect in heats of hydration of liquid nonelectrolytes, Russian Journal of Physical Chemistry 59 (1) (1985) 212-14.

155. Chai, X.-S., Falabella, J. B., and Teja, A. S., A relative headspace method for Henry's constants of volatile organic compounds, Fluid Phase Equilibria 231 (2) (2005) 239-245.

156. Collins, K. D., Ion hydration: Implications for cellular function, polyelectrolytes, and protein crystallization, Biophysical Chemistry 119 (3) (2006) 271-281.

157. Falabella To be published. Unpublished Work.

158. Robbins, G. A., Wang, S., and Stuart, J. D., Using the static headspace method to determine Henry's law constants, Analytical Chemistry 65 (21) (1993) 3113-18.

159. Gorgenyi, M., Dewulf, J., and Van Langenhove, H., Temperature dependence of Henry's law constant in an extended temperature range, Chemosphere 48 (7) (2002) 757-762.

160. Sultanov, R. C., Skripka, V. C., and Namiot, A. Yu., Solubility of methane in water at high temperatures and pressures, Gazova Promyshelnnost 17 (1972) 6-7.

161. Blanco C., L. H. and Smith, N. O., The high pressure solubility of methane in aqueous calcium chloride and aqueous tetraethylammonium bromide. Partial molar properties of dissolved methane and nitrogen in relation to water structure, Journal of Physical Chemistry 82 (2) (1978) 186-91.

162. Moore, J. C., Battino, R., Rettich, T. R., Handa, Y. P., and Wilhelm, E., Partial molar volumbes of gases at infinite dilution in water at 298.15 K, Journal of Chemical and Engineering Data 27 (1) (1982) 22-4.

163. Duan, Z., Moller, N., Greenberg, J., and Weare, J. H., The prediction of methane solubility in natural waters to high ionic strength from 0 - 250 ^{o}C and from 0 - 1600 bar, Geochimica et Cosmochimica Acta 56 (4) (1992) 1451-60.

164. Falabella, J. B., Kizzie, A. C., and Teja, A. S., Henry's constants of gases and volatile organic compounds in aqueous solutions, Fluid Phase Equilibria 241 (1-2) (2006) 96-102.

165. Shires, T. M.; Harrison, M. R. *Methane Emissions from the Natural Gas*

Industry;GRI-94/0257.23 and EPA-600/R-96-080f; Jun, 96.

166. *ASPEN Plus,* version 2004.1; ASPEN Technologies, inc.: Cambridge, MA,

.

VITA

James was born in Massachusetts on September 10th 1978. As lifelong resident of the state James attended public school in the suburbs of Boston. Growing up, James enjoyed playing sports, creating art, fishing, classical music, and gardening. He enrolled at Northeastern University in September of 1996 and completed his Bachelor's degree in Chemical Engineering in June of 2001 with almost 2 years of industry experience through co-op. James continued studying chemical engineering in the graduate program at Northeastern University, and earned his Masters in chemical engineering in June 2003 in the research group of Professor Nurcan Baç (currently the chair of the department of chemical engineering at Middle East Technical University in Ankara, Turkey). While at Northeastern University, James presented his work yearly at the departmental seminar series and twice at the annual meeting of the North American Membrane Society (NAMS)

After completing his Master's degree at Northeastern University, James immediately began pursuing a PhD in the School of Chemical and Biomolecular Engineering at Georgia Tech in the group of Professor Amyn Teja. In his time at Georgia Tech, James published several articles in peer reviewed journals and presented his work at the Georgia Tech School of Chemical and Biomolecular Engineering Graduate Student Symposium, at the annual meeting of the American Institute of Chemical Engineers (AIChE), and at the Eleventh International Conference on Properties and Phase Equilibria for Product and Process Design (PPEPPD).